

**FOSSIL  
FUELS  
RESEARCH**

DOE/ET/12382-11

**CORRELATION OF PETROLEUM COMPONENT  
PROPERTIES FOR IMPROVED WATERFLOODING**

**Final Report**

Work Performed for the Department of Energy  
Under Contract No. DE-AS19-78ET12382

Date Published—August 1982

University of Southern California  
Los Angeles, California



**Bartlesville Project Office  
U. S. DEPARTMENT OF ENERGY  
Bartlesville, Oklahoma**

## DISCLAIMER

"This book was prepared as an account of work sponsored by an agency of the United States Government. Neither the United States Government nor any agency thereof, nor any of their employees, makes any warranty, express or implied, or assumes any legal liability or responsibility for the accuracy, completeness, or usefulness of any information, apparatus, product, or process disclosed, or represents that its use would not infringe privately owned rights. Reference herein to any specific commercial product, process, or service by trade name, trademark, manufacturer, or otherwise, does not necessarily constitute or imply its endorsement, recommendation, or favoring by the United States Government or any agency thereof. The views and opinions of authors expressed herein do not necessarily state or reflect those of the United States Government or any agency thereof."

Available from the National Technical Information Service, U.S. Department of Commerce, Springfield, Virginia 22161.

### NTIS price codes

Paper copy: \$12.00

Microfiche copy: \$4.00

**CORRELATION OF PETROLEUM COMPONENT  
PROPERTIES FOR IMPROVED WATERFLOODING**

**Final Report**

T. F. Yen, *Principal Investigator*  
University of Southern California  
School of Engineering  
University Park  
Los Angeles, California 90007

Gary D. Peterson, *Technical Project Officer*  
San Francisco Operations Office  
1333 Broadway  
Oakland, California 94612

Work Performed for the Department of Energy  
Under Contract No. DE-AS19-78ET12382

Date Published—August 1982

## TABLE OF CONTENTS

Section I.	Background Information in Literature	
	1. Origin and Transformation of Petroleum.....	1
	2. History of Alkaline Flooding.....	2
	3. Field Tests.....	2
	4. Alkali Materials Studied.....	3
	5. Mechanistic Studies.....	3
	6. Interfacial Phenomenon.....	7
Section II.	Research Objectives and Approach	
	1. General Chemical Characterization of Crude Oil.....	11
	2. Characterization of Alkali Sensitive Interfacially Active Fraction from Crude Oil.....	11
	3. Development of an Equilibrium Chemical Model for the Observed Interfacial Phenomenon.....	11
	4. Enhancement of Interfacial Activity.....	13
Section III.	Materials and Instruments Used	
	1. Chemicals.....	15
	2. Analytical Instruments.....	15
	3. Crude Oils.....	16
Section IV.	Experimental Procedures	
	1. Interfacial Tension Measurement.....	17
	2. Vacuum Distillation of Crude Oil.....	18
	3. Isolation of Pigments from the Volatiles.....	25
	4. Solvent Fractionation of the Nonvolatiles.....	25
	5. Fractionation by Polarity.....	26
	6. Isolation of Porphyrins.....	29
	7. Molecular Weight Measurement.....	32
	8. Bulk Viscosity Measurement.....	32
	9. Density Measurement of Liquid Sample.....	33
	10. Infrared Absorption Measurement.....	33
	11. Sand-Packed Core Flooding Experiments.....	33
	12. Extraction of Soap-Forming Acids by Alkali.....	38
	13. Acid Treatment of Oil.....	39
Section V.	Results and Discussion	
	1. Definition of Interfacial Activity.....	41
	2. Reliability of Interfacial Tension Data.....	41
	3. Comparison of Sodium Hydroxide and Sodium Orthosilicate in Interfacial Behavior.....	41
	4. Characterization of the Volatiles and Nonvolatiles of Crude Oil.....	43

(Cont.)

5.	Concentration of Activity: Fraction 3 and its Characterization.....	50
6.	Porphyryns: Characterization and Their Role in the Alkali Induced Interfacial Activity.....	64
7.	Effects of Sodium Ions on the Activity Onset pH....	67
8.	Experimental Evidence for the Equilibrium IFT Model.....	73
9.	Sequential Activation of Acids in the Crude.....	78
10.	Generation of Additional Soap-Forming Acids From Crude Oil.....	84
11.	Evidence for the Mechanism of the Generation of Additional Activity by Acid Treatment.....	91
Section VI.	Conclusions.....	100
Reference.....		103

### List of Tables

Table 1.	Documented Known Field Tests of Alkali Floods .....	5
Table 2.	High Resolution Mass Measurements of Carboxylic Acids from California Crude. (Ref. 44) .....	8
Table 3.	The pH Values of Alkaline Solutions and their Stability with Storage Time. Stored in half-filled bottles. Solutions contain 7,500 ppm NaCl. ....	8
Table 4.	Weight Percentage Breakdown of Cuts from Crude Oils .....	45
Table 5.	High Resolution Mass Spectroscopic Identification of Carotenoid Fragments from Crude Oil, 12 ev., 180°C. ....	49
Table 6.	NMR Structural Characterization of Long Beach Cuts .....	52
Table 7.	Mass Balance and Average Molecular Weights of Crude Oil Fractions Separated by Silica Gel Column Chromatography .	56
Table 8.	Elemental Analysis of Long Beach Crude and its Fractions 1, 2 and 3 .....	61
Table 9.	Viscosity Effect of Asphaltic Materials and Fraction 3 ..	63
Table 10.	Distribution of Activity among Crude Oil (Long Beach) Cuts .....	63
Table 11.	Elemental Analysis of Materials Extracted from Crude Oil with Alkaline Solution and Acid Solution .....	75
Table 12.	Oil Recovery from a Sand-Packed Core by Alkali Flood ....	83
Table 13.	Amount of Acid Extracted Out by Alkali from Crude Oil after each Acid Reactivation .....	83
Table 14.	Increased Alkaline Flooding Oil Recovery from a Sand- Packed Core through Acid Treatment .....	90

### List of Figures

Figure 1.	In-Situ Emulsification of Oil in Reservoir .....	4
Figure 2.	Operation Procedure of Interfacial Tension Measurement using a Spinning Drop Interfacial Tensiometer .....	19
Figure 3.	Interfacial Tension versus Time of a Spinning Crude Oil Sample Drop in Alkaline Solution .....	20
Figure 4.	Schematic Diagram of Vacuum Distillation Setup .....	22
Figure 5.	Calibration Curve of Refractive Index versus Composition of a Binary Mixture of Methylcyclohexane and Toluene .....	23
Figure 6.	Graphical Determination of the Number of Theoretical Plates in a Packed Glass Bead Column. All Concentrations are Mole Fractions of Methylcyclohexane in a Mixture with Toluene .....	24
Figure 7.	Diagram of a Silica Gel Column for Chromatography Use .....	28
Figure 8.	Structure of Chlorophyll a and Vanadyl DPEP .....	30
Figure 9.	Equipment Used for Density Measurement of Liquid Sample .....	34
Figure 10.	Schematic Diagram of Core Flood Apparatus .....	36
Figure 11.	Interfacial Activity of Long Beach Crude Measured in Five Separate Runs .....	42
Figure 12.	A Comparison of the Effects of Sodium Hydroxide and Sodium Orthosilicate on the Interfacial Activity of the Three Crude Oils .....	44
Figure 13.	Mass Spectrum of Pink Pigment from Long Beach Crude, 12 ev., 180°C .....	47
Figure 14.	Mass Spectrum of Pink Pigment from Huntington Beach Crude. 12 ev., 180°C .....	48
Figure 15.	Structures of Two Carotenoids: Lutein and Zeaxanthin.	49
Figure 16.	A Typical Proton Nuclear Magnetic Resonance Spectrum of an Oil Sample .....	51

(Cont.)

List of Figures (Cont.)

Figure 17. Interfacial Activity of Huntington Beach Crude and its Oil-Resin .....	53
Figure 18. Interfacial Activity of Long Beach Crude and its Oil-Resin .....	54
Figure 19. Interfacial Activity of Arkansas Crude and its Oil-Resin .....	55
Figure 20. Reconstitution of Long Beach Crude from its Fractions 1, 2 and 3 (weight ratio 72:18:8) .....	58
Figure 21. Interfacial Activity of Samples with Different Concentrations of Fraction 3 in Toluene .....	59
Figure 22. Interfacial Activity of Samples with Different Concentrations of Long Beach Crude Oil in Toluene ....	60
Figure 23. Infrared Spectra of Fractions 1, 2 and 3 .....	61
Figure 24. Interfacial Activity of Fraction 3's Isolated from Gas Oil, Resin and Asphaltene .....	65
Figure 25. Visible Absorption Spectrum of Metal-Porphyrins from Long Beach Crude .....	66
Figure 26. Visible Absorption Spectrum of Metal-Free Porphyrins from Long Beach Crude .....	68
Figure 27. Mass Spectrum and Structures of Metal-Free Porphyrins from Huntington Beach Crude. MS: 12 ev., 180°C .....	69
Figure 28. Interfacial Activity of Long Beach Crude in the Presence of NaCl .....	72
Figure 29. Infrared Spectrum of Material Extracted from Crude Oil with Alkali .....	76
Figure 30. Interfacial Activities of Acid A (Undissociated) and Acid B (Dissociated) Extracted from Crude Oil .....	77
Figure 31. Interfacial Activity of Extracted Acids (1:1 Acid A to Acid B) at Different Concentrations in Toluene ....	79
Figure 32. Effects on Crude-Water IFT of Addition of Sodium as NaCl and as NaOH to a 3,000 ppm NaOH Aqueous Solution.	80
Figure 33. Depletion of Activity by Incremental Alkali Treatment.	82
Figure 34. Reactivation of Alkali Exhausted Crude Oil by Acid ...	86

(Cont.)

List of Figures (Cont.)

Figure 35. Increased Activity of Crude Oil by Acid Treatment .....	87
Figure 36. Repeated Reactivation of Crude Oil by Acid Treatment ..	88
Figure 37. Acid-Induced Interfacial Activity of Fraction 2 (10 % Sample) .....	92
Figure 38. Acid-Induced Interfacial Activity of Oleic Acid-Methyl Ester: a 1% sample Pre-exhausted with Alkali .....	93
Figure 39. Acid-Induced Interfacial Activity of Oleic Monoethanolamide: a 1 % Sample Pre-exhausted with Alkali .....	94
Figure 40. Acid-Induced Interfacial Activity of L- $\alpha$ -Phosphatidyl- choline (Lecithin): a 1 % Sample Pre-exhausted with Alkali .....	95
Figure 41. Infrared Spectrum of Material Extracted from Crude Oil with 0.2N HCl Solution .....	97
Figure 42. Interfacial Activity of Amino Material Extracted from Crude Oil with 0.2N HCl Solution: a 1 % Sample. A 0.5 % Sample of Active Acid Extracted by Alkali is Included for Comparison .....	98

We would like to acknowledge the following scientists and engineers for helping and advising during the span of this project.

Dr. Dick Weinbrandt  
of Aminoil (past) and EORCO (now)

Dr. Tom Campbell  
of PQ Corporation (past) and Aminoil (now)

Mr. Ed Mayer  
of Thums Long Beach Co.

Mr. George Bernard  
of Union Oil

Dr. Bob Berg  
of DOE (past) and Aminoil (now)

Dr. Charles Ritz  
of Chevron Oil Field Research Co. (past) and  
Chaplain Oil (now)

The following research personnel have participated in the research.

Research Associates:

Rong Hwang  
Win Chung Lin

Visiting Scholar:

Wen Hui Wu

Graduate Students:

Paul Farmanian  
Mankin Chan  
Jonathan T. Kwan  
P.F. Lin  
M.M. Sharma  
Long-Kwan Jang  
Youim Chang

Undergraduate Students:

Jeff Miller  
Norman Davis  
Robert Casteneda  
John Olenyn  
Joe O'Neill  
John Chen

## BACKGROUND INFORMATION IN LITERATURE

### Origin and Transformation of Petroleum

In order to study the chemical and physical interactions in enhanced oil recovery, it is essential to have a good understanding of the origin and transformation of petroleum which is responsible for the final oil composition.

It is generally believed that petroleum has a biogenic origin.<sup>1,2</sup> However, according to opinions of the majority of the contemporary investigators, petroleum was not created in a ready-made form by living organisms, but rather is the result of complex geochemical transformations of the various constituents of living cells. No one single class of cellular material is responsible for all the petroleum forming substances. For example, the existence of nitrogen compounds suggests substances like protein and chlorophyll. The presence of sulfur also suggests the participation of sulfur containing proteins. The presence of fatty acids also makes it impossible to exclude fats or lipids.

Petroleum-forming substances are believed to accumulate initially in basins (marine or lagoon type). Porfirev and his collaborators<sup>3,4</sup> believed that these substances were accumulated in the form of a homogeneous organic deposit, which is possible only in aquatic basins of the closed or semiclosed type with an anaerobic medium, which implies a lagoonal nature. Other investigators, including Brod and Eremenko<sup>5</sup>

and Cox<sup>6</sup>, gave support to a marine nature of sediments. Still other investigators supported the accumulation of these substances in salty and brackish lakes<sup>7</sup> and fresh water lakes<sup>8</sup>.

The following external factors have been recognized as assisting the transformation of organic substances in sedimentary rocks in the direction of petroleum formation: (i) temperature; (ii) pressure or strata depth; (iii) biochemical processes which include bacterial action ; and (iv) presence of mineral catalysts.

Finally, it should be pointed out that tectonic movement is believed to have caused, in some cases, migration of petroleum from its source rock to distant oil reservoirs. A detailed discussion on the above topics can be found elsewhere<sup>9</sup>.

#### History of Alkaline Flooding

The interfacial activity, that is, the lowering of interfacial tension (IFT) of acid-containing hydrocarbons in water by alkali agents was recognized by Donnan as far back as 1899<sup>10</sup>. Later Hartridge and Peters<sup>11</sup>, and Peters<sup>12</sup> found that this fall in IFT is a function of the pH of the aqueous medium. The range of pH over which the tension starts to change is close to the ionization pH of the acids, although Danielli<sup>13</sup> suggested that the surface pH may be lower than the bulk solution pH due to surface charge effects. The pH dependent reaction has long been applied to the commercial manufacturing of soap<sup>14,15</sup>. Its application to the oil recovery business resulted in many patents<sup>16,17,18,19</sup>. Nutting<sup>20,21</sup> also described the use of weak salts such as sodium carbonate for improving water flooding by his so-called "soda process".

#### Field Tests

A complete documentation of all field tests on alkaline flooding EOR is not available (Fig 1). However, from the view by Mayer, et al<sup>22</sup> a partial list of documented known field tests are compiled in Table 1. Results of these tests vary greatly from one case to another, because of the differences in injection chemical, injection rate and quantity, nature of reservoir and oil, etc. Also many of the detailed results are not available to the public. Overall, the recovery is not very impressive. In other words, more study needs to be done before we can come up with a consistent way to carry out successful alkaline floodings. Currently two projects are in progress in Southern California, namely the Aminoil and the THUMS.

#### Alkali Materials Studied

The alkali material used in most recent floodings is either sodium hydroxide or sodium orthosilicate. The latter is a silicate buffer system of sodium hydroxide, and its reactions in water were described in detail by Campbell<sup>32</sup>. The average formula of the orthosilicate is  $\text{Na}_4\text{SiO}_4$ , but its basic reacting element is still sodium hydroxide, although Campbell<sup>33</sup> has claimed that the orthosilicate form is slightly more effective in cases when calcium ions were present in the injection fluids.

Other alkali materials such as sodium carbonate, ammonium hydroxide, hydroxyl amine and polyphosphate<sup>34</sup> also have been investigated, although they do not seem to offer any improvement over sodium hydroxide. In fact calcium hydroxide and magnesium hydroxide do not even cause significant lowering of IFT<sup>35</sup>.

#### Mechanistic Studies

Johnson<sup>36</sup> has reviewed the mechanisms which have been proposed over the years, and classified them into the following

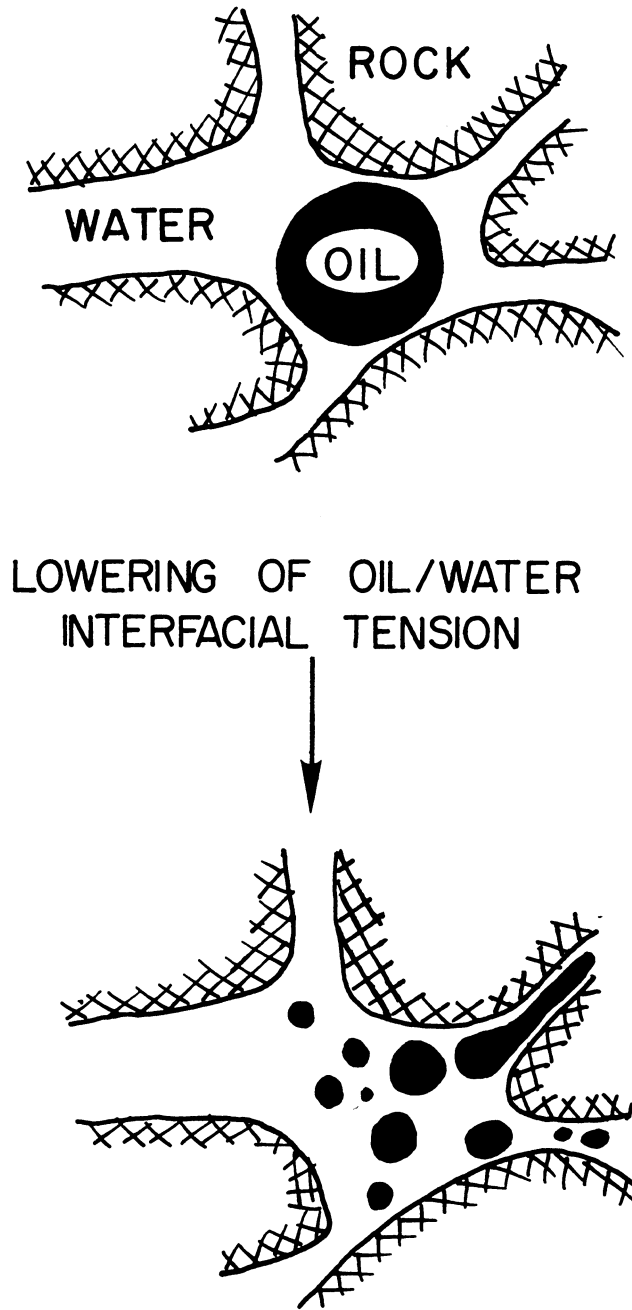


Figure 1. In-Situ Emulsification of Oil in Reservoir.

Table 1. Documented Known Field Tests of Alkali Floods

<u>Field</u>	<u>Alkali Used</u>	<u>Reference</u>
Completed Field Tests:		
Bradford Field, Pennsylvania	sodium carbonate	20, 21
South East Texas (Exxon)	sodium carbonate	22
Harrisberg Field, Nebraska	sodium hydroxide	23
Nagylengyel Field, Hungary	ammonium hydroxide	24
North Ward-Estes Field, Texas	sodium hydroxide	25
Singleton Field, Nebraska	sodium hydroxide	26
Whittier Field, California	sodium hydroxide	27
Wainwright Field, Alberta	sodium hydroxide	28
Brea Orlinda Field, California	sodium orthosilicate	19
Orcutt Hill Field, California	sodium orthosilicate	29
Field Tests in Progress (1980):		
Biason Basin Field, Wyoming	sodium hydroxide	22
Epping Field, Saskatchewan	sodium hydroxide	22
Huntington Beach Field, Calif.	sodium orthosilicate	30
North Ward-Estes Field, Texas	sodium hydroxide	22
Smackover Field, Arkansas	sodium carbonate	31
Toborg Field, Texas	sodium hydroxide	22
Wilmington Field, California	sodium orthosilicate	22

categories:

- (i) Emulsification and Entrainment -- Subkow<sup>18</sup> and Reisberg and Doscher<sup>37</sup> believed that in-situ emulsification of the crude oil resulted from the lowering of IFT by the action of the alkali, and its entrainment into a continuous flowing alkali water phase represent the major means of oil recovery from the reservoir. A picture of in-situ emulsification of oil is shown in Figure 1.
- (ii) Emulsification and Entrapment -- Jennings et al.,<sup>38</sup> in their laboratory coreflood experiments, showed that in-situ emulsification, which is produced when the IFT falls below 0.01 dyne/cm., leads to the movement of the residual oil downstream for a distance, and will be entrapped again by smaller pores where the oil is more efficient in blocking the flow of water, and helps to divert into water regions that would be normally bypassed, thus leading to better oil recovery. This is especially useful for viscous oil reservoirs where waterflood sweep efficiency is believed to be poor.
- (iii) Wettability Reversal -- Wagner and Leach<sup>39</sup> and Mungan<sup>40</sup> and Ehrlich et al.<sup>41</sup> described laboratory experiments which showed enhanced recovery by alkaline flooding through changing the reservoir from oil-wet to water-wet.

Cooke et al.<sup>22</sup>, however, observed that some

crude oils and porous media were converted from water-wet to oil-wet during alkaline flooding, providing a continuous wetting pathway for the otherwise trapped oil. At the same time an emulsion of water in oil due to the low IFT was formed, blocking flow, and thus creating a high pressure gradient which, in turn, is said to overcome capillary force and reduce residual oil saturation further.

The mechanism of interactions of oil, water and the rock phases may indeed vary from reservoir to reservoir. Yet in all situations, the lowering of oil-water interfacial tension is considered to be the necessary requirement for a successful recovery.

#### Interfacial Phenomenon

It is generally accepted that the formation of soap molecules from the interaction of alkali and the acids in the oil lowers the interfacial tension. Seifert et al.<sup>42,43</sup> had carried out thin layer chromatography-mass spectrometry identification of these acids<sup>44</sup>. The presence of straight-chain, polynuclear aromatic as well as naphtheno-aromatic structures was indicated. Molecular sizes ranging from 260 to 430 were observed, with the higher concentrations around C<sub>18</sub> and C<sub>19</sub> (see Table 2). This is also the ideal molecular size for many commercial soaps<sup>14,15</sup>. That also explains the lack of correlation reported<sup>46</sup> between interfacial activity or recovery magnitude and the acid number which is the alkali neutralizing capacity of the crude, because only the right size acids can form good soaps.

Dunning et al.<sup>45</sup> had claimed that porphyrins in the crude are

Table 2. High Resolution Mass Measurements of Carboxylic Acids from California Crude. (Ref. 44)

<u>Observed Mass</u>	<u>Formula</u>	<u>Calculated Mass</u>	<u>Mass Meas. Error, ppm</u>	<u>Relative Peak Height</u> *
264.1146	$C_{18}H_{16}O_2$	264.1150	-2	+
264.2086	$C_{17}H_{28}O_2$	264.2089	-1	++++
266.1309	$C_{18}H_{18}O_2$	266.1307	+1	+
266.2244	$C_{17}H_{30}O_2$	266.2246	-1	+++
268.1090	$C_{17}H_{16}O_3$	268.1099	-3	+
268.1462	$C_{18}H_{20}O_2$	268.1463	-0	+
268.2394	$C_{17}H_{32}O_2$	268.2402	-3	++
270.1267	$C_{17}H_{18}O_3$	270.1256	+4	+
270.1610	$C_{18}H_{22}O_2$	270.1620	-4	+++
270.2542	$C_{17}H_{34}O_2$	270.2559	-6	+
272.1765	$C_{18}H_{24}O_2$	272.1776	-4	+++
274.1010	$C_{19}H_{14}O_2$	274.0994	+6	+
274.1926	$C_{18}H_{26}O_2$	274.1933	-3	+++
276.1165	$C_{19}H_{16}O_2$	276.1150	+5	+
276.2081	$C_{18}H_{28}O_2$	276.2089	-3	++++
278.2239	$C_{18}H_{30}O_2$	278.2246	-3	
384.3035	$C_{26}H_{40}O_2$	384.3028	+2	
386.3177	$C_{26}H_{42}O_2$	386.3185	-2	
388.2401	$C_{27}H_{32}O_2$	388.2402	-0	
414.3128	$C_{27}H_{42}O_3$	414.3134	-1	
416.3650	$C_{28}H_{48}O_2$	416.3654	-1	
418.3789	$C_{28}H_{50}O_2$	418.3811	-5	
428.2697	$C_{30}H_{36}O_2$	428.2715	-4	

\* ++++ Represents the most intense peaks within a mass range of 14. Relative heights were measured only for those peaks so marked.

interfacially active. However, their activity under alkaline condition has not been studied.

Shah et al.<sup>47</sup> correlated minimum IFT with maximum electrophoretic mobility which reflects the increase in charge density of the oil surface by acid ionization. The  $pK_a$  values of these acids, however, have not been determined due to the pH difference between the bulk solution and the hard-to-measure interface.

Excessive alkali concentration was found to raise the IFT values. It has been suggested<sup>47</sup> that this may be the result of formation of undissociated soap of the acid, although no direct evidence was reported. Some investigators, on the other hand, suspected that the acids which introduced into the bulk aqueous solution, thereby depleting the surface of acids.

Salt has been found to help in enhanced oil recovery<sup>30</sup>. Jennings et al.<sup>38</sup> have observed that the presence of some NaCl reduces the alkali concentration required to achieve low IFT. A detailed study of the effects of a wide range of salt concentrations, however, has not been reported.

Divalent ions have been shown<sup>38</sup> to have detrimental effects on interfacial activity. Probably because of this reason, calcium and magnesium hydroxides were found to be ineffective in bringing about low IFT<sup>35</sup>.

DeZabala et al.<sup>48</sup> had developed a simple equilibrium chemical model to describe the observed interfacial activity. It was based only on the ionization of acids at alkaline pH. The equation developed was

$$(A^-) = \frac{(Na^+)}{1 + K/(HA)}$$

where interfacial activity, as represented by concentration of acid anion  $A^-$ , will be positively correlated to the sodium concentration and concentration of acids in the crude. Here the sodium concentration was used to represent the hydroxyl ion concentration. This model is far from being satisfactory because it fails to predict the effect of the presence of NaCl and the negative effect of excess NaOH.

## RESEARCH OBJECTIVES AND APPROACH

### General Chemical Characterization of Crude Oil

An understanding of the composition and chemical properties of crude oil is important to the development of recovery processes. Three crudes are studied: two from California and one from Arkansas. Fractionation of the crude according to the traditional classification of volatiles, gas oil, resin and asphaltene was carried out. Studies on components including suspected surfactants such as porphyrins.<sup>45</sup> were conducted.

### Characterization of Alkali Sensitive Interfacially Active Fraction from Crude Oil

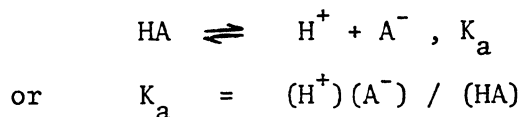
The active (judged by interfacial tension response in alkaline solution) components are isolated both by chromatographic separation based on polarity and by extraction with alkaline solution. These components are then chemically characterized to give information on their composition and structure (elemental analysis and infrared spectroscopy), molecular size (vapor pressure osmometry) and effects on certain physical properties of the crude.

### Development of an Equilibrium Chemical Model for the Observed Interfacial Phenomenon

In view of the inadequacy of the DeZabala model<sup>48</sup> mentioned in Chapter 2, a new chemical model is proposed. The existence of a minimum in the IFT versus alkali concentration curve calls for a deactivation of the interfacial activity by either excess  $\text{Na}^+$  or  $\text{OH}^-$ .

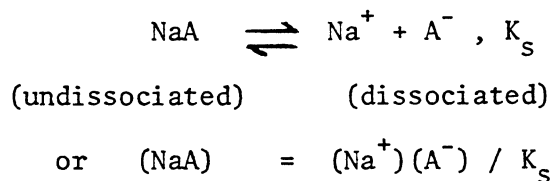
The observation by many investigators that a pure monocarboxylic acid also shows this kind of response suggested that excess  $\text{OH}^-$  cannot do anything to the already ionized acid species. In other words, it is probably the excessive  $\text{Na}^+$  which is detrimental to the interfacial activity.

Therefore we propose an equilibrium chemical model based on two competing reactions. The activation reaction is the ionization of the acids in the oil (represented here by a single species HA) to become the active  $\text{A}^-$  ion:



where concentrations within brackets are those at the interface.

The  $\text{A}^-$  may actually associate loosely with  $\text{Na}^+$  in the form of a dissociated soap molecule at the interface. The dissociated soap in turn is in equilibrium with an undissociated form of the soap:



The formation of undissociated soap, then, is the deactivation reaction which is competing with the activation reaction.

Two more equations can be written. They are the mass balance of the acid species,



where  $\text{HA}_0$  is the concentration of acids originally in the oil, and

water dissociation

$$(H^+) (OH^-) = K_w$$

Solving equations

$$(A^-) = \frac{HA_o}{\frac{(H^+)}{K_a} + \frac{(Na^+)}{K_s} + 1}$$

Now, consider the case in which NaCl is present. Then the sodium term can be split into sodium hydroxide derived sodium  $(Na^+)_{OH}$  and sodium chloride derived sodium  $(Na^+)_{Cl}$ . That is,

$$(A^-) = \frac{HA_o}{\frac{(H^+)}{K_a} + \frac{(Na^+)_{OH}}{K_s} + \frac{(Na^+)_{Cl}}{K_s} + 1}$$

The assumption is that the lowering of IFT is positively correlated to the interfacial concentration of  $A^-$ . IFT data was obtained to try to support the validity of this model on the interfacial activity of the crude.

The plan included isolating acids with distinctly different  $K_s$  values, showing that their interfacially activities are affected by  $(Na^+)$  differently. The model also predicts at high pH,  $(Na^+)_{OH}$  and  $(Na^+)_{Cl}$  should have the same effect on IFT. IFT measurements at various  $(Na^+)_{OH}$  and  $(Na^+)_{Cl}$  have been carried out to support this.

#### Enhancement of Interfacial Activity

The understanding that the interfacial activity probably relies on the presence of free organic acids in the crude leads to an attempt

to increase the amount of these available acids. The presence of organic acid-bearing compounds such as esters and amides has been shown by many investigators<sup>49,50,51</sup>. Also, the well-known presence of basic nitrogen compounds such as pyridine, indoline and hydroxycarbazole almost guarantees the existence of the base-acid associates through the interaction of these basic molecules with organic acids in the crude. Here studies have been made on the feasibility of liberating these acids from their derivatives in the crude by an acid catalyzed hydrolysis reaction. Dilute mineral acid solutions have been used to treat the crude and the resulting change in the IFT behavior was monitored. Samples containing pure model compounds such as esters (including fats) and amides have also been tested to support the theory.

Sand-packed core flooding experiments have been conducted to show the effectiveness of such acid treatment in enhancing oil recovery from a laboratory simulated reservoir.

## MATERIALS AND INSTRUMENTS USED

### Chemicals

- \*  $\text{MgSO}_4$ ,  $\text{MgCO}_3$ , sodium acetate, NaCl, NaOH pellets, pentane, toluene, methylene chloride and methanol (all analytical reagent grade)--Mallinckrodt Chemical Works.
- \* Compressed liquid propane--Manchester C. Tank.
- \* Oleic acid (99%), oleic acid-methyl ester (99%) and L- $\alpha$ -phosphatidyl choline or lecithin (60%)--Sigma Chemical Co.
- \* Methanesulfonic acid--Eastman Kodak Co.
- \* HCl and  $\text{H}_2\text{SO}_4$  concentrates, silica gel (60-200 mesh, for chromatographic use)--Baker Chemical Co.
- \* Sodium orthosilicate (wt ratio  $\text{SiO}_2/\text{Na}_2\text{O} = 3.22$ ; 41.0 Be)--PQ Corp., Valley Forge, PA.
- \* Ottawa sand (100 mesh)--Matheson Coleman & Bell Manufacturing Chemists.

### Analytical Instruments

- \* Spinning drop interfacial tensiometer, model 300--Chemistry Department, University of Texas, Austin.
- \* Pendent drop interfacial tensiometer--Petroleum Engineering Department, University of Southern California.
- \* Infrared Spectrophotometer, model Acculab 6--Beckman Instruments.

- \* Pump for core flood: Tubing pump, model 375A (max. flow rate 100 ml/hr)--Sage Instruments.
- \* Elemental Analysis--Hoffman Lab., Wheatridge, Colorado.
- \* Vapor pressure osmometer--Mechrolab Inc., Model 301
- \* Viscometer: HBT Wells--Brookfield Micro Viscometer--Brookfield Engineering Lab., Inc.
- \* Sample syringe for IFT measurement: Microliter 701 (10  $\mu$ l); Needle: gauge 26 (Type B)--Hamilton.
- \* Balance: Microbalance (0.1 mg-100 g)--Sartorius; Digital balance (0.1 g-200 g)--Fisher, Model 2000.
- \* Vacuum pump (duo-seal)--Welch, Model 1400.
- \* Rotary evaporator--Buchi Rotavapor-R
- \* Mass spectrometer--Chemistry Department, University of California, Los Angeles.
- \* Nuclear magnetic resonance (NMR)--Varian, Model T60

#### Crude Oils

Three oils were obtained in 1979 from the following sources:

- \* Aminoil, well S-47, Lower Main Zone, Huntington Beach Field, California (API 24).
- \* Thums, well C-331, Ranger Zone, Long Beach Field, California (API 22).
- \* Phillips Petroleum, well Hurt 4, Smackover Field, Nacatoch formation, Arkansas (API 26).

## EXPERIMENTAL PROCEDURES

### Interfacial Tension Measurement

Low interfacial tension (IFT) values of an oil-aqueous system were measured using a spinning drop interfacial tensiometer. The basic principle is to introduce a drop (about 2  $\mu$ l) of an oil sample into a glass capillary tube (1.5 mm I.D., 78 mm long) filled with the aqueous medium. The tube is then spun about its main axis. The oil drop will elongate to a length determined by the IFT value of the system. Details of the theory can be found elsewhere<sup>52</sup>. According to the manufacturer, the formula used to calculate low IFT values is

$$\text{IFT(dyne/cm)} = 1.234 \frac{(\Delta d)^3 \Delta \rho}{p^2}$$

where  $\Delta d$  = the thickness of the elongated oil drop in cm;

$\Delta \rho$  = density difference between the oil and the aqueous phase in gm/ml;

$p$  = period of spinning in sec.

The oil sample was first loaded into a micro syringe fitted with a needle which has an inner diameter large enough to let the viscous oil go through under normal pressure. Then a drop of the oil sample was introduced through the needle vertically upward into the center interior of the glass capillary tube which was filled with the aqueous solution under study. The needle was withdrawn fast to break

off any hanging drop at the tip. The tube was then capped and placed in the spinning chamber which then spun the tube about its main axis at the chosen speed. In my studies, a spinning speed of around 125 revolutions/second was used. The console of the tensiometer would show the spinning period in milliseconds. A strobe light synchronized to the spinning speed was used to facilitate reading of the oil drop dimension (thickness) through a calibrated microscope. A picture of the operation steps is shown in Figure 2. All oil sample drops, whether they are raw crudes or toluene solutions, take some time (the crude takes several minutes, and dilute toluene solution takes about 30 seconds) to reach their equilibrium, which is also the minimum thickness. A time study of the spinning crude oil sample is shown in Figure 3. The corresponding IFT value will be referred to as the IFT for the given oil-aqueous interface.

Between runs, the capillary tube was flushed with distilled water a few times and preflushed with the next aqueous medium. Between samples, the inside of the syringe and needle were cleaned by flushing with toluene, and dried by passing compressed air through for at least one minute.

High IFT values (greater than 10 dyne/cm), such as in the case of no activity, were determined by the pendent drop method which involves the measurement of the dimensions of the hanging drop. It was done by the Petroleum Engineering Department of the University of Southern California, and therefore details will not be discussed here.

#### Vacuum Distillation of Crude Oil

In order to preserve the components in the crude, vacuum distil-

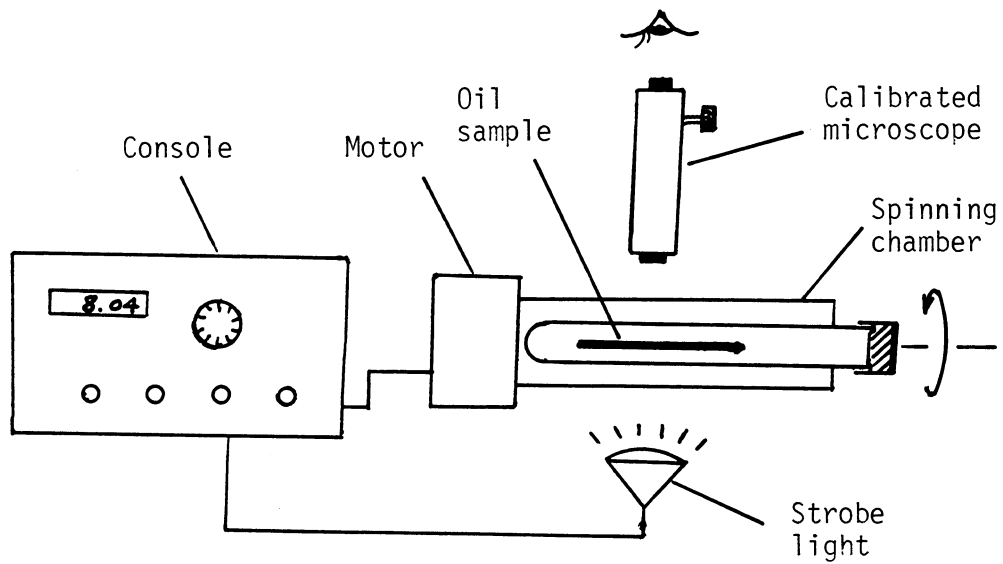
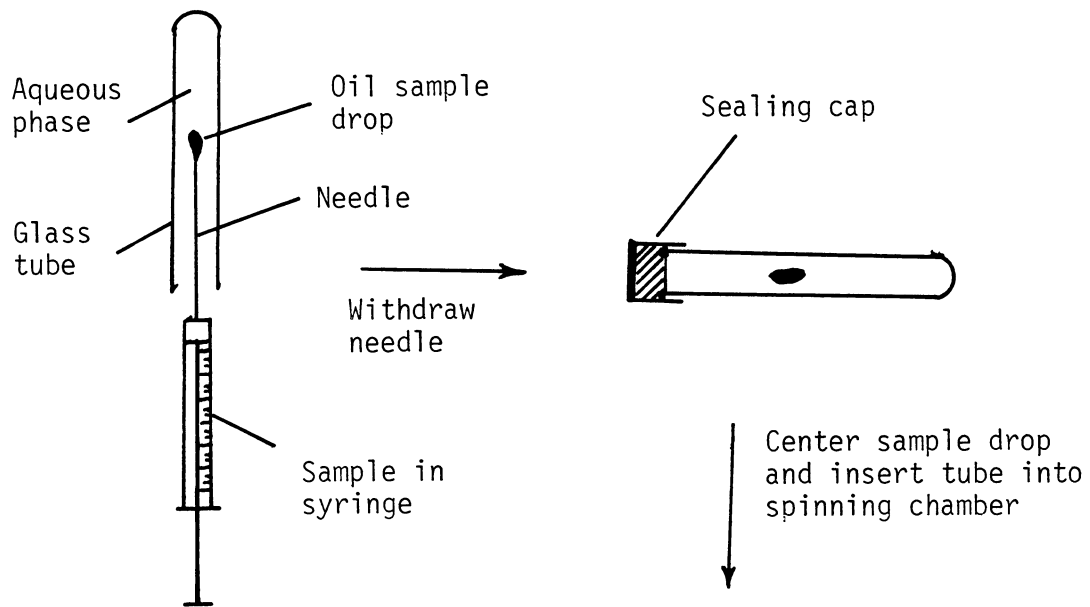


Figure 2. Operation Procedure of Interfacial Tension Measurement using a Spinning Drop Interfacial Tensiometer.

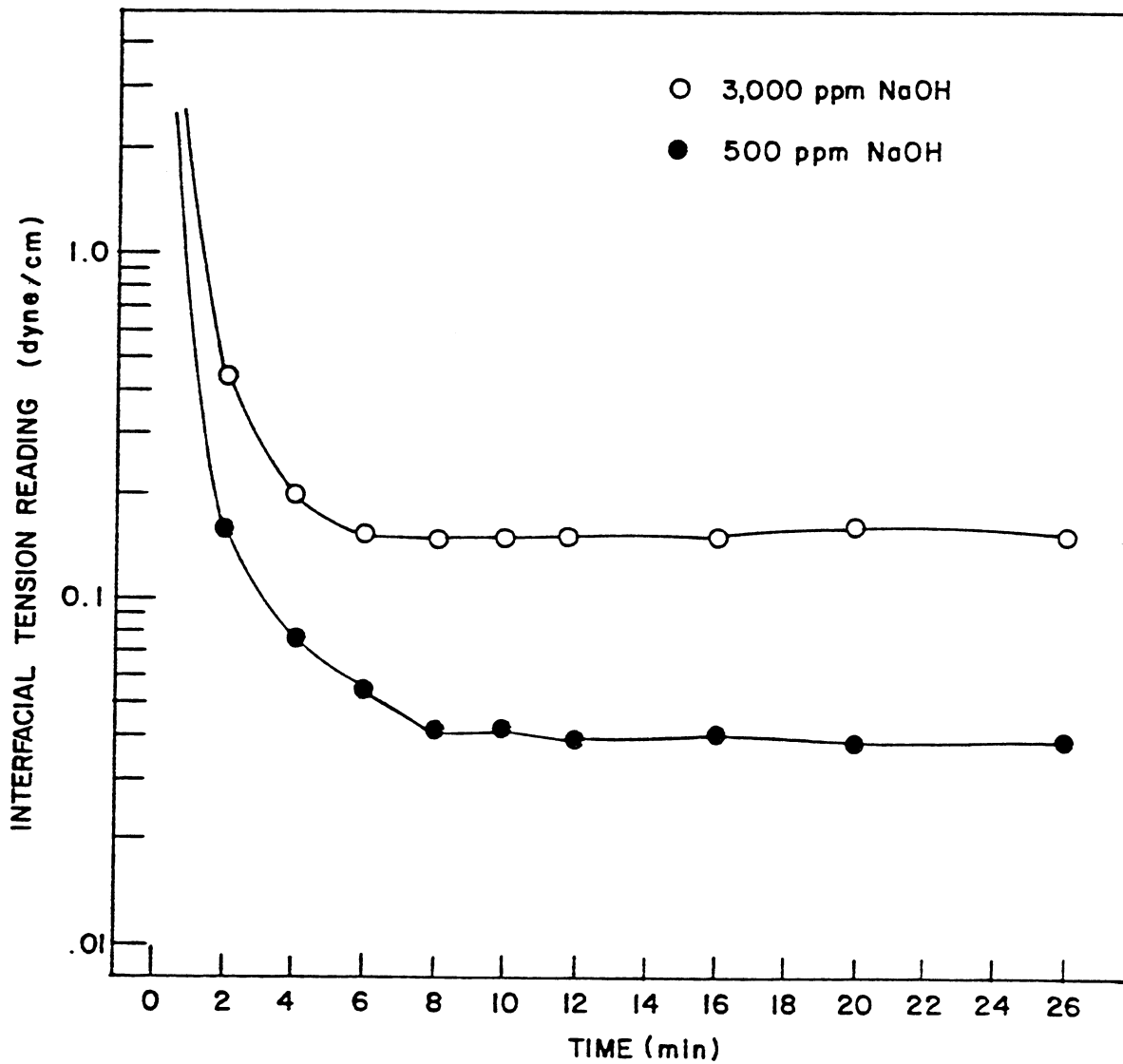


Figure 3. Interfacial Tension versus Time of a Spinning Crude Oil Sample Drop in Alkaline Solution.

lation was used to reduce the risk of high temperature cracking and oxidation. Therefore standard API distillation was not attempted.

A vacuum jacketed glass column (3 cm I.D., 45 cm Ht) was packed with spherical glass beads of 4 mm in diameter. It was connected to a head with adjustable reflux ratio. The system was connected to a vacuum pump. A liquid nitrogen cold trap was put between the pump and the system to prevent volatile vapor from contaminating the pump. The pot (2 liter size) was immersed in a silicone oil bath which was heated by heating electrical wire submerged in the oil. The distillate was condensed by cold running water and collected by a receiving flask which was cooled by ice. A schematic of the setup is shown in Figure 4.

To calibrate the column, the binary system of methylcyclohexane (boiling point  $101^{\circ}\text{C}$ ) and toluene (boiling point  $110.6^{\circ}\text{C}$ ) was picked because it is a common system to use for columns with around ten theoretical plates.

In order to quickly analyze the composition of samples from the binary mixture, a physical method was devised. It was done by making use of the fact that the refractive index of the binary mixture differs with different composition. It was found that with increasing mole fraction of toluene, the refractive index increases almost linearly. Such a calibration curve is shown in Figure 5. With data on the composition of samples from the pot and the distillate at total reflux, one was able to determine the number of theoretical plates in the column by a graphical method on the vapor-liquid equilibrium curve of the system. Subsequent distillation of the methylcyclohexane-toluene system at a reflux ratio of 10 yielded results shown in Figure 6, indicating that

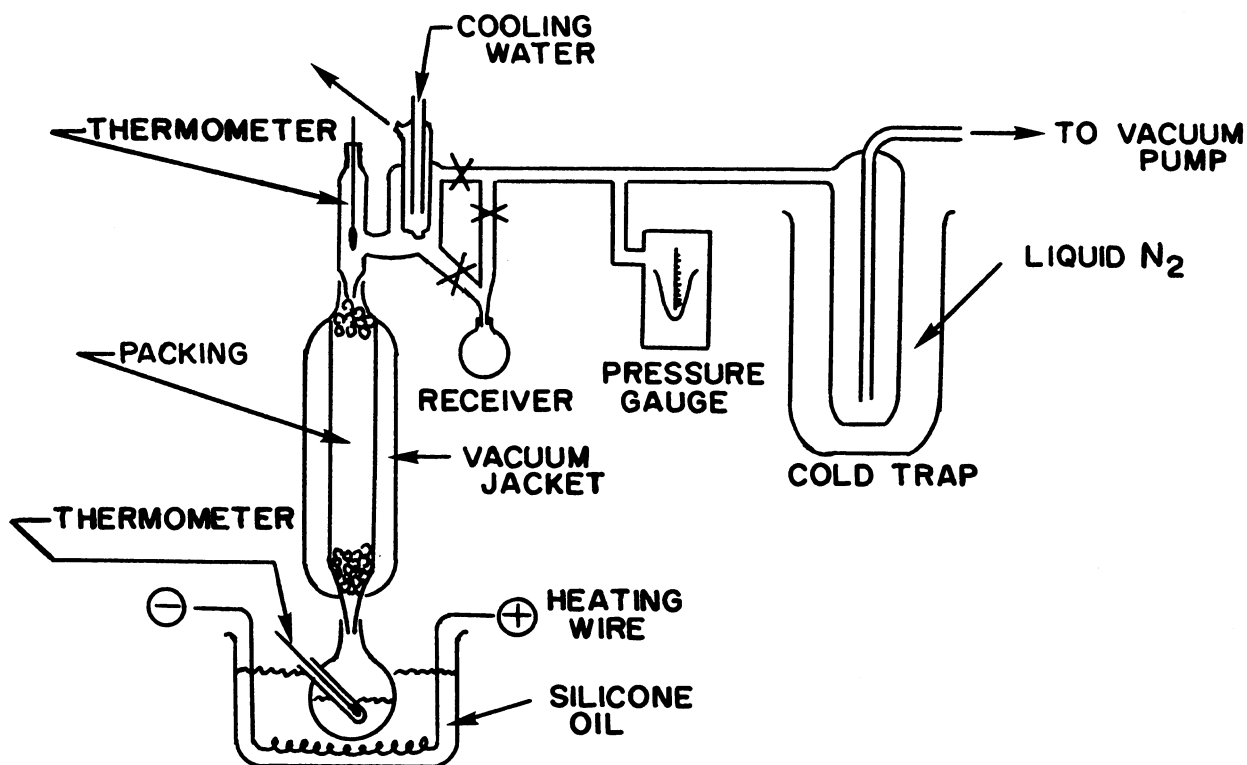


Figure 4 Schematic Diagram of Vacuum Distillation Setup.

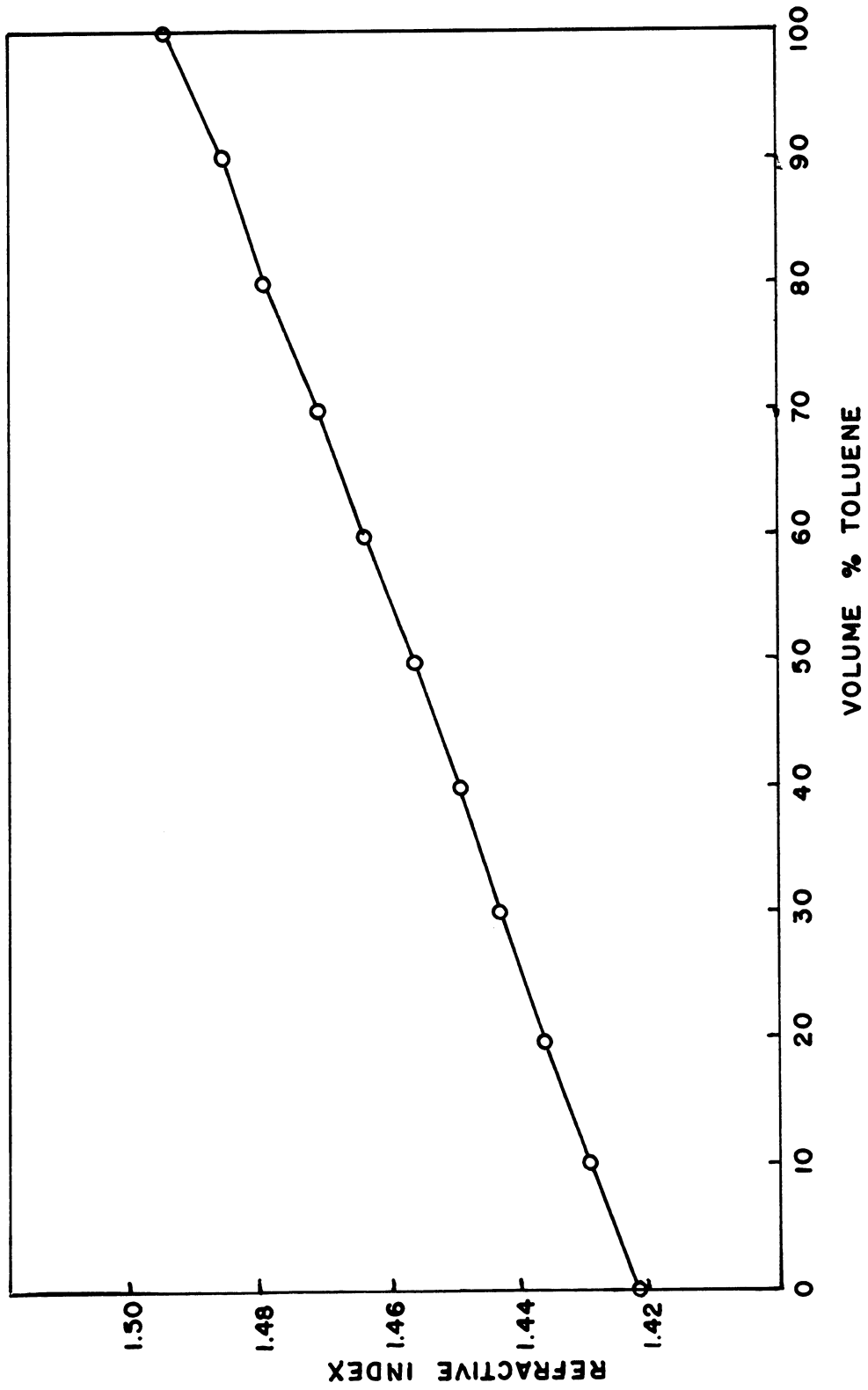


Figure 5 Calibration Curve of Refractive Index versus Composition of a Binary Mixture of Methylcyclohexane and Toluene.

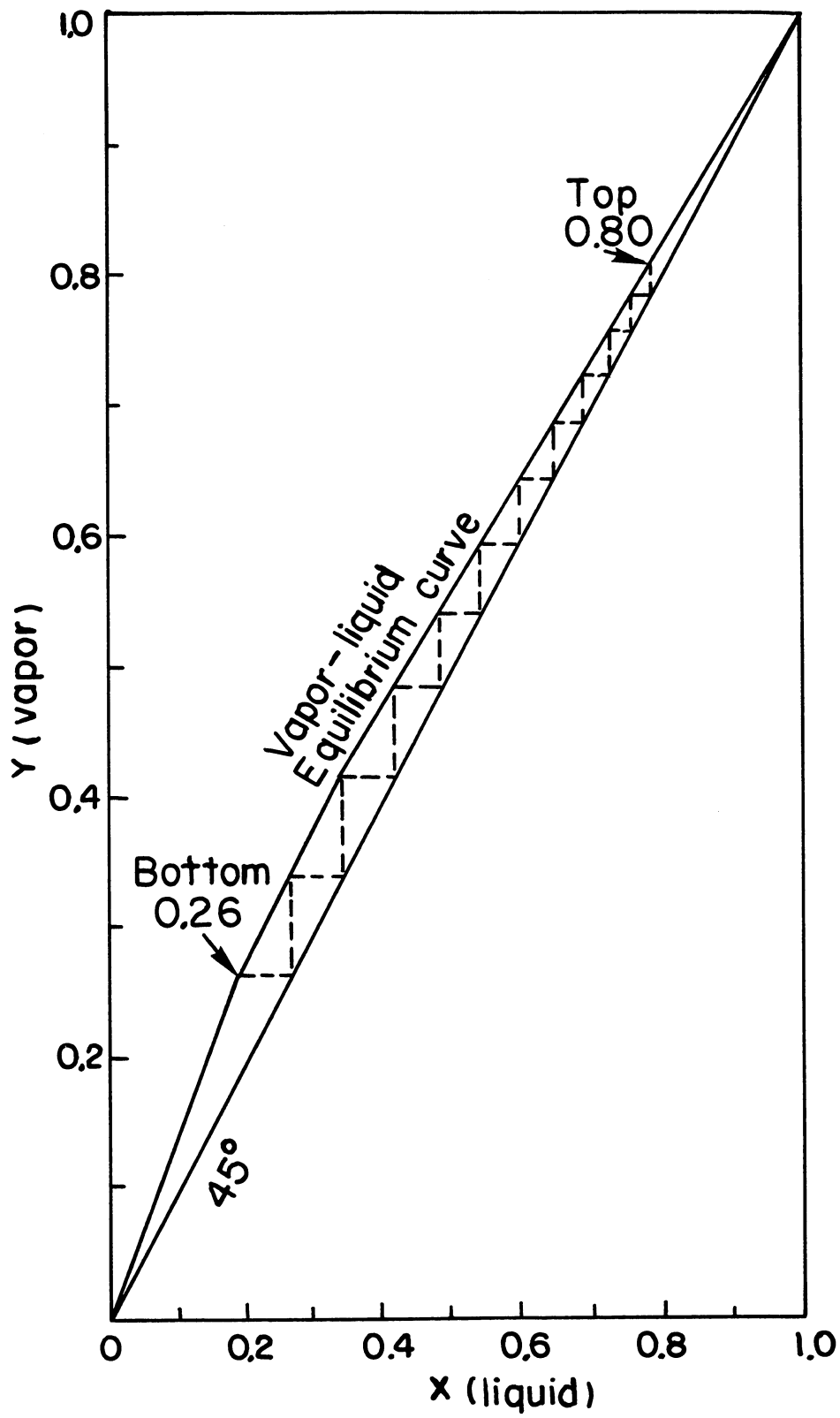


Figure 6. Graphical Determination of the Number of Theoretical Plates in a Packed Glass Bead Column. All Concentrations are Mole Fractions of Methylcyclohexane in a Mixture with Toluene.

the packed column has 11 theoretical plates when calibrated at atmospheric pressure with the above system.

Finally, when distillation of crude oil was carried out using the set up described above, a vacuum of 0.05 mm Hg was achieved. The volatiles started coming out around an overhead temperature of 28°C, and were collected up to 80°C. Throughout the distillation, the pot temperature was maintained at less than 210°C, and air was let into the system only after everything had been cooled down to room temperature. The clear distillate is defined as the volatiles, and the dark viscous materials remaining in the pot as the nonvolatiles.

#### Isolation of Pigments from the Volatiles

The pigment material could be extracted by adsorbing on an adsorbant such as  $\text{CaCO}_3$ ,  $\text{MgSO}_4$ , or  $\text{MgCO}_3$ , washed with a nonpolar solvent such as hexane, and finally eluted out using a polar solvent such as acetone. In the case of Long Beach volatiles, since the pigment, on sitting for days, settled and stuck to the bottom of the glass container, it could be recovered in the same manner as above except that the glass container surface took the place of the adsorbants. The pigment isolated was then dried under vacuum at room temperature.

#### Solvent Fractionation of the Nonvolatiles

The nonvolatiles obtained from the vacuum distillation of the crude were further fractionated according to the following method into gas oil (propane soluble), resin (propane insoluble, pentane soluble) and asphaltene (pentane insoluble, toluene soluble):

One hundred grams of the crude nonvolatiles was dissolved in

100 ml of toluene. The solution was added slowly with stirring into 4,000 ml of pentane. The final solution was poured through thimbles to filter off the insoluble material. The insolubles were then Soxhlet extracted with more fresh pentane overnight. The pentane soluble portions were then combined and dried by stripping off the pentane in a rotary evaporator. This fraction is the gas oil-resin mixture, or called oil-resin. Because no preasphaltene (toluene insoluble) was found in the crude studied, the pentane insoluble material remaining in the thimble after the Soxhlet extraction is the asphaltene. The asphaltene can now be dried by rotary evaporation followed by freeze drying under vacuum.

One hundred grams of the oil-resin mixture was then put into a one liter stainless steel bomb. The bomb was cooled with dry ice, and filled to half full with compressed liquid propane. The sealed bomb was shaken gently overnight using an automatic shaker. At the end of the reaction, the bomb was allowed to sit in a position with one of the two outlets facing down vertically. The resin portion, which is propane insoluble, would settle to the bottom of the bomb and thus come out first as solid when the outlet was opened. A small amount of propane liquid would come out together with the resin but would evaporate off rapidly. When no more solid resin was coming out, liquid propane solution containing the gas oil would exit. The propane evaporated off rapidly at room temperature and pressure, leaving the gas oil which is a dark liquid.

#### Fractionation by Polarity

An oil sample may be fractionated based on polarity difference

using silica gel chromatography. Silica gel (60-200 mesh) was first activated by drying at 120°C for 24 hours. After cooling down to room temperature, 4 weight percent distilled water was added to the gel drop by drop with intermittent shaking. The moistened gel was kept in a stoppered flask overnight to let the moisture equilibrate through the gel. The prepared gel must be used within a few days before it absorbs too much moisture from the air.

A gel-hexane slurry was prepared. It was then loaded little by little into a 1.5" diameter glass column half filled with hexane. By eluting the hexane at the same time the slurry was being added, the gel was packed in place forming a column. A final gel column of 5" high was packed. Ottawa sand was then layered on top of the gel to a thickness of half an inch, while the whole thing was still under solvent level. A diagram of the setup is shown in Figure 7. When an oil sample was ready to be run, the level was lowered to just beneath the top sand surface by draining out excess solvent at the bottom outlet of the column. The sample, which was usually less than 3 grams of oil dissolved in minimum amount of toluene, was added onto the top. By draining again, the sample body was drawn into the sand packing. Several one-mls size hexane were added and drained similarly. At this point, all of the oil sample had passed the sand packing into the gel part. One may now add large quantities of hexane on top to continuously elute the column. The elution rate in our case is about 2 drops every second. At no time during column use should the solvent level be allowed to fall below the gel surface. In other words, the gel, once packed, should be submerged in solvent at all times. The

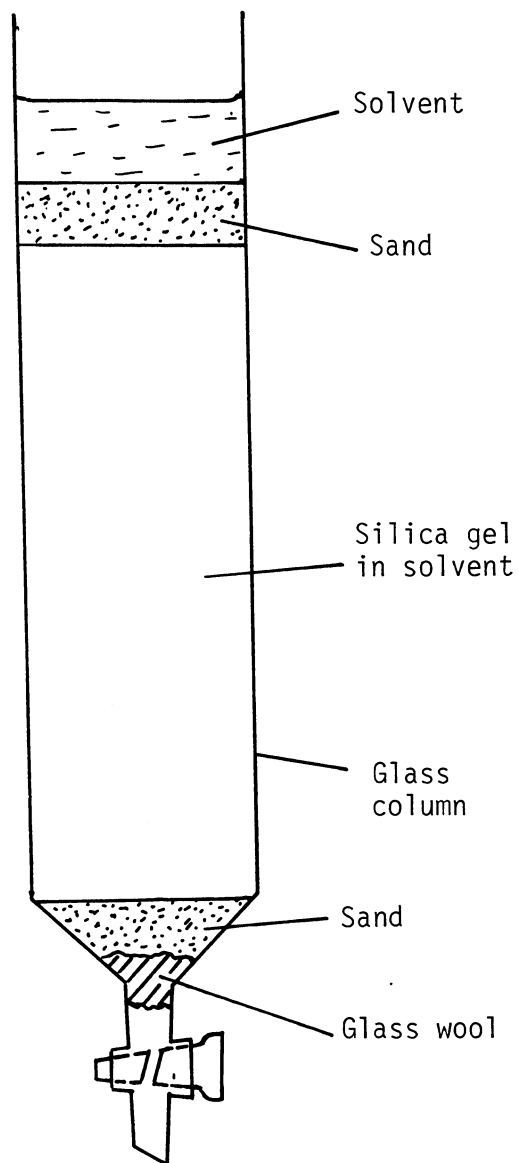


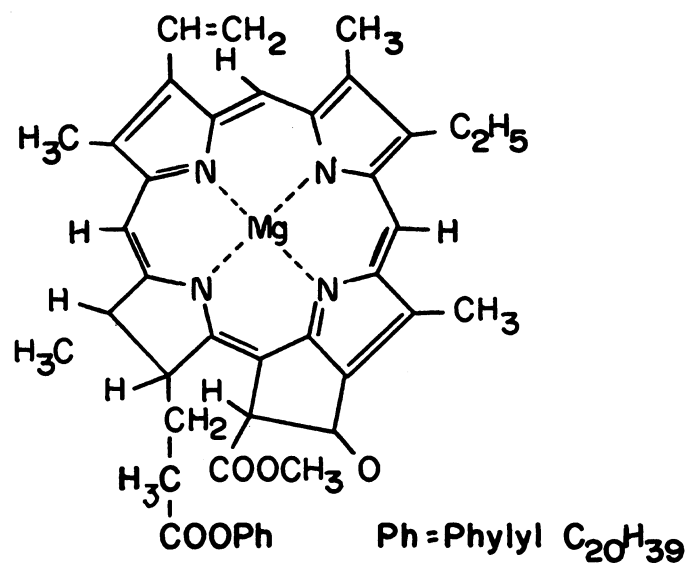
Figure 7. Diagram of a Silica Gel Column for Chromatography Use.

collected hexane eluted fraction, which is judged visually by its yellow color, was called Fraction 1. After elution of Fraction 1 is finished, i.e., hexane coming out is no longer yellow, the solvent level was again lowered to the sand surface and toluene was added in place of hexane. A second brownish fraction was then eluted out with toluene, and is called Fraction 2. The remaining portion of the sample was finally eluted out with a 3:1 toluene:methanol mixture which removed practically all the rest of the oil sample from the silica gel column. This final dark brown fraction is called Fraction 3. The gel column, after the toluene-methanol elution, cannot be reused, and was therefore discarded. Solvents were stripped off from Fractions 1, 2, and 3 using a rotary evaporator. Fraction 3 was further dried by freeze drying under vacuum. Typically a 7:2:1 ratio of Fractions 1, 2, and 3 would be obtained.

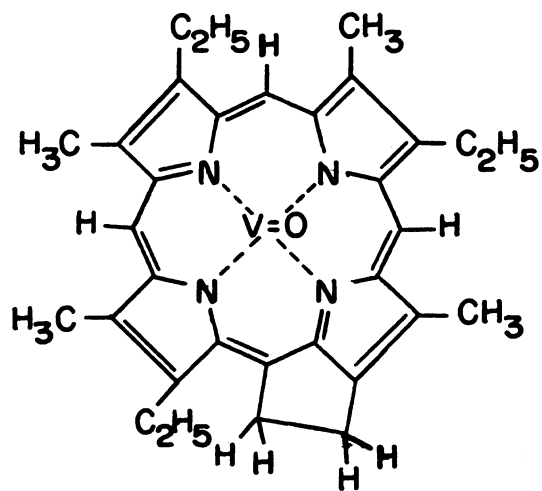
For the crudes studied, after drying, Fraction 1 was a light orange liquid; Fraction 2 was an extremely viscous dark material; and Fraction 3 was a dark asphalt-like solid. Since polarity of the eluting solvent increases from one to the next, Fraction 1 is nonpolar, Fraction 2 is slightly more polar, and Fraction 3 is the most polar portion of the crude.

#### Isolation of Porphyrins

All porphyrins have the basic macrocyclic structure composed of carbon, hydrogen and nitrogen atoms. They are believed to originate from chlorophylls which share the same basic ring skeleton. A comparison of the two structures is shown in Figure 8. In nature the porphyrins have a metal in the center of the ring, usually vanadium or nickel.



**Chlorophyll a**



**Vanadyl DPEP**

Figure 8. Structure of Chlorophyll a and Vanadyl DPEP.

The metal-porphyrins can be obtained from an oil sample by simply running the sample through a silica gel column as described in previous sections. They will fall into the toluene eluted fraction. Their presence and their metal type can be identified by their characteristic absorption in the visible wavelengths.

The metal-free porphyrin base was extracted by following a modified version of Erdman's method<sup>53</sup>. Thirty grams of crude (or any nonvolatile fraction) was mixed with about 100 grams of methane-sulfonic acid in a 250 ml flask. The mixture was shaken vigorously for 2 minutes to obtain a fairly homogeneous emulsion. It was then immediately put in a 110°C oil bath and stirred continuously to prevent layer separation of the oil and aqueous phases. After five hours of incubation, crushed ice was added to make up the volume to 400 ml. This stopped the reaction. The mixture was then filtered by suction through two layers of filter paper to remove the oil sludge. The pink acid filtrate which contained the porphyrin base was washed in a separatory funnel with fresh toluene repeatedly until the toluene became only very light yellow. The acid-dissolved porphyrins were then extracted into methylene chloride. The methylene chloride was then adjusted to neutral pH by shaking with a sodium acetate solution. It was dried by stirring with anhydrous magnesium sulfate overnight followed by filtration. After stripping off the volatile methylene chloride, the crude porphyrin sample was passed through a silica gel column as described previously. Reasonably pure porphyrin base would come out as red band during toluene elution. These base types could be identified both by their characteristic visible absorption spectrum and by mass spectrum.

### Molecular Weight Measurement

A vapor pressure osmometer (VPO) was used to measure molecular weights (MW). It was based on the depression of vapor pressure,  $P$ , of the solvent in the presence of some relatively less volatile solute. The  $\Delta P$  which is measured in terms of  $\Delta T$ , the temperature difference between the solvent drop and the sample drop, is then proportional to the molarity  $n$  by the Ideal Gas Law. For a given volume (constant drop size) and a known solute weight in the sample,  $n$  is equal to weight divided by the molecular weight. Therefore  $\Delta T$  will be proportional to  $1/MW$ .

By using benzil (MW = 210.2) as standard, a calibration curve of  $\Delta T$  versus different known molar concentrations (from 5 to 30 g/l) in each chosen solvent was plotted. For polar samples, tetrahydrofuran (THF) was the solvent used to break up association. Other samples were measured in benzene. For each solvent system, the slope of the calibration curve (normally a straight line) gave the proportionality constant between  $\Delta T$  and  $n$ . In this case the constants for benzene and THF were 309.59 and 367.9, respectively.

Samples with a known weight concentration of the solute, a measured  $\Delta T$ , which corresponded to a certain  $n$  from the calibration curve, gave the molecular weight of the solute. In this study, molecular weight measurement of a least three samples with different solute concentrations were run, and the MW versus concentration plot was extrapolated to zero concentration which gave the molecular weight of an association-free monomer.

### Bulk Viscosity Measurement

A Brookfield microviscometer (cone and plate type) was used. It

was found from working with the instrument that using enough sample (about 1 to 2 cc) to cover the rim of the cone piece gave the most reproducible result. The shear rate used depended on the range of viscosity the sample had. Eight different shear rates are available covering the appropriate viscosity range. If possible, measurements at two different shear rates were done for each sample to confirm viscosity data.

#### Density Measurement of Liquid Sample

A small glass container (about 1.8 cc) with a ground glass stopper was used to carry the liquid sample. The capillary in the center of the stopper allowed excess sample to escape when the stopper was capped onto the sample container. The set up is shown in Figure 9. A container filled with the sample and another container of the same size filled with distilled water (density = 1 g/l) were weighed. The ratio of the two weights gave the sample density in gram per ml.

#### Infrared Absorption Measurement

A double-beamed infrared (IR) spectrophotometer was used. For liquid samples, null salt discs were used to hold the sample film. For solid samples, either a film was spread onto the salt disc surface by first dissolving the sample in a volatile solvent such as carbon tetrachloride which was then evaporated off the solvent from the top of the salt disc, or a solid KBr compressed disc containing 2 mg/250mg KBr was used. In all cases air was used as a reference.

#### Sand-Packed Core Flooding Experiments

A sand-packed column was used to simulate a porous medium such as

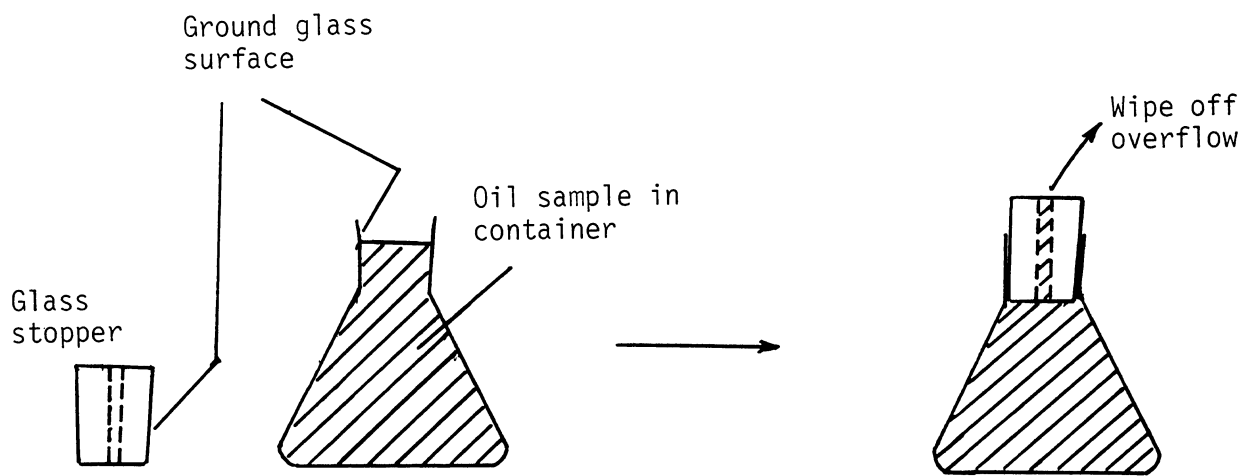


Figure 9. Equipment Used for Density Measurement of Liquid Sample.

an oil reservoir. Each core was a piece of 12" long, 1" I.D. lucite tubing fitted on each end with a 500-mesh metal screen both to hold the sand in and help even out fluid distribution. Each end was then plugged with a lucite disc sealed with a rubber O-ring. The plugs were fitted with Swagelock adaptors for 1/8" tubings. Reinforced plastic tubings were then fitted onto both ends of the core, one leading to the source pump and the other to the collector. Pressure gauges (0 to 100 psi) were placed on the ends of the core to monitor pressure drop readings. The pump worked by exerting peristaltic compression on the soft carrier tubing from the feed reservoir. The entire set up is shown in Figure 10. The sand was packed vertically while beating on the outside of the column to effect even packing.

The packed core was then evacuated with a vacuum pump, and saline solution (7,500 ppm NaCl, which is the salt concentration present in all aqueous flooding solutions used in this study) was sucked in gradually to fill up the space created by the vacuum. The difference in weight before and after water infiltration divided by the solution density gave the pore volume of the column.

For oil recovery runs, the crude was first put in the feed reservoir, and pumped into the horizontal saline-filled packed core at a rate of 10 ml/hr, which was the flooding rate used for all runs. During this initial oil saturation, the core was rotated 180° about its main axis every two hours to effect even oil front movement. When no more water came out (judged visually), oil saturation was complete. The volume of water displaced gave the volume of oil held in the core.

Secondary water flooding was then carried out by flooding the oil saturated core with saline solution until no more oil came out (water

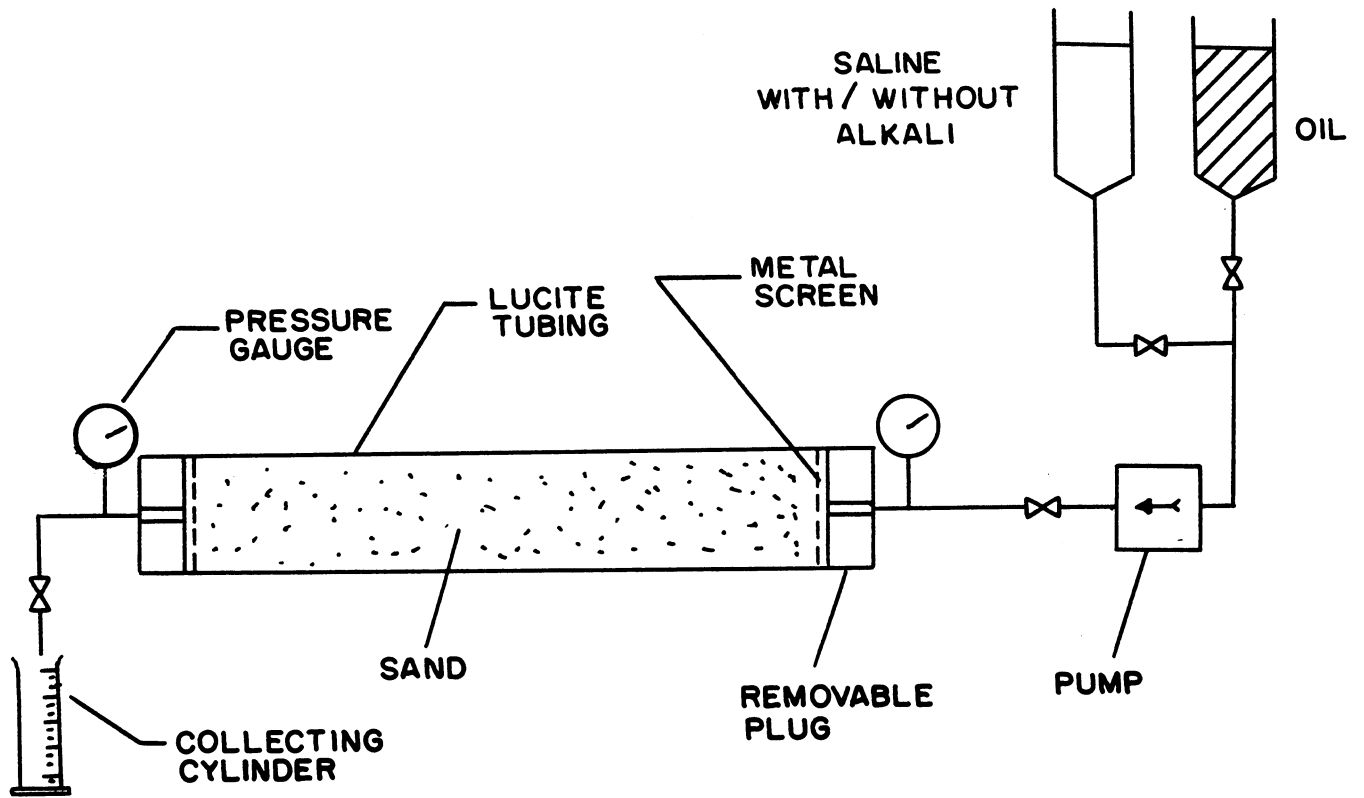


Figure 10. Schematic Diagram of Core Flood Apparatus.

to oil ratio greater than 50). The difference between the amount of oil held in the core before the secondary water flooding and the amount of oil displaced gave the amount of residual oil after the secondary water flooding. This constituted the residual oil saturation value which the later alkaline flooding tertiary enhanced oil recovery percentages were based upon. After the water flood, the core was ready for flooding with any test solution for enhanced oil recovery.

In order to find the effective alkali concentrations to use, different cores were flooded with sodium orthosilicate solutions of different concentrations, and recovery percentages were compared.

To test the effects of acid pretreatment on alkaline flooding enhanced oil recovery, two sets of experiments were carried out with cores packed with sand which were predigested with 0.2N HCl for 48 hours followed by rinsing with water. Predigestion was to eliminate possibility of enhanced oil recovery due to increased packing porosity from acid digestion. The experiments are outlined as follows:

- (i) A round of regular alkaline flooding (250 followed by 500 and 3,000 ppm alkali, flooded at each concentration until oil was no longer recovered); then the cores was rinse-flooded with four pore volumes of saline solution followed by acid flooding with four pore volumes of 0.2N HCl solution. Finally, the core was rinse-flooded again as described above, and a second round of regular alkaline flooding was carried out.
- (ii) Acid flooding with four pore volumes of 0.2N HCl solution, rinse-flooded with saline, followed by

a round of the above described regular alkaline flooding procedure.

The rinse-flooding with saline solution served to reduce residual acid or base to minimize consumption of incoming base and acid respectively.

Eluent from the core was collected using graduated cylinders. Because some of the oil was sticking to the wall of the cylinder, natural separation by gravity of the oil and water was not enough to allow simple reading of volumes. A method was devised to overcome this problem. It was done by adding a known volume of toluene to the oil-water mixture. Toluene is not miscible with water. With slight stirring, the toluene would pick up the oil remaining on the glass wall, which resulted with a clean separation between the top oil layer (sample oil plus toluene) and the bottom aqueous phase. Volumes were then read off easily from the graduation. A controlled experiment with known volumes of toluene, oil and water showed that the volumes were additive on mixing, and loss of toluene from evaporation was negligible.

#### Extraction of Soap-Forming Acids by Alkali

This is based on the fact that sodium salt molecules formed

by the reaction between sodium hydroxide and acids in the oil sample are insoluble in the oil phase. In other words, the acid salts or soap will either be dissolved in the alkaline solution or exist as insoluble precipitate suspended in the aqueous solution. Extraction was done by vigorously shaking a 2:1 mixture of 10,000 ppm NaOH solution was then centrifuged at 2,000 rpm for 3 minutes to separate the phases. Three phases were obtained, the top oil layer, a middle white precipitate (acid salts) and the bottom turbid alkaline aqueous solution which also contained some dissolved acid salt. The oil layer was carefully transferred to another test tube to repeat the extraction with fresh alkaline solution. Extraction was repeated until no suspended materials were visible.

The precipitate-plus-aqueous portions were combined, centrifuged for another 3 minutes, and washed gently on the top with a small amount of benzene. The aqueous phase was then drawn out and placed in a separatory funnel. Diluted HCl solution was added to bring the pH to slightly acidic. At this point, the dissolved acid salt was converted back to acid form. Shaking with methylene chloride would then extract all the acids into the organic phase. The methylene chloride was then stripped off by blowing nitrogen over it, and the final acid extract was dried in a vacuum.

The acid salt precipitate from the alkali extraction was mixed with distilled water, acidified and similarly extracted with methylene chloride.

#### Acid Treatment of Oil

An oil sample was repeatedly treated with fresh 0.2N HCl by

shaking a 2:1 oil-aqueous mixture in a test tube followed by centrifugation for 3 minutes at 2,000 rpm. Every time the aqueous phase was drawn out and combined. Treatment of the oil phase was repeated until no yellow tint was present in the aqueous acid phase. The combined aqueous portion, which presumably contained dissolved organic bases, was extracted with methylene chloride and dried in a vacuum.

## RESULTS AND DISCUSSION

### Definition of Interfacial Activity

In my analysis, a sample is said to be interfacially active if it displays an interfacial tension (IFT) value of 0.1 dyne/cm or less in aqueous solutions containing alkali concentrations up to 10,000 ppm. In the absence of alkali, the Huntington Beach Crude, Long Beach Crude and Arkansas Crude show IFT values of 21, 26, and 16 dyne/cm, respectively.

### Reliability of Interfacial Tension Data

Reliable and reproducible IFT data is very important to this study. Because crude oil is a complex mixture composed of thousands of different compounds, homogeneity variation between sample drops is always a concern. Despite this, IFT measurements taken of drops of the same sample yielded reproducible equilibrium IFT values. Results of five separate runs of the sample are shown in Figure 11. It is noticed that data scattering is more significant towards the lower end of the alkali concentration range. But the overall scattering falls within 10% of the mean value, which is considered good enough for the logarithmic scale IFT response.

### Comparison of Sodium Hydroxide and Sodium Orthosilicate in Interfacial Behavior

As far as IFT is concerned, fresh sodium hydroxide and sodium orthosilicate with the same NaOH concentration have practically the same pH. They, as expected, showed identical effects on the IFT of the

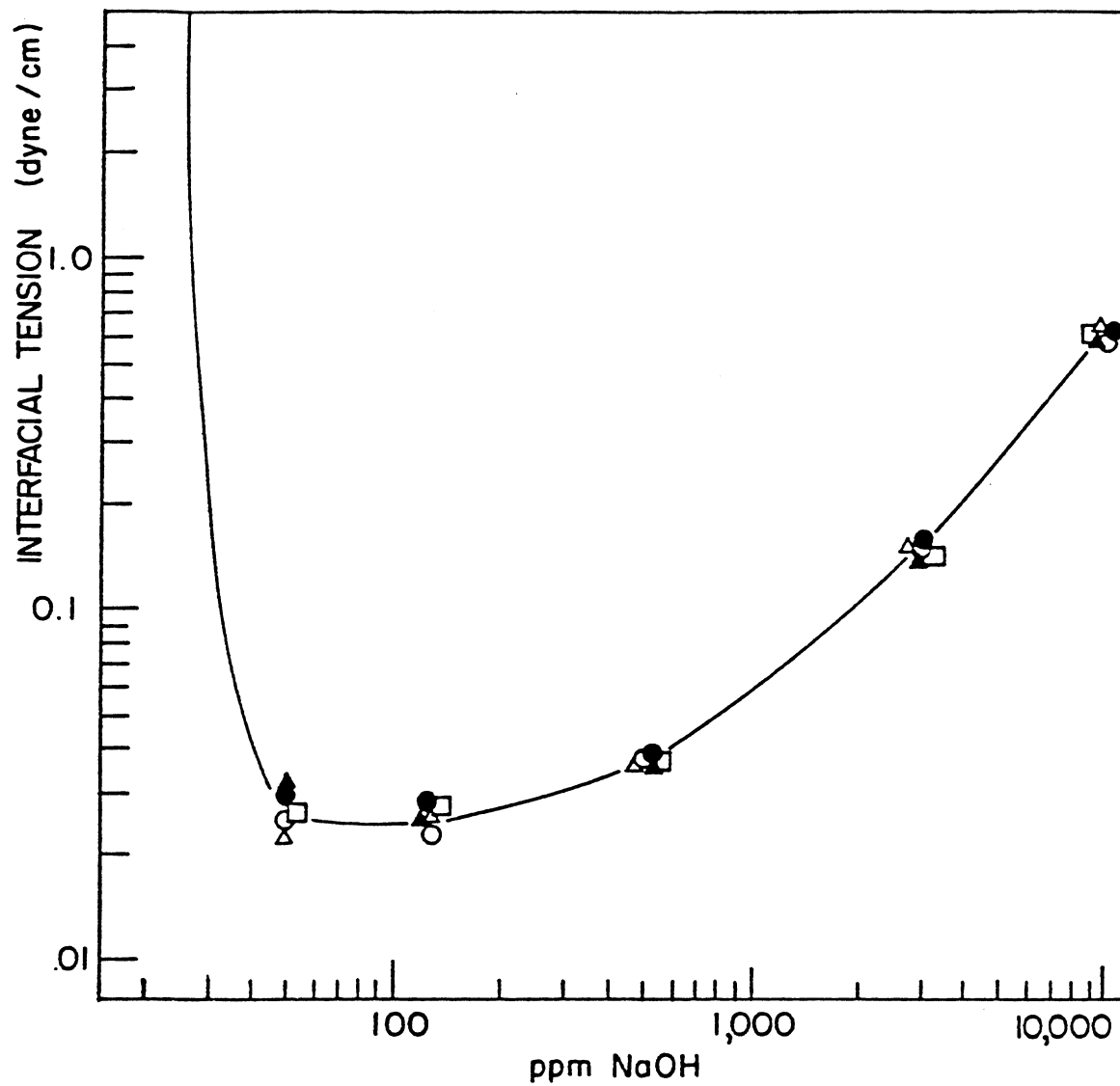


Figure 11. Interfacial Activity of Long Beach Crude Measured in Five Separate Runs.

crude oils (Figure 12). Sodium orthosilicate, being a buffered solution of sodium hydroxide, does have the advantage of resisting pH change caused by carbon dioxide in the air. Table 3 shows the pH values corresponding to different alkali concentrations and their stability with storage time. Therefore, for convenience reasons, sodium orthosilicate solution was used in all my IFT measurements because it eliminated the need to prepare fresh sodium hydroxide solutions each time for IFT measurement. As a result, data are more reproducible. Solutions containing low alkali concentrations such as 125 ppm or below, however, need to be prepared fresh to be safe. For simplicity alkali concentrations are labelled ppm NaOH rather than sodium orthosilicate on the IFT response graphs given in this report.

#### Characterization of the Volatiles and Nonvolatiles of Crude Oil

As the result of the vacuum distillation and solvent fractionation, the percentage breakdown of the crude into volatiles and nonvolatiles, and the nonvolatiles into gas oil, resin and asphaltene for the three crudes used are shown in Table 4. The Arkansas crude, which is a lighter oil than the two California crudes, surprisingly showed a lower volatile percentage. However, it also showed a lower asphaltene content, supporting the belief that the asphaltene content, rather than the volatile content, is primarily responsible for the apparent "lightness" of a crude.

The volatile fraction was a clear liquid with a strong smell of hydrogen sulfide. In the two California crudes, the volatile cut changed from light yellow right after distillation to pink on storage (stored in the dark in nitrogen in a refrigerator, but presence of

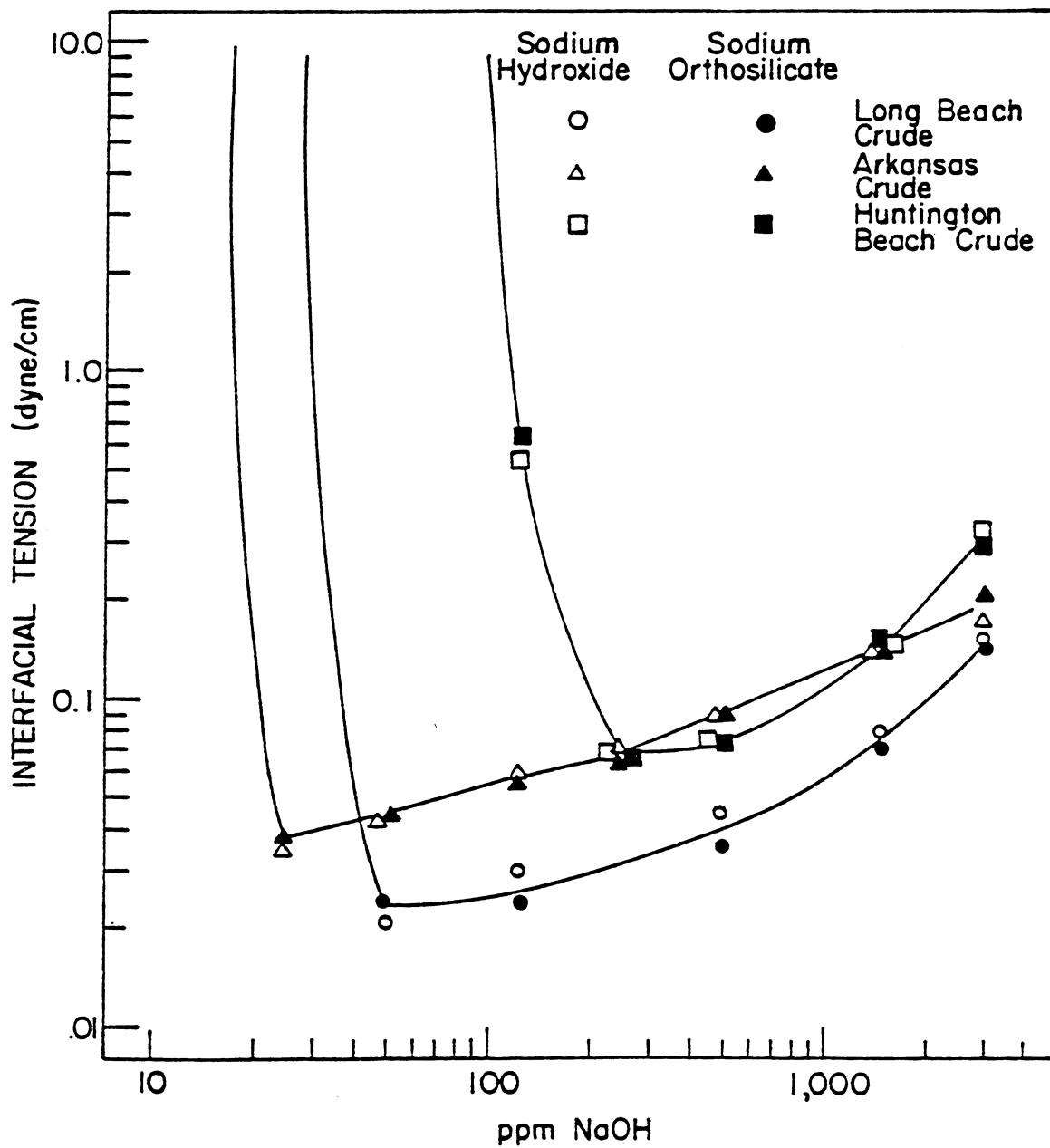


Figure 12. A Comparison of the Effects of Sodium Hydroxide and Sodium Orthosilicate on the Interfacial Activity of the Three Crude Oils.

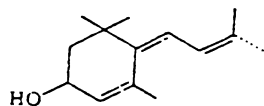
Table 3. The pH Values of Alkaline Solutions and their Stability with Storage Time. Stored in half-filled bottles. Solutions contain 7,500 ppm NaCl.

<u>Alkali Concentration (ppm)</u>	<u>pH</u>			
	<u>Sodium Hydroxide</u>		<u>Sodium Orthosilicate</u>	
	<u>Fresh</u>	<u>After 2 weeks</u>	<u>Fresh</u>	<u>After 2 weeks</u>
5	9.1	7.2	9.1	8.9
12.5	10.0	8.0	9.9	9.6
25	10.3	8.2	10.2	10.0
50	10.7	8.25	10.6	10.4
125	11.3	8.5	11.1	10.9
250	11.6	9.0	11.4	11.3
500	11.8	11.6	11.6	11.5
1,500	12.0	12.0	12.0	12.0
3,000	12.2	12.2	12.3	12.3
10,000	12.5	12.5	12.5	12.5
50,000	13.1	13.1	13.1	13.1

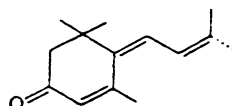
Table 4. Weight Percentage Breakdown of Cuts from Crude Oils

<u>Cut</u>	<u>Separation Definition</u>	<u>Weight, %</u>		
		<u>Huntington Beach</u>	<u>Long Beach</u>	<u>Arkansas</u>
Volatiles	0.05 mm Hg overhead 80°C	32.5	26.7	17.2
Nonvolatiles				
Gas oil	Propane soluble	41.7	57.6	63.7
Resin	Pentane soluble	10.4	10.2	9.5
Asphaltene	Toluene soluble	10.7	5.8	3.9

oxygen is guaranteed due to frequent opening of the container). The pink color darkened faster with exposure to air and sunlight. These pigment materials were isolated according to the procedure outlined in Chapter 5. Dried samples were analyzed by mass spectroscopy (MS). The spectra of pigments from the two crudes are shown in Figures 13 and 14, respectively. They showed the MS pattern of carotenoids<sup>54</sup>. High resolution MS identified a few major peaks to be fragments containing one oxygen atom (see Table 5). This coincides with the composition of a very common class of carotenoid end groups with the following structures:



(a)



(b)

Furthermore, the oxidation<sup>48</sup> of the hydroxy form (a) which is yellow to the keto form (b) which is red is consistent with the color change observed. Examples of carotenoids with such end groups are lutein and zeaxanthin<sup>55</sup> which are extremely common in animals, algae, and plants, the kind of materials that petroleum is believed to originate from. Their structures are shown in Figure 15.

Volatiles from the Arkansas crude did not show any color, and are therefore believed to contain no such carotenoids.

The study of the presence of certain groups of pigments in the crude could be useful for petroleum exploration and recovery because these molecules could be used as biomarkers in studying the age, origin, maturation and migration of the crude.

A typical proton nuclear magnetic resonance (nmr) spectrum is

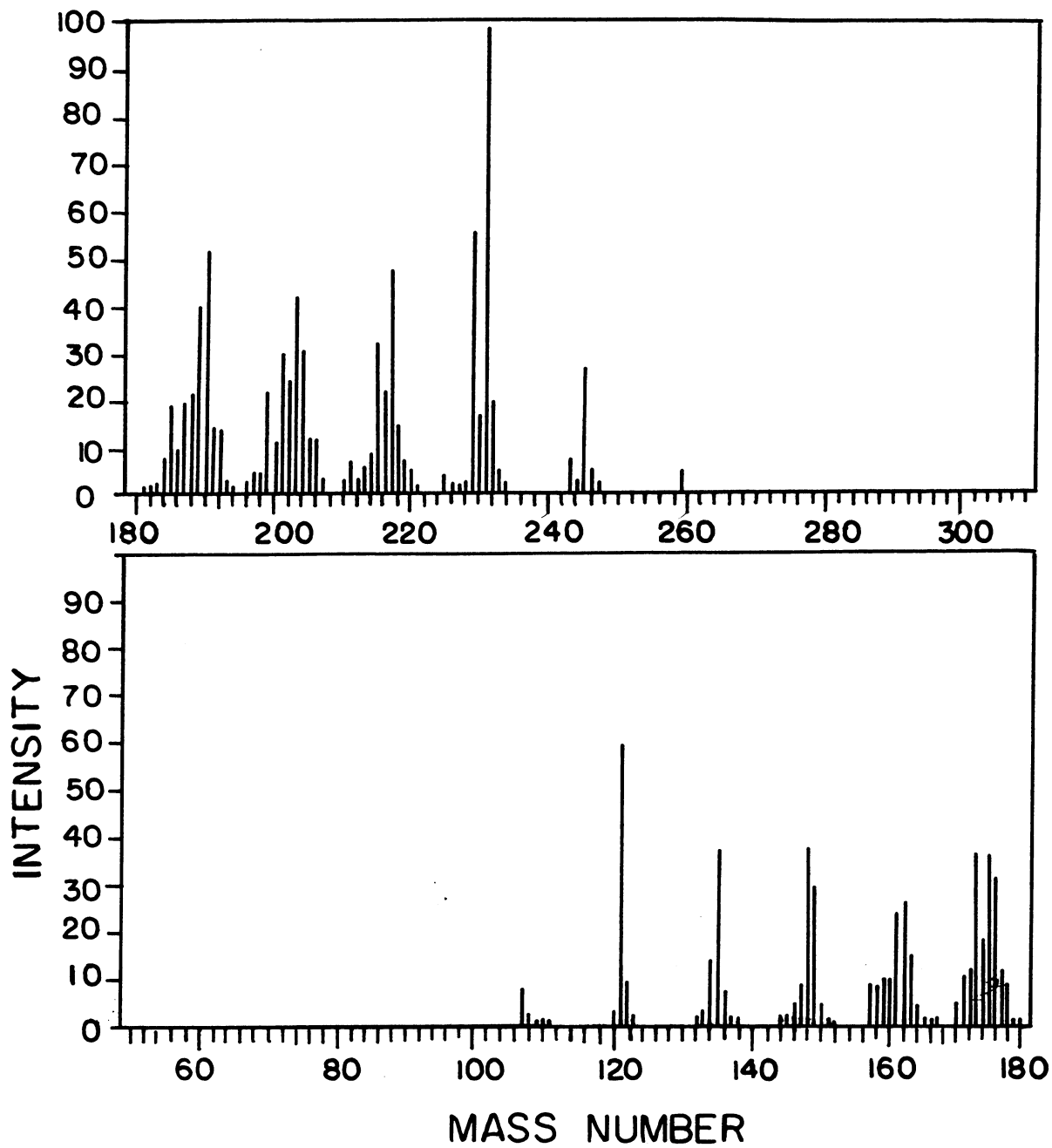


Figure 13. Mass Spectrum of Pink Pigment from Long Beach Crude, 12 ev., 180°C.

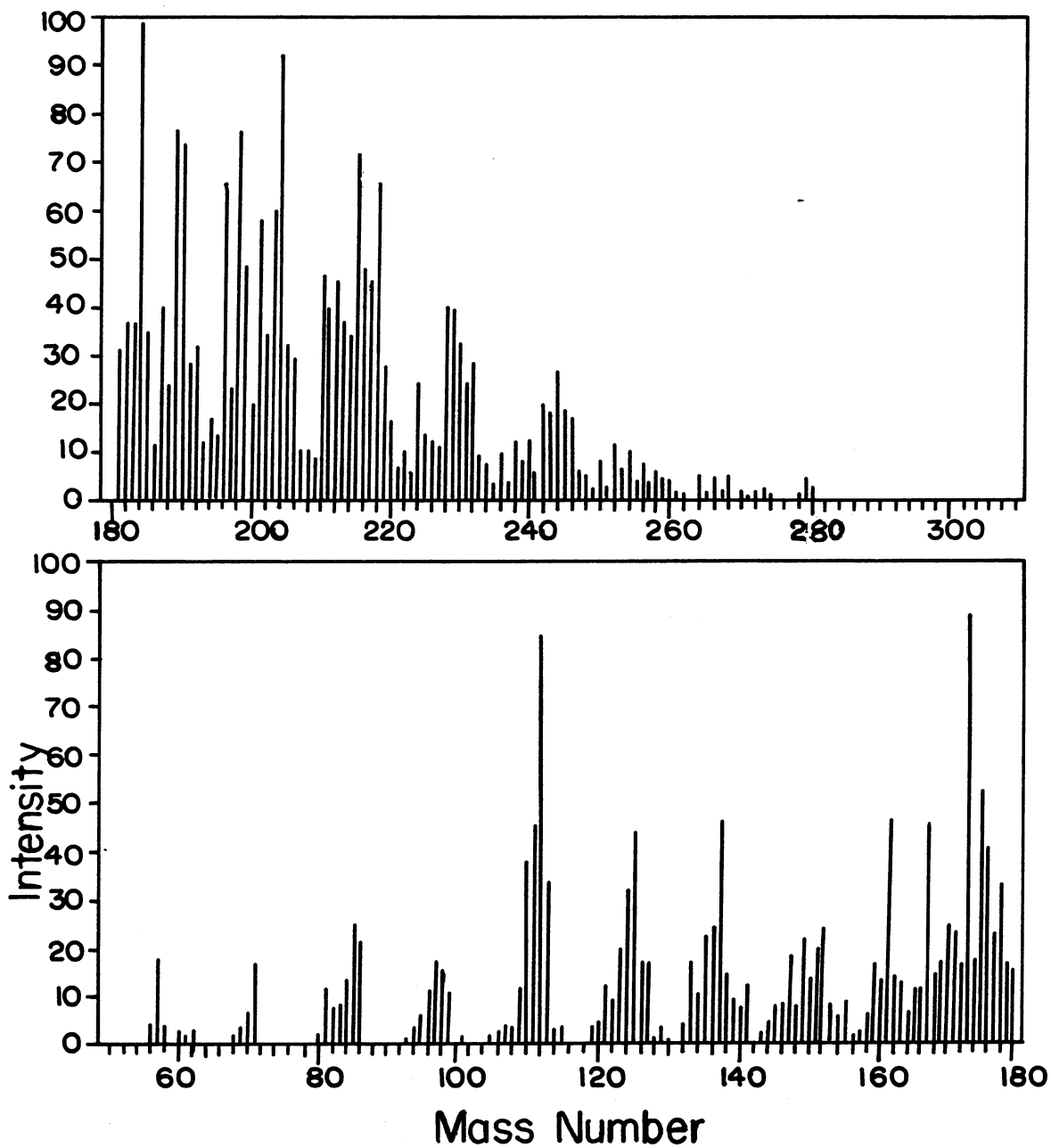


Figure 14. Mass Spectrum of Pink Pigment from Huntington Beach Crude. 12 ev., 180°C.

Table 5. High Resolution Mass Spectroscopic Identification of Carotenoid Fragments from Crude Oil, 12 ev., 180°C.

<u>Measured Mass of Peak</u>	<u>Closest Matching</u>	
	<u>Formula</u>	<u>Mass</u>
111.072	C <sub>7</sub> H <sub>11</sub> O	111.081
137.090	C <sub>9</sub> H <sub>13</sub> O	137.097
181.156	C <sub>12</sub> H <sub>21</sub> O	181.159
190.139	C <sub>13</sub> H <sub>18</sub> O	190.136

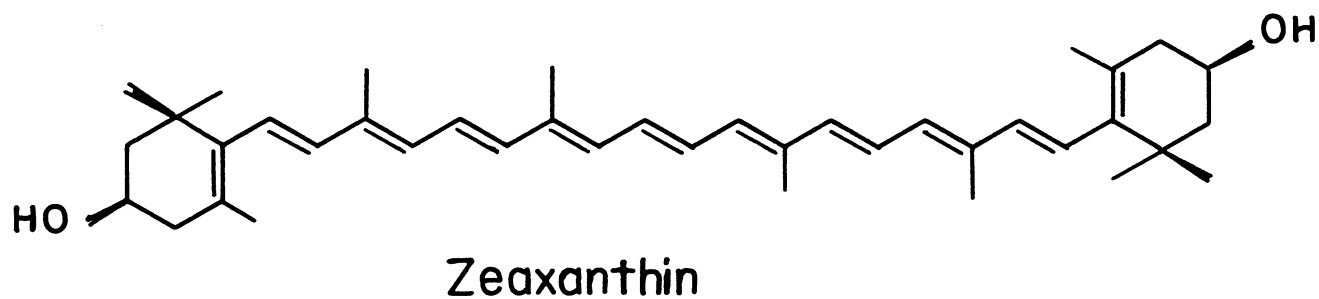
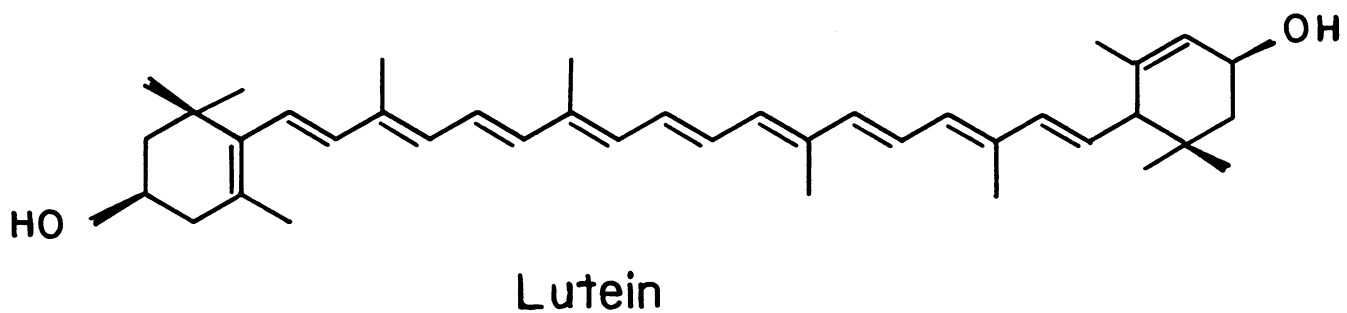


Figure 15. Structures of Two Carotenoids: Lutein and Zeaxanthin.

shown in Figure 16. Analyses of the aromatic proton to aliphatic protons, protons adjacent to heteroatoms and terminal methyl groups are done. The asphaltene, showing the highest proportion of protons adjacent to heteroatoms, obviously has the most heteroatoms, i.e., atoms other than hydrogen and carbon. The molecular weight, and chain length which is estimated by the ratio of middle chain proton to terminal methyl proton, also increases down the nonvolatile list. The results are summarized in Table 6.

IFT measurements of these cuts in alkaline solutions showed that the volatiles are not active, and all activities are distributed among the nonvolatiles. The IFT response of the oil-resin, as expected, is very close to that of the crude. They are shown in Figures 17, 18, and 19, respectively for the three crudes.

Also noticed was that the three showed very similar response with respect to alkali concentration range except the Arkansas oil has a slightly lower onset alkali concentration. Therefore in the rest of the experiments, only the Long Beach crude was studied in detail.

#### Concentration of Activity: Fraction 3 and its Characterization

As the result of silica gel column chromatography, each crude was broken down into three fractions: Fraction 1 which is hexane eluted, Fraction 2 which is toluene eluted, and Fraction 3 which is toluene-methanol eluted. The weight percentage breakdown and average molecular weights of the three fractions for the three crudes are listed in Table 7. Fraction 3, the smallest (about 8%) but heaviest (largest MW) fraction in the crude, was found to be the only fraction that showed activity. Because it is an asphalt-like solid, it was

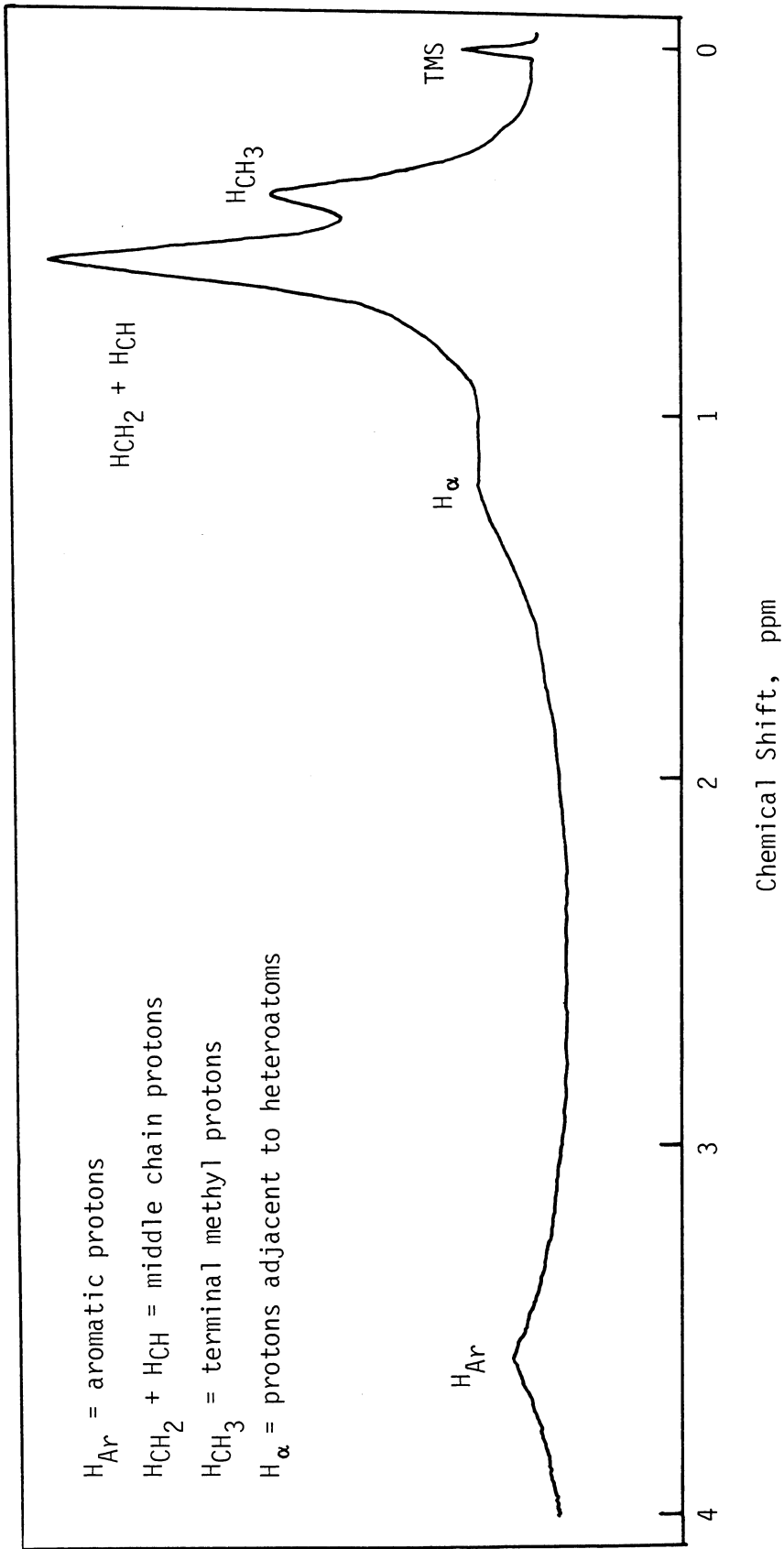


Figure 16. A Typical Proton Nuclear Magnetic Resonance Spectrum of an Oil Sample.

Table 6. NMR Structural Characterization of Long Beach Cuts

<u>Fraction</u>	$\frac{H_{Ar}}{H_0}$ *	$\frac{H_a}{H_0}$	$\frac{(H_{CH_2} + H_{CH})}{H_{CH_3}}$	Molecular Weight **
Volatiles	0.023	0.116	1.64	206
Gas Oil-Resin	0.050	0.158	2.08	461
Asphaltene	0.049	0.222	2.31	2,740

---


$$* H_0 = H_{Ar} + H_{CH} + H_{CH_2} + H_{CH_3} + H_a$$

\*\* THF used as solvent for VPO.

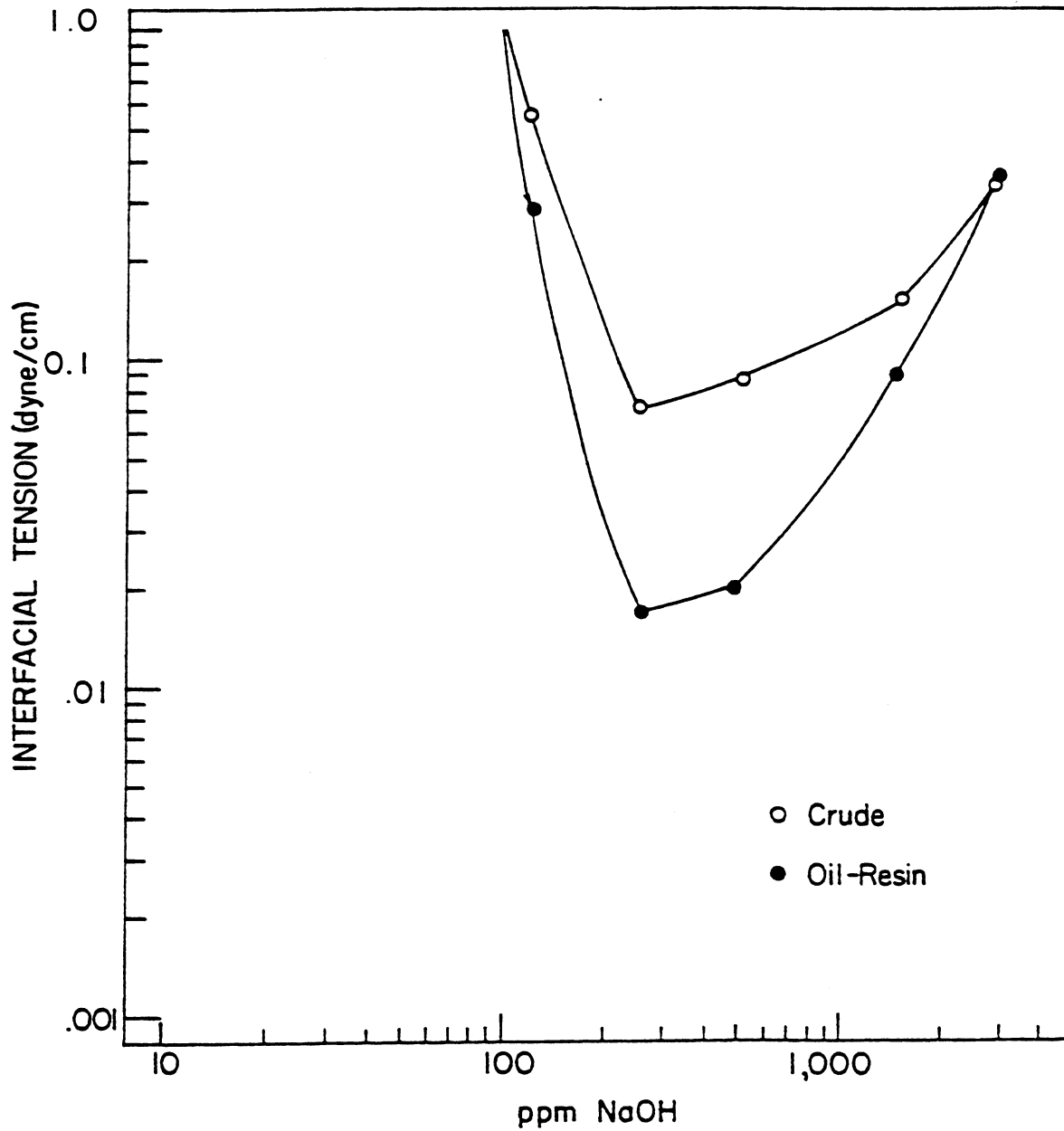


Figure 17. Interfacial Activity of Huntington Beach Crude and its Oil-Resin.

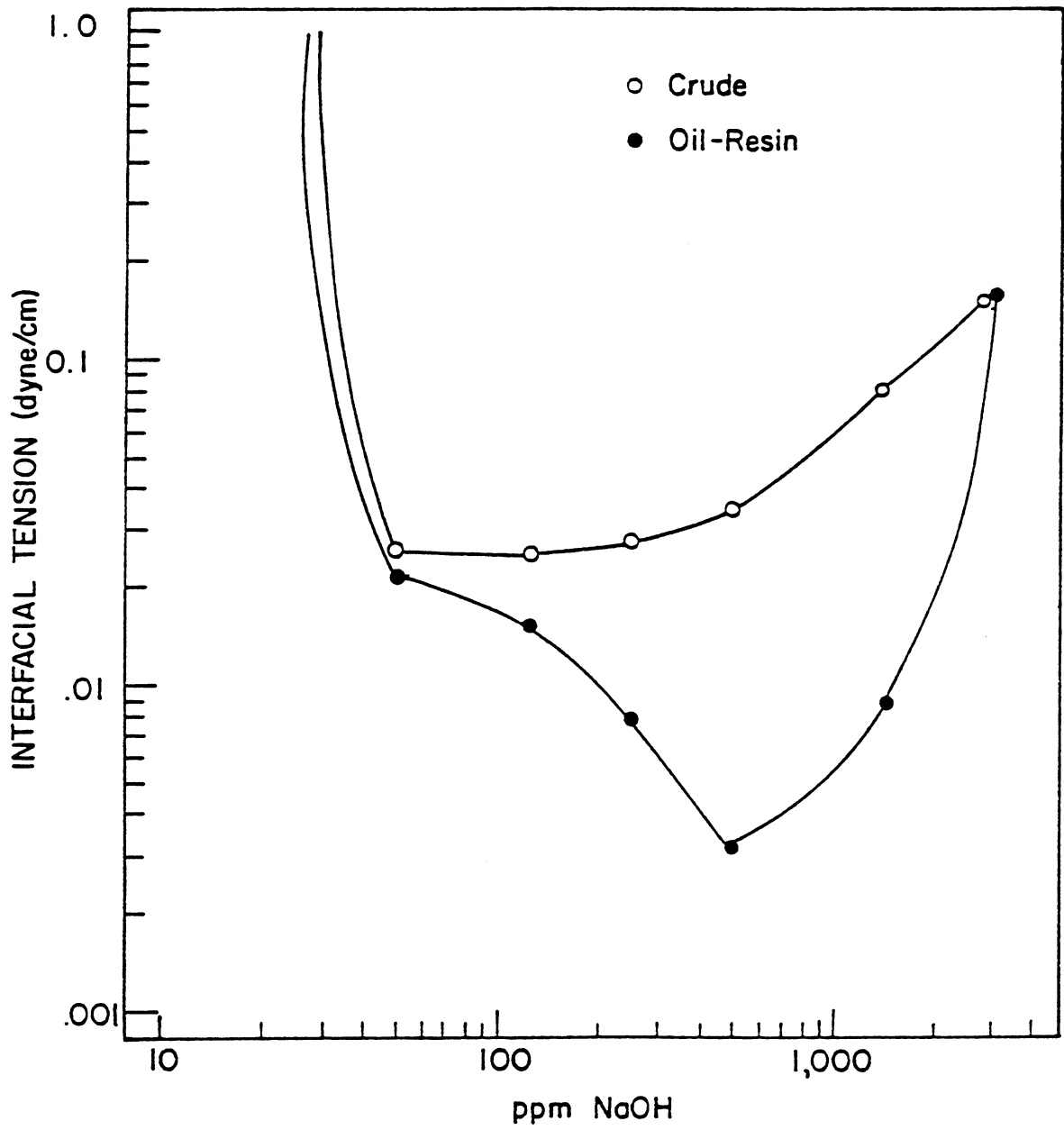


Figure 18. Interfacial Activity of Long Beach Crude and its Oil-Resin.

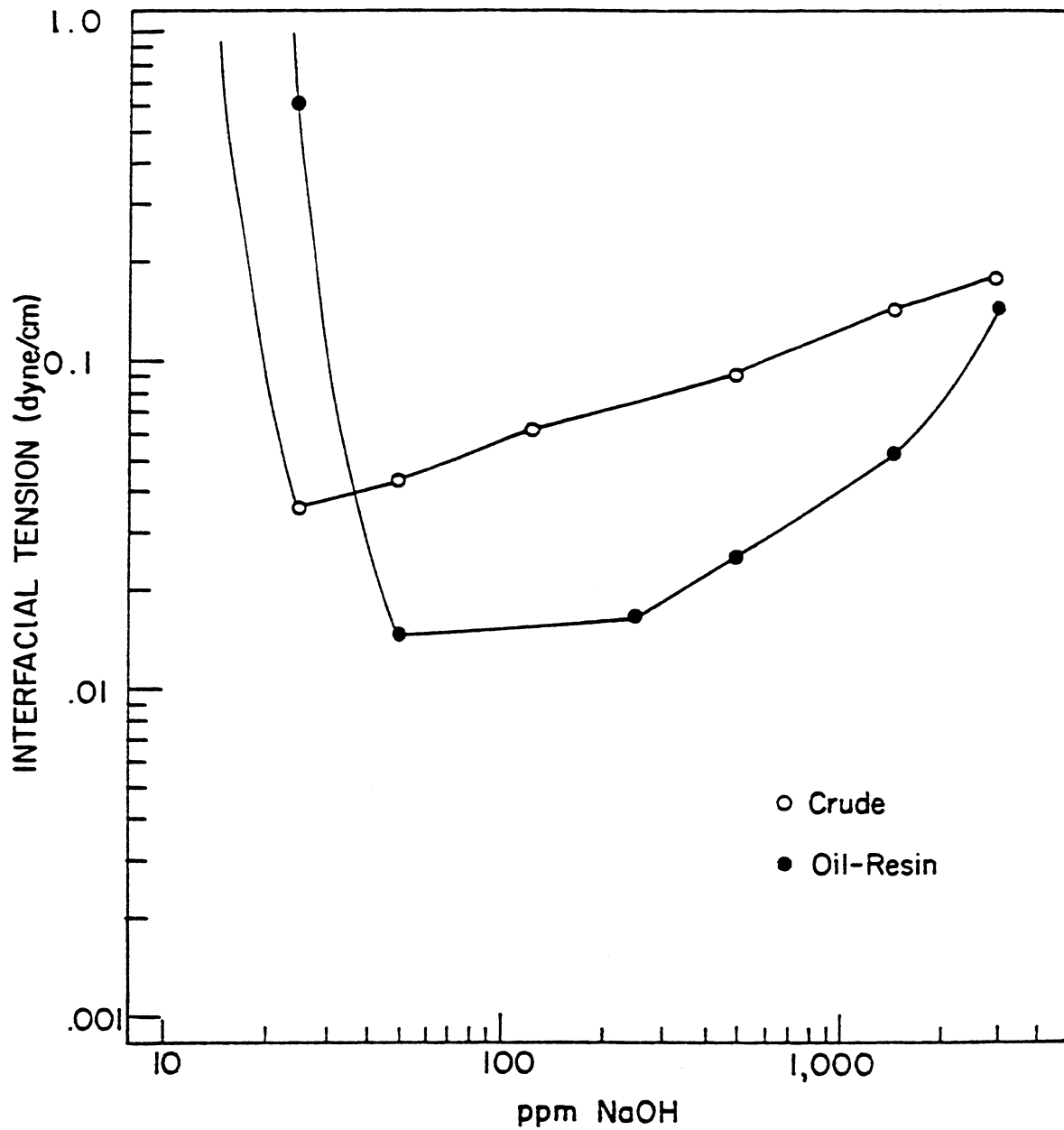


Figure 19. Interfacial Activity of Arkansas Crude and its Oil-Resin.

Table 7. Mass Balance and Average Molecular Weights of Crude Oil Fractions Separated by Silica Gel Column Chromatography.

<u>Fraction #</u>	<u>Eluting Solvent</u>	<u>Weight %</u>			<u>Average Molecular Weight *</u>
		<u>Huntington Beach</u>	<u>Long Beach</u>	<u>Arkansas</u>	
1	Hexane	61.0	71.9	79.4	240
2	Toluene	23.4	17.7	14.8	585
3	Toluene-Methanol	13.9	8.2	4.5	820

---

\* Benzene used as solvent for VPO

dissolved in toluene before IFT was measured. While undiluted Fraction 1 and 10% Fraction 2 in toluene did not show any activity, a 1% solution of the Fraction 3 exhibited very high activity. In other words, silica gel chromatography represents a simple, clear cut method of concentrating the active compounds from the crude. The technique does not alter the interfacial property of the crude components as shown by the observation that a crude reconstituted with the three fractions showed the same activity as the original crude (Figure 20.)

In general, interfacial activity increased with increasing concentration of Fraction 3 in the sample (Figure 21), up to a point where it was beginning to account for a substantial percentage (10% or more) of the molecules in the sample that it actually changed the bulk properties, including IFT, of the original toluene sample. Such transition was observed with the increasing crude oil concentration in a toluene solution sample (Figure 22). Anyway, the above results showed that this minor fraction of the crude represents a concentrate of the active components which are responsible for the interfacial activity of the crude in alkaline solution.

Infrared spectrum of the polar Fraction 3 showed a strong carbonyl (C = O) absorption band at  $1,700 \text{ cm}^{-1}$  compared with those of Fractions 1 and 2 (all shown in Figure 23). This is in agreement with the fact that carboxylic acids (RCOOH) are generally eluted last from a silica gel column due to their highly polar nature. The O-H stretching bands around  $3,000 \text{ cm}^{-1}$  were not as broad as those expected from pure carboxylic acids, probably due to the presence of other components that hinder the O-H --- O-H hydrogen bonding interaction which accounts for the normally observed broad O-H absorption.

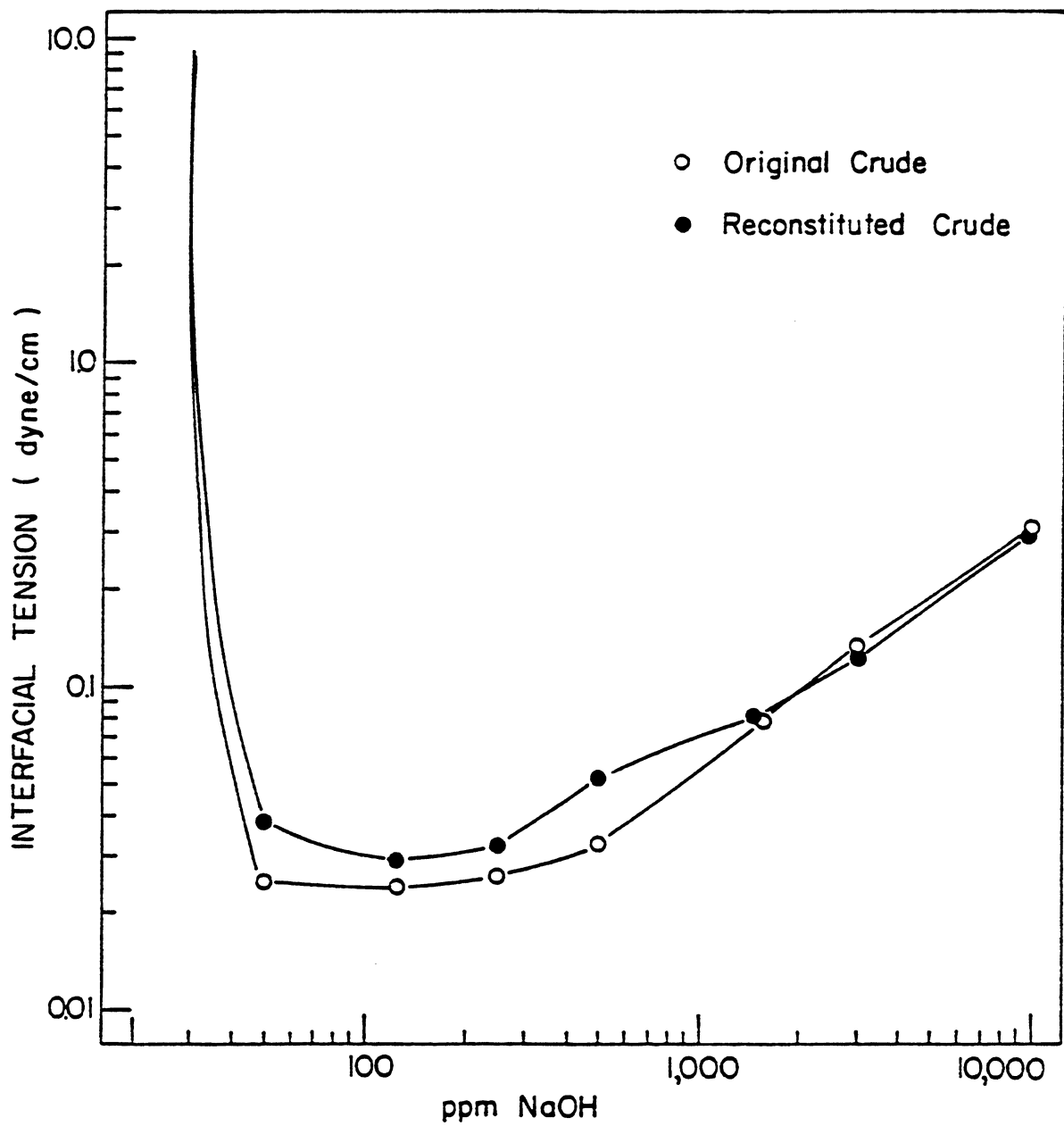


Figure 20 Reconstitution of Long Beach Crude from its Fractions 1, 2 and 3 (weight ratio 72:18:8)

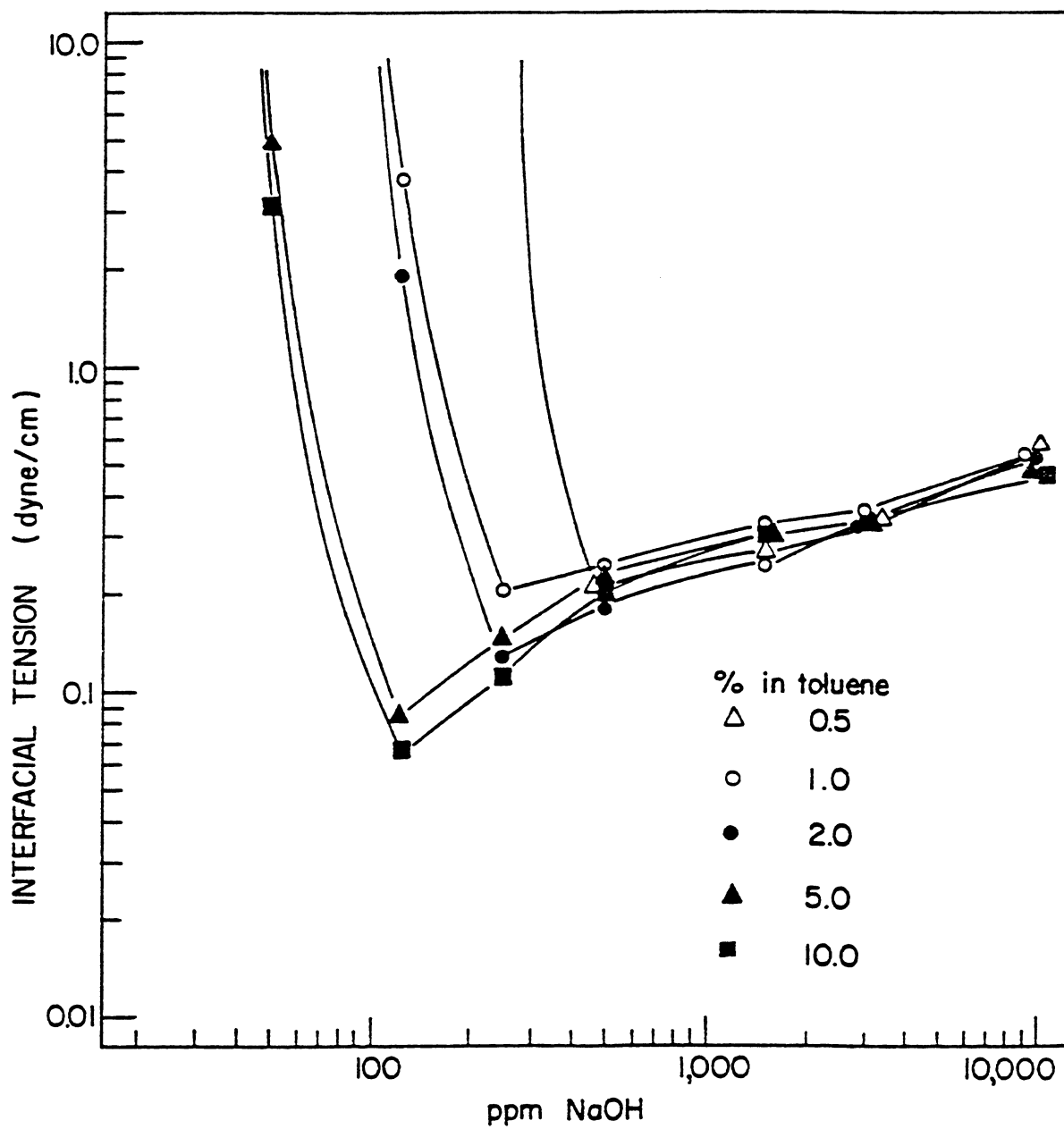


Figure 21 Interfacial Activity of Samples with Different Concentrations of Fraction 3 in Toluene.

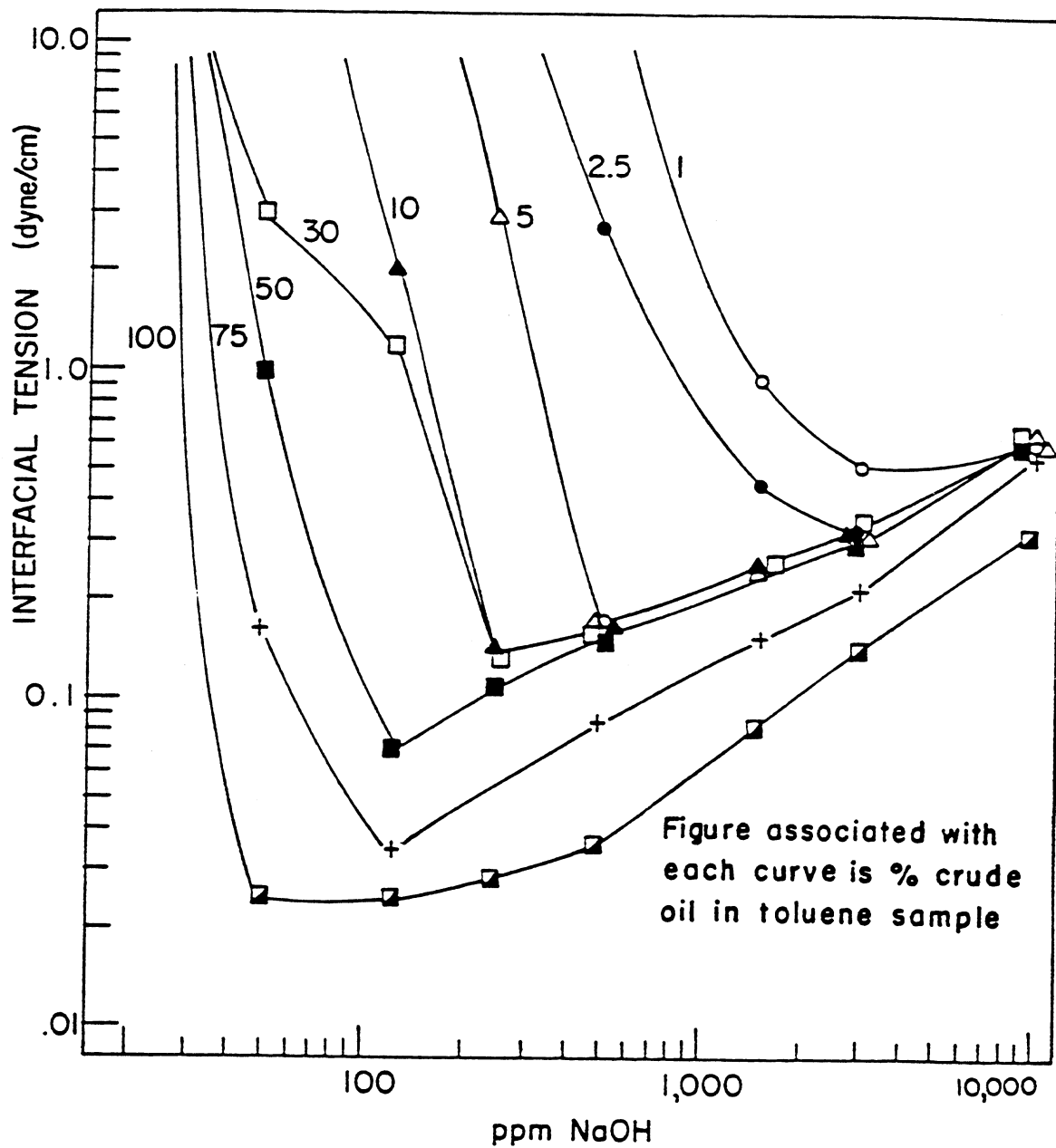


Figure 22. Interfacial Activity of Samples with Different Concentrations of Long Beach Crude Oil in Toluene.

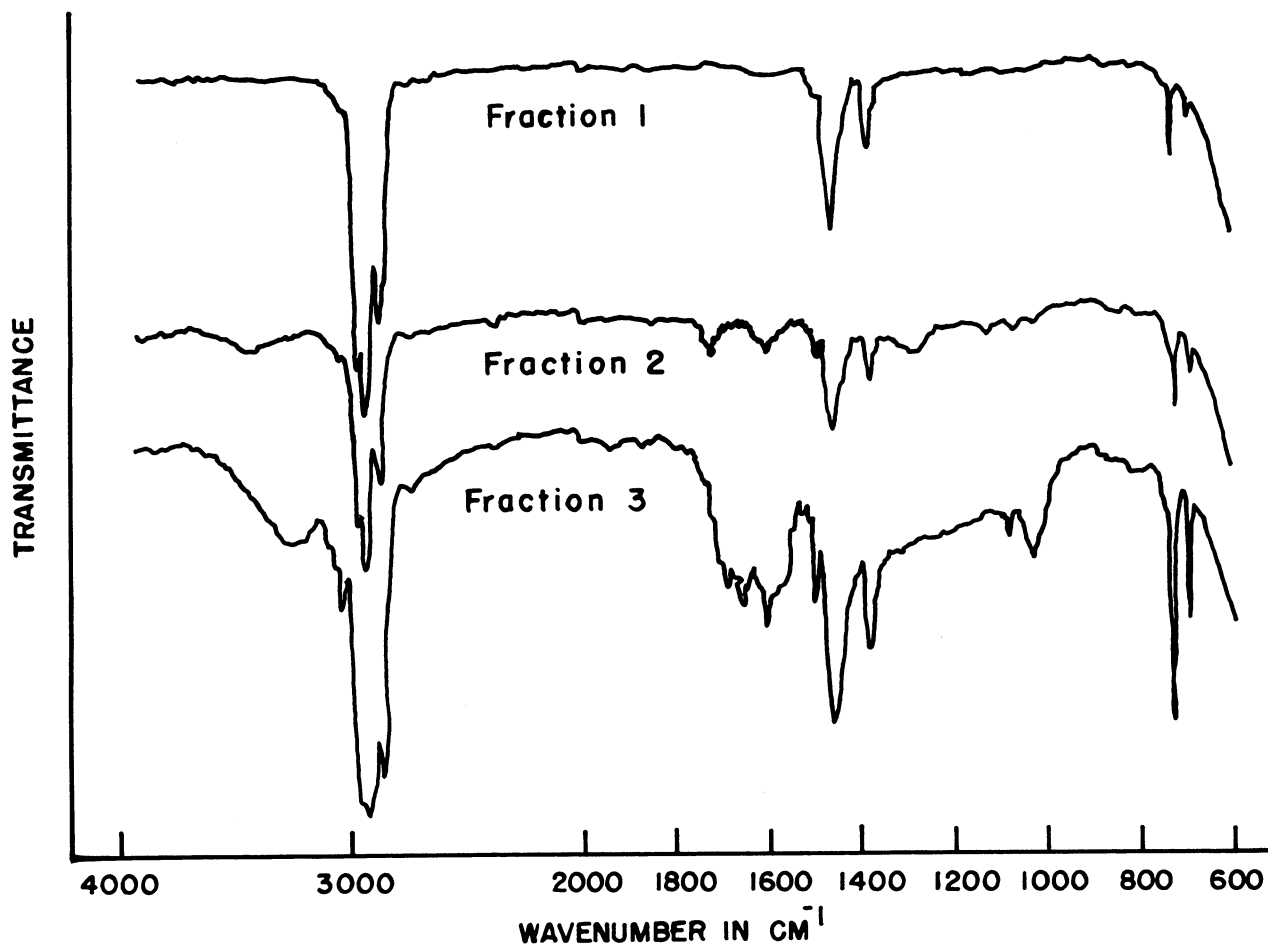


Figure 23. Infrared Spectra of Fractions 1, 2 and 3.

Table 8. Elemental Analysis of Long Beach Crude and its Fractions 1, 2 and 3.

	<u>Weight %</u> *				
	<u>C</u>	<u>H</u>	<u>N</u>	<u>S</u>	<u>O</u>
Crude Oil	84.99	11.70	0.57	1.53	0.95
Fraction 1	85.21	12.8	0.16	1.25	0.48
Fraction 2	84.54	9.89	1.72	2.10	1.21
Fraction 3	78.52	9.62	1.84	2.88	4.89

\* Direct Determination

Elemental analysis (Table 8) also confirmed the abundance of oxygen in Fraction 3, although other heteroatoms such as nitrogen and sulfur were also present at a higher level than the original crude in both Fractions 2 and 3. The higher content of nitrogen supported my speculation that some kind of amine-acid associates may be present in Fractions 2 and 3, and that it makes sense to try liberating these acids from their bound complexes for enhancing alkaline flooding efficiency.

The separation of crude into gas oil, resin and asphaltene serves to better understand the properties of the oil as a whole, because the presence of asphaltic materials is generally considered essential to some of these properties. As shown by results given in Table 9, asphaltic materials are responsible for the viscous nature of the oil, a property which is not desirable from the oil refiner's point of view. On the other hand, due to their aromatic nature and presence of heteroatoms, asphaltic materials give the crude a good dissolving power and serve as a sink for many undesirable reactions such as oxidation and photoreactions. Therefore a study of the distribution of the active components among these three cuts would be useful. When samples from each of these three cuts were each run through silica gel columns, substantial amounts of Fraction 3 were obtained from all of them, with per gram concentration highest in the resin, less in the asphaltene, and least in the gas oil. However, due to the large amount of gas oil in comparison with those of resin and asphaltene, the gas oil ended up containing more overall active components (based on the weights of Fraction 3 isolated) than asphaltene and resin. The breakdown of the

Table 9. Viscosity Effect of Asphaltic Materials and Fraction 3

<u>Sample</u>	<u>Viscosity (cps) at 25°C</u>
Crude Oil (Long Beach)	147.5
Gas Oil	184.3
Gas Oil + Resin	270.3
Nonvolatiles (Gas Oil + Resin + Asphaltene)	7,741.4*
Crude Oil with Fraction 3 removed	50.2

\* A shear rate of  $19.2 \text{ sec}^{-1}$  was used.  
For all other samples a shear rate of  $192 \text{ sec}^{-1}$  was used.

Table 10. Distribution of Activity among Crude Oil (Long Beach) Cuts

<u>Cut</u>	<u>Cut wt. % in Crude</u>	<u>Active Fr. 3 in Cut (Wt. %)</u>	<u>Contribution (wt %) to Total Activity of Crude</u>	<u>Fraction 3 Molecular Weight *</u>
Volatiles	26.7	0.0	0.0	
Gas Oil	57.6	6.4	41.8	440
Resin	10.2	34.4	39.8	756
Asphaltene	5.8	28.0	18.4	1,927

\* Benzene used as solvent for VPO

percentages of activity in each cut and in the crude overall are presented in Table 10. This finding is new since Wasan's report<sup>56</sup> which indicated that active components were present in the resin and asphaltene. It also refuted the report by Farmanian et al.<sup>57</sup> that the volatiles contain the active species. The mistake has been attributed by the authors to an accidental carrying over of some nonvolatiles to the distillate during distillation. The Fraction 3's from the three cuts were found to have practically the same activity potency, as shown in Figure 24. They probably belong to some homologous series of acids which have the same functional groups, but differ in molecular sizes. This is supported by the molecular weights (Table 10) of the three classes of Fraction 3. They were found to be 440, 756, and 1,927, respectively for the Fraction 3 from gas oil, resin and asphaltene.

As expected from the high asphaltic content of Fraction 3, its removal from the crude, i.e., leaving only Fractions 1 and 2, leads to a substantial drop in viscosity (see Table 9). Therefore it seems that the presence of these highly surface active molecules would cause the undesirable effect of increased oil viscosity. On the other hand, this may give us a hint that heavy oils, which are more viscous than light oils, may contain more active components and thus be more suitable for alkaline flooding enhanced oil recovery.

#### Porphyryns: Characterization and Their Role in the Alkali Induced Interfacial Activity

Metal-porphyrins and metal-free porphyrin base were extracted from the Huntington Beach crude and the Long Beach crude (Isolation of Porphyrins). The visible absorption spectrum (Figure 25 of the metal-porphyrin concentrate showed on absorption peak at 550 nm, and another one at 510 nm at a

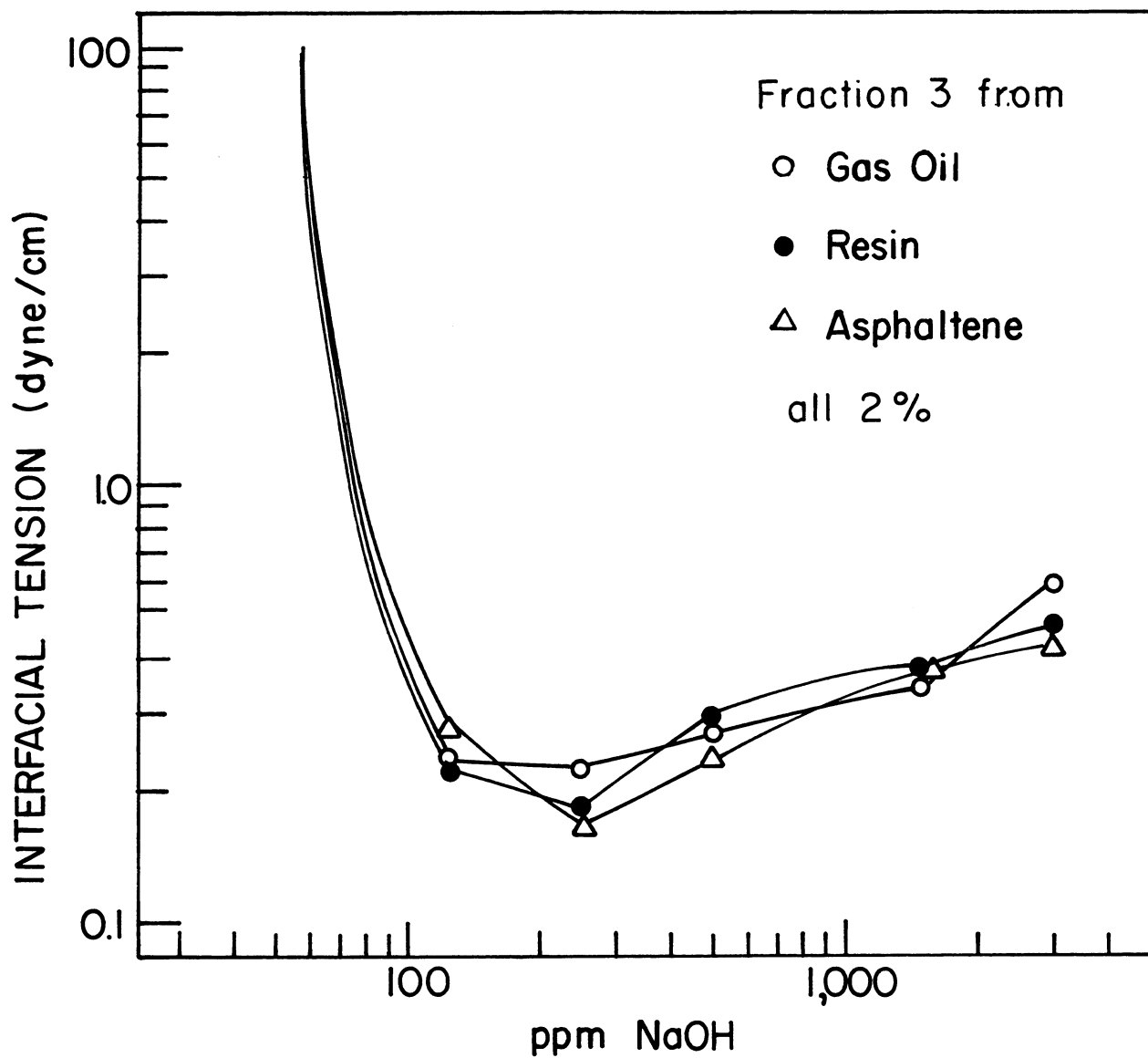


Figure 24. Interfacial Activity of Fraction 3's Isolated from Gas Oil, Resin and Asphaltene.

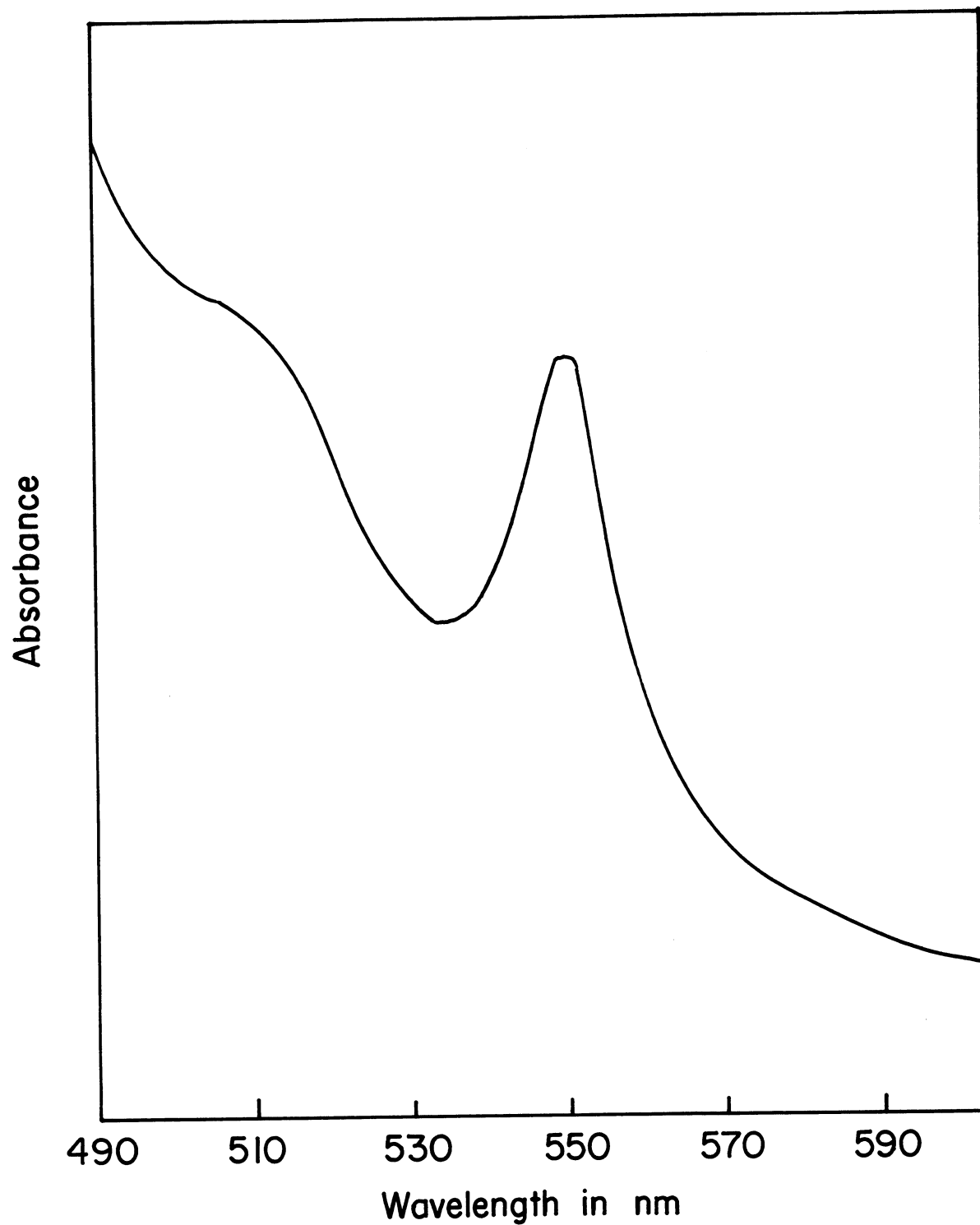


Figure 25. Visible Absorption Spectrum of Metal-Porphyrins from Long Beach Crude.

lesser intensity. These are the absorption peaks of nickel complex as opposed to vanadium complex which should have absorptions at 550 and 570 nm instead<sup>45</sup>. Visible spectrum (Figure 26) of the metal-free porphyrin base showed the characteristic four-peak pattern<sup>58</sup>. Mass spectrum taken of the base identified the molecules to be a mixture of etio (mass number  $310 + 14n$ ) and DPEP (mass number  $308 + 14n$ ), where  $n$  is the number of methylene groups added onto the basic ring structure. The mass spectrum and the structures of the two porphyrin bases are given in Figure 27. By summing the intensities of the peaks belonging to the same type, the ratios of the amounts of DPEP to etio type in the Huntington Beach and Long Beach crudes were found to be 1.1 and 1.2, respectively. In other words, these two crudes contain nickel porphyrins composed of etio and DPEP types present in about equal amount.

Since the porphyrins came out from the silica gel column in the toluene eluted fraction, i.e., Fraction 2 which according to Section 6 does not show any activity at alkaline pH, it seems unlikely that porphyrins are among the active components in the crude.

#### Effects of Sodium Ions on the Activity Onset pH

An ionic double layer is believed to exist on the surface of the oil in which the negatively charged acid species generate a negative potential on the surface which, in turn, creates another layer of counter ions, namely the positive sodium ions, at the adjacent surrounding. This electrical double layer problem has been studied theoretically by Gouy<sup>59</sup>, Chapman<sup>60</sup>, and later by Stern<sup>61</sup>. Such a negatively charged surface film will cause an electrostatic exclusion of hydroxide ions from the interface. In fact, Davies and Rideal<sup>62</sup>

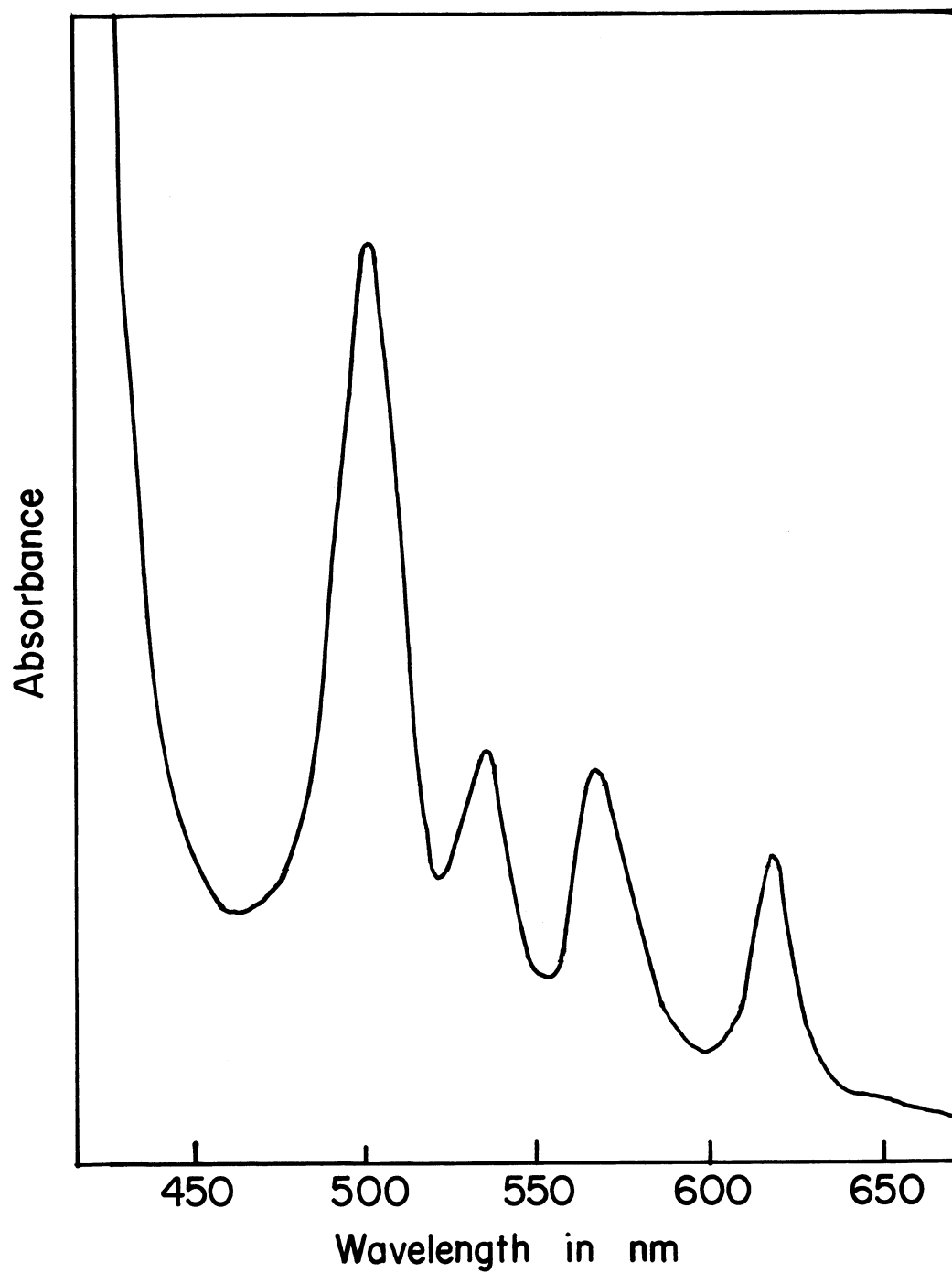
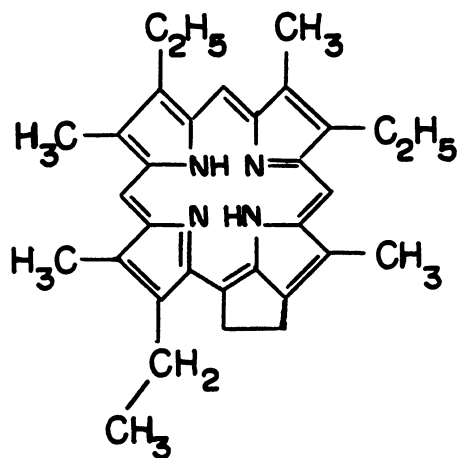
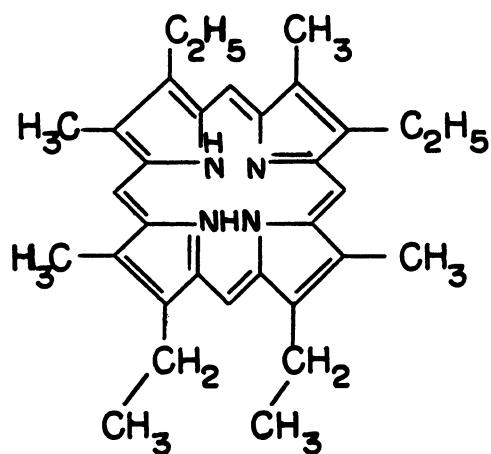
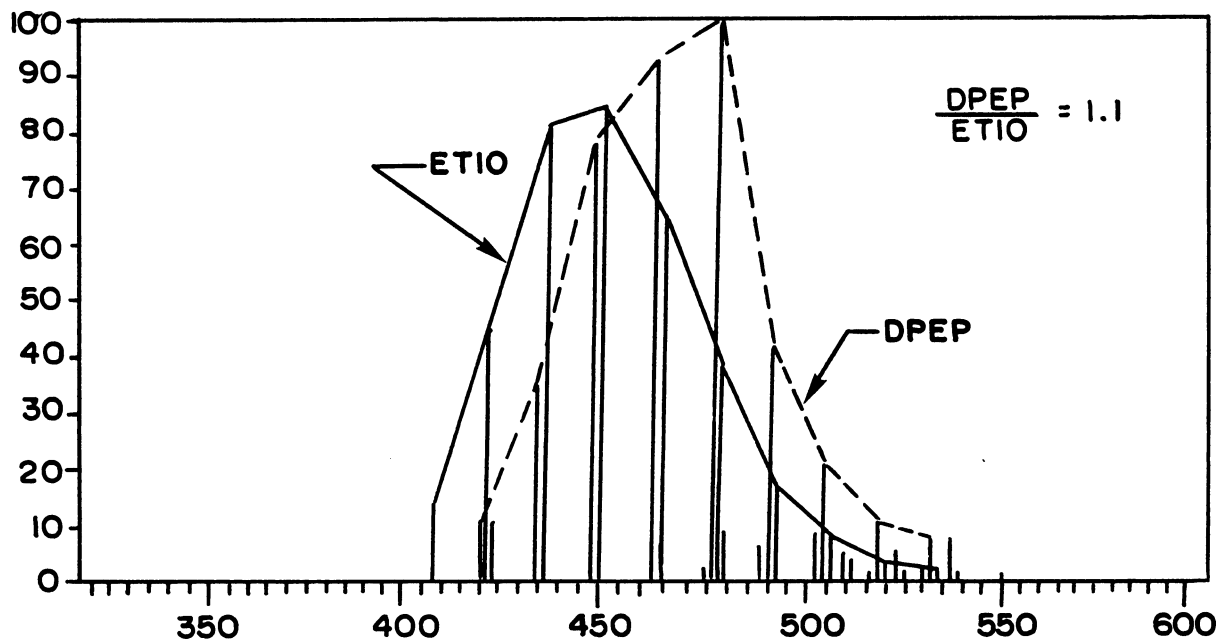


Figure 26. Visible Absorption Spectrum of Metal-Free Porphyrins from Long Beach Crude.



Etioporphyrin (ETIO)

Deoxyphylloerythro -  
etiochlorin (DPEP)

Figure 27. Mass Spectrum and Structures of Metal-Free Porphyrins from Huntington Beach Crude. MS: 12 ev., 180°C.

in dealing with the alkaline hydrolysis of monoacetylsuccinate ions, and Payens<sup>63</sup> in dealing with alkaline treatment of acidic oil, have recognized that the local concentration of hydroxide ions would be lower than that in the bulk solution. Here, the Donnan condition can be applied by equating the sodium hydroxide activities in the bulk (b) and in the interface (i):

$$C^+_b \cdot A^-_b = C^+_i \cdot A^-_i$$

In this case, cation  $C^+$  is sodium ion and anion  $A^-$  is hydroxide ion.

Assuming electroneutrality in the interface, we have:

$$Z^2 = (Y + X)X$$

where Z is the bulk sodium hydroxide concentration and X is its concentration at the interface, while Y is the  $C^+$  associated with the negatively charged acid film.

For a given sample the value of Y can be considered constant. Therefore the value of X will approach that of Z if the latter becomes much larger than Y. Since the molecular sizes and activity coefficients of the chloride and hydroxide ions are very close, one may assume that at all times  $OH^-_b/Cl^-_b$  is approximately equal to  $OH^-_i/Cl^-_i$ , then  $A^-$  can be treated as  $OH^- + Cl^-$ . This analysis suggests that an addition of sodium chloride will also lead to the approach of the hydroxide concentration or pH of the interface to that of the bulk phase.

In the absence of salt, the Long Beach crude starts to show activity at a bulk solution pH of 11.4. At this point, the interfacial pH reaches the  $pK_a$  value of the native acids in the crude and the latter are thus ionized to form interfacially active charged acid

species. This leads to the sudden drop of IFT•

The curves in Figure 28 showed the different IFT responses of the crude in the presence of different salt concentrations in the aqueous alkaline solution. Addition of salt was found to lower the bulk alkali concentration or the bulk pH needed to achieve the onset of the IFT drop, i.e., the point where the interfacial pH is equal to the  $pK_a$  values of the acids in the crude cannot be higher than 9. This is a more reasonable  $pK_a$  ceiling estimate than the apparent value of 10 to 11 observed when little or no salt is present.  $pK_a$  values of these large native acids are not available in the literature primarily due to their low solubility.

Therefore, sodium chloride can be used to promote ultra-low interfacial tension of crude oils at a lower onset bulk aqueous pH. In other words, in cases where too high an alkali concentration is undesirable due to either economic or environmental reasons, salt can be used to lower the amount of alkali required to bring about the low IFT. One drawback is that one is sacrificing IFT activity for this because the sodium ion concentration buildup accompanying the salt addition deactivates the soap formed and therefore increases the IFT value, as shown in Figure 28.

From experimental results like those given in Figure 28, a compromise salt concentration could be picked to give a reasonably broad alkali response range without sacrificing too much in IFT. In the case with the Long Beach crude, a salt concentration of around 10,000 ppm is good. That also explains why a salt concentration of 7,500 ppm was used in all solutions in this study.

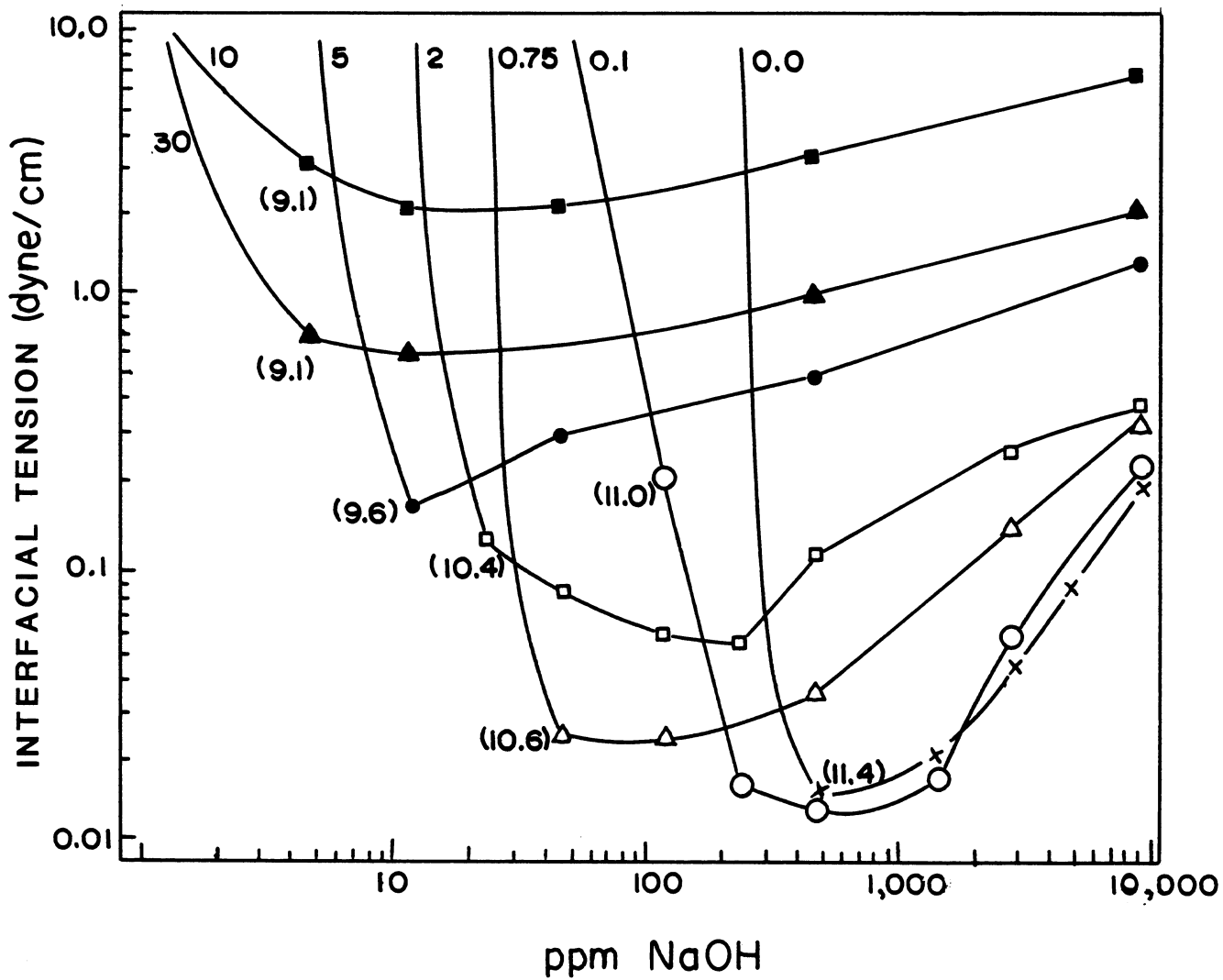


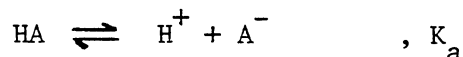
Figure 28. Interfacial Activity of Long Beach Crude in the Presence of NaCl. The Figures on top are percent NaCl in Aqueous Solution. Those in brackets are the Onset Solution pH.

Experimental Evidence for the Equilibrium IFT Model

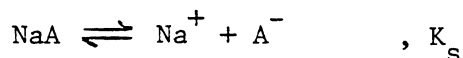
The model developed previously says that the interfacial concentration of active species  $A^-$ , which is believed to correlate positively to the IFT activity of the oil, is given

$$A^- = \frac{HA_o}{\frac{H^+}{K_a} + \frac{Na^+}{K_s} OH + \frac{Na^+}{K_s} Cl + 1}$$

where



is the activation reaction, and



(undissociated)                      (dissociated)

is the deactivation reaction.

The IFT of the crude oil shows a sudden drop when the acids start to ionize. That is, the drop occurs at the point where pH is equal to the  $pK_a$  of the acids, or  $H^+ / K_a = 1$ . Further increase of alkali concentration beyond this point reduces the value of the  $H^+ / K_a$  to much less than 1, and the  $Na^+ OH / K_s$  term at the same time approaches or exceeds the value of 1. Soon the sodium term becomes more significant and causes the IFT to go up. Therefore, the results indicate that, in the domain of low IFT, the change of value of the order of 1 or more in the denominator will be reflected significantly in the IFT curve.

Now, to support the proposition that the deactivation step involves the formation of undissociated, tight complex of sodium soap molecules

which may precipitate out, the acids in the crude were extracted using a 10,000 ppm NaOH aqueous solution in a manner described previously. As a result two kinds of acids were obtained: one which formed the undissociated soap precipitate and therefore should have small  $K_s$  value, and one which formed the loosely associated soluble soap and therefore should have larger  $K_s$  value. They are labeled Acid A and Acid B, respectively, and their soaps are called Soap A and Soap B accordingly. Both acids isolated are reasonably pure carboxylic acids as indicated by the IR spectrum (Figure 29) with typical carbonyl (C=O) absorption at  $1,700\text{ cm}^{-1}$  and the broad O-H stretching absorption in the  $3,500$  to  $2,500\text{ cm}^{-1}$  region. Elemental analysis also indicated the abundance of oxygen (see Table 11). After dissolving in toluene (2 wt. % solutions), the two acids were tested for IFT response in alkaline solutions. Results shown in Figure 30 indicate that Acid A, which has smaller  $K_s$  value, is greatly affected by increasing NaOH concentration after the ionization onset at around 100 ppm NaOH. Whereas Acid B, which has larger  $K_s$  value, is relatively unaffected by increasing alkali concentration up to 10,000ppm. Also, as expected, Acid A was found to have larger molecular size than Acid B (average MW of 340 versus 260).

To estimate the values of  $K_s$  of soap formed from these native acids, one can make use of the above analysis that a change of the order of 1 or more in the denominator in expression will be reflected significantly in the IFT response after the onset pH. In Figure 30, a reasonably significant IFT change from 0.15 to 0.4 dynes/cm was picked. Acid B took an additional 1 M. sodium to achieve that while Acid A required only  $2 \times 10^{-2}$  M. sodium. In other words,

Table 11. Elemental Analysis of Materials Extracted from Crude Oil with Alkaline Solution  
and Acid Solution, •

	<u>C</u>	<u>H</u>	<u>N</u>	<u>O</u>
Long Beach Crude	84.99	11.70	0.57	0.95
Material extracted by Alkali	78.08	9.89	0.36	9.35
Material extracted by Acid	78.36	9.11	4.49	2.51

---

\* Direct Determination

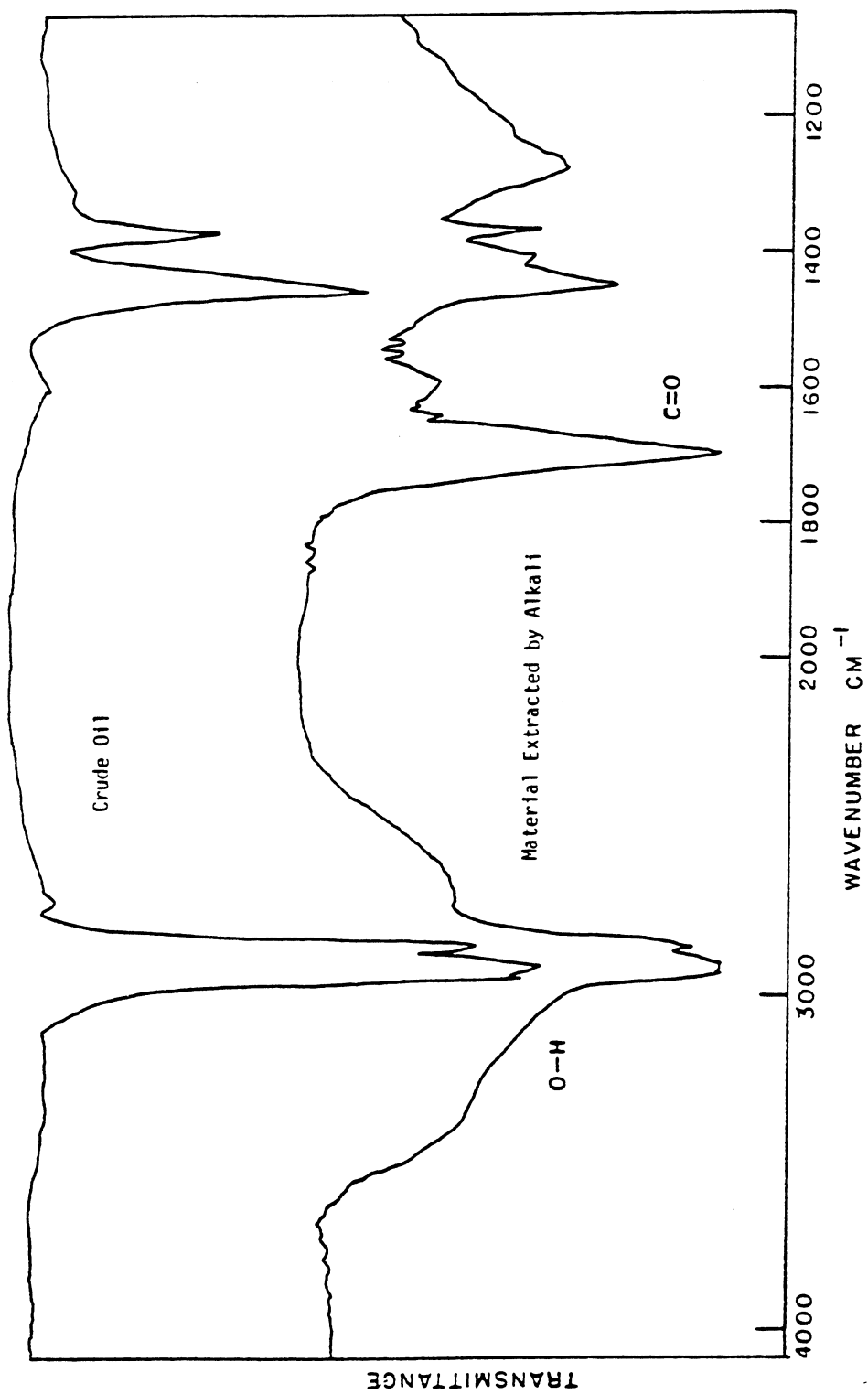


Figure 29. Infrared Spectrum of Material Extracted from Crude Oil with Alkali.

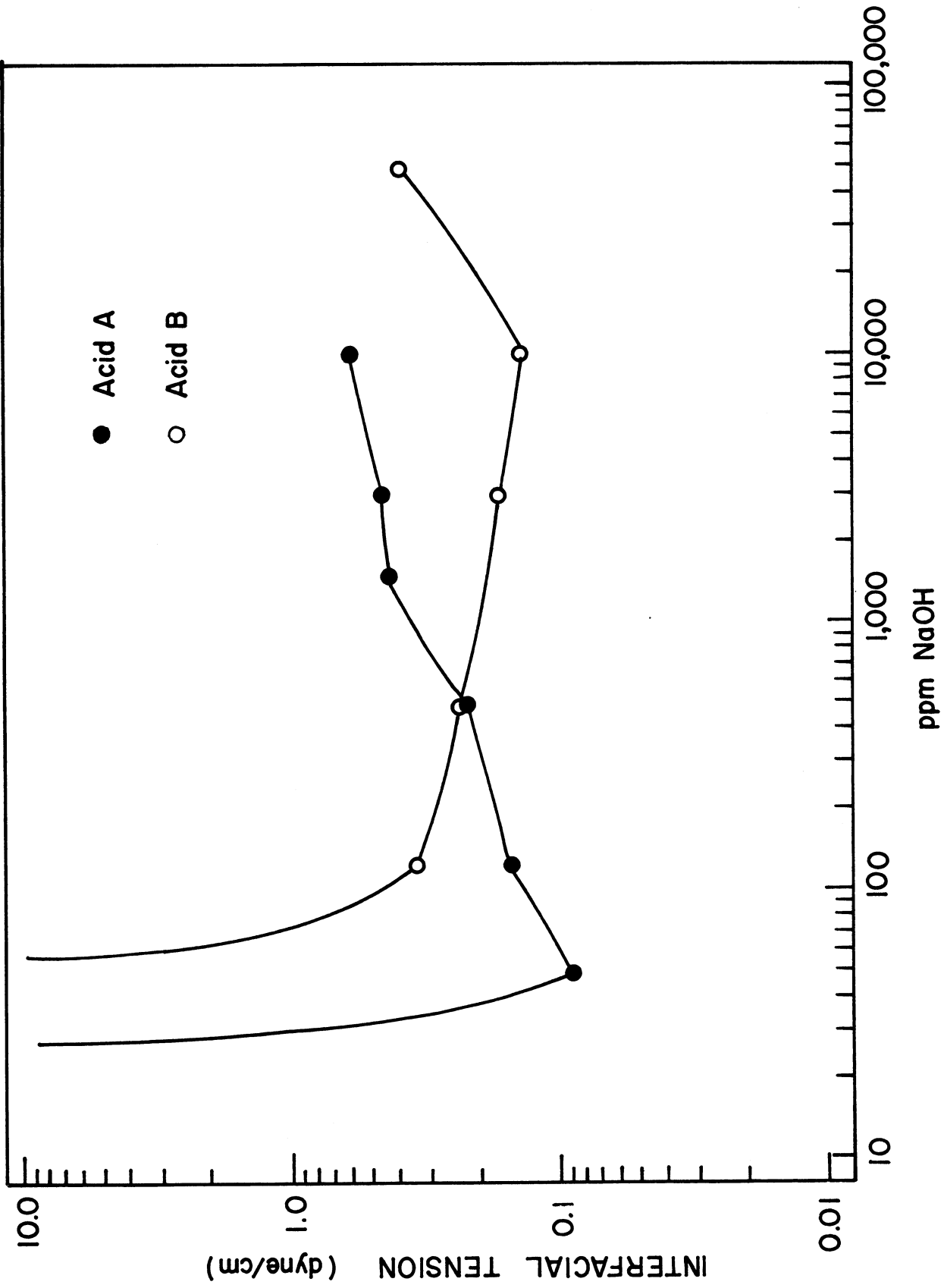


Figure 30 Interfacial Activities of Acid A (Undissociated) and Acid B (Dissociated) Extracted from Crude Oil.

for  $\Delta \text{Na}^+ / K_s$  to be 1, the  $K_s$  value for Soap A and Soap B will be in the order of 1 and  $10^{-2}$ , respectively. These values are reasonable because a "dissociated" soap should have a  $K_s$  value of at least 1, and an "undissociated" soap should have very small  $K_s$ , such as  $10^{-2}$  or smaller. The ratio of the amounts of the two types of acids extracted in this case was found to be around 1.

With the acids extracted, we may now show the positive correlation between interfacial activity and  $\text{HA}_0$ . IFT measurements of the acids (a 1:1 mixture of Acids A and B) showed increasing interfacial activity with the increasing acid concentration in the sample. Results are shown in Figure 31.

As with the NaCl in the system, its positive effect, which has to do with the lowering of the bulk alkali concentration required to achieve the onset of interfacial activity due to its effects on the electrical double layer, has been discussed previously. After the onset pH is reached, however, NaCl will only cause an increase of IFT as described above by this model. The model also predicts that at pH above the onset pH, i.e.,  $\text{H}^+ / K_a \ll 1$ ,  $\text{Na}^+_{\text{OH}}$  has the same detrimental effect as  $\text{Na}^+_{\text{Cl}}$ . Experimental results gave support to this. Starting with a highly alkaline solution, say at 3,000 ppm alkali, addition of sodium in the forms of NaOH and NaCl was found to give practically the same rise in IFT of the crude (Figure 32).

#### Sequential Activation of Acids in the Crude

Since the acids in the crude could not be a single species, their differences in structure and size is expected to give them slightly different  $\text{pK}_a$  values. They may also have different molecular orientation at the interface which means that they may experience

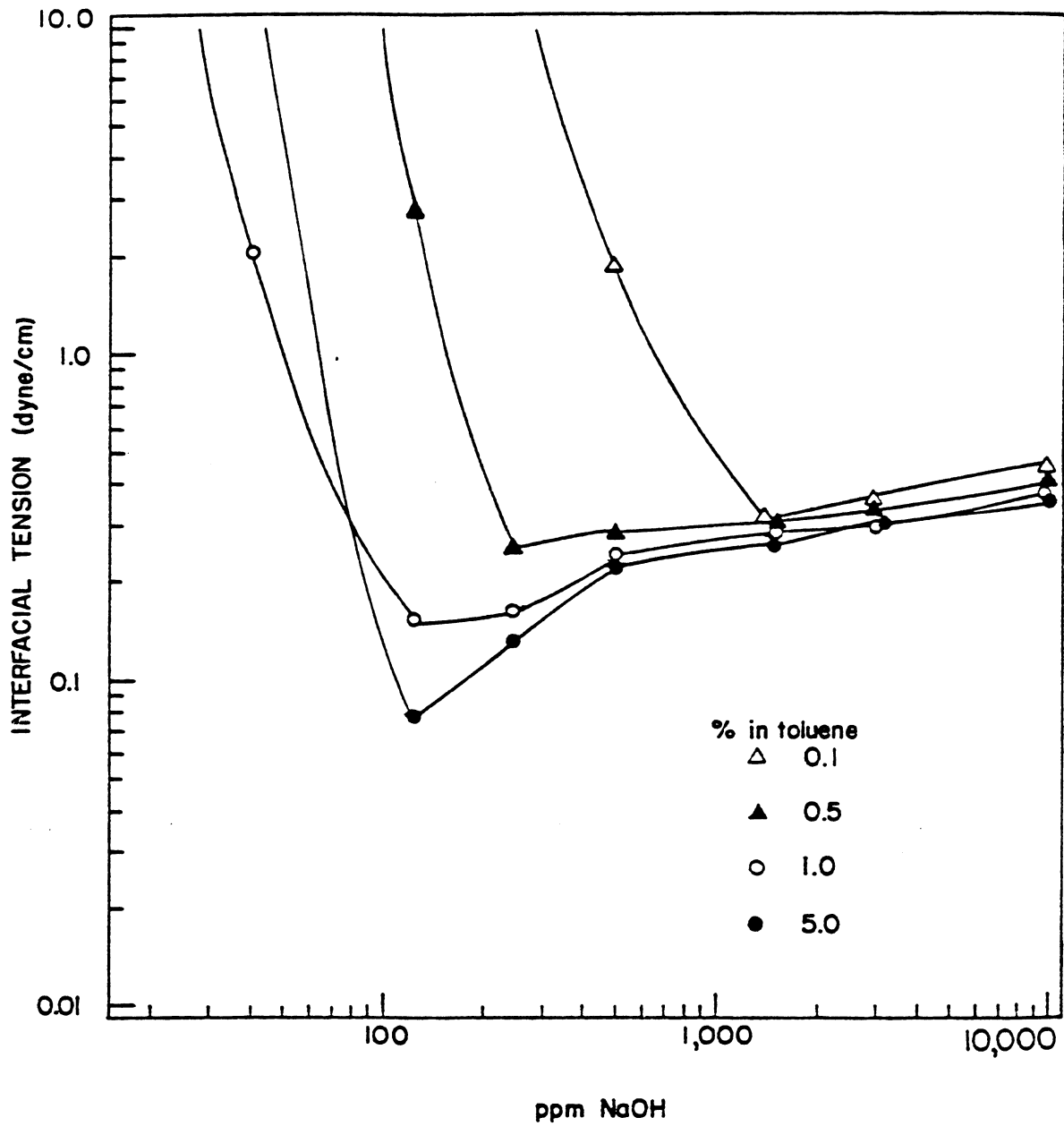
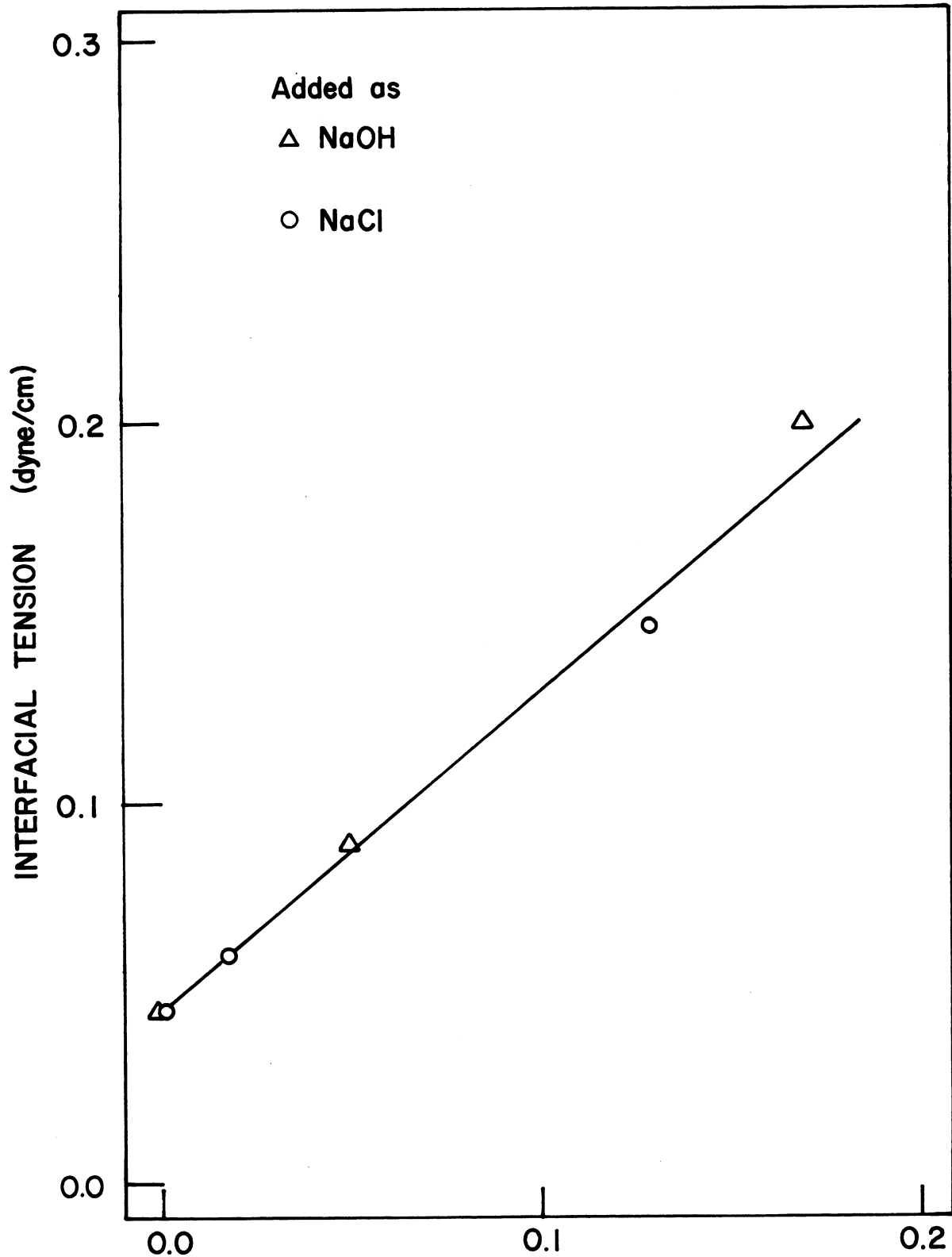


Figure 31. Interfacial Activity of Extracted Acids (1:1 Acid A to Acid B) at Different Concentrations in Toluene.



**ADDITIONAL Na<sup>+</sup> CONCENTRATION (mole/liter)**  
Figure 32. Effects on Crude-Water IFT of Addition of Sodium as NaCl and as NaOH to a 3,000 ppm NaOH Aqueous Solution.

different local interfacial pH and thus may not be activated by the same bulk solution pH. This was confirmed by the results of the alkali treatment of the crude. When the crude was treated, in a manner described in Section IV, with a 125 ppm NaOH (the alkali concentration corresponding to minimum IFT in the presence of 7,500 ppm NaCl) solution, the crude was deactivated in alkali range of up to and including ppm NaOH. IFT test showed that at higher alkali concentration the crude became active again. This indicated that the 125 ppm NaOH is good enough to ionize and thus remove only some of the acids originally in the crude, with the remaining acids activated only at a higher pH. The remaining activity of the crude from 250 ppm NaOH up showed a new IFT minimum at 500 ppm NaOH. Now treating this crude sample with 500 ppm alkali solution was found to remove some more acids, leaving a crude which showed activity only at very high alkali concentration of 1,500 ppm and above. Finally, treating the sample with a 3,000 ppm alkali solution removed all activity up to and including 10,000 ppm NaOH. Results of the activity depletion by this incremental alkali treatment are shown in Figure 33.

The above results suggested that if alkaline flooding were to be carried out with incremental alkali concentrations, it would yield better total recovery than with a single high concentration of alkali which is known to give higher IFT values. This was supported by the core flooding result which showed an average total tertiary recovery of 33% by flooding in the sequence of 250, 500, and 3,000 ppm NaOH, compared with only 14% if flooded with a 10,000 ppm NaOH solution (see Table 12). Flooding with a single concentration of 500 ppm alkali

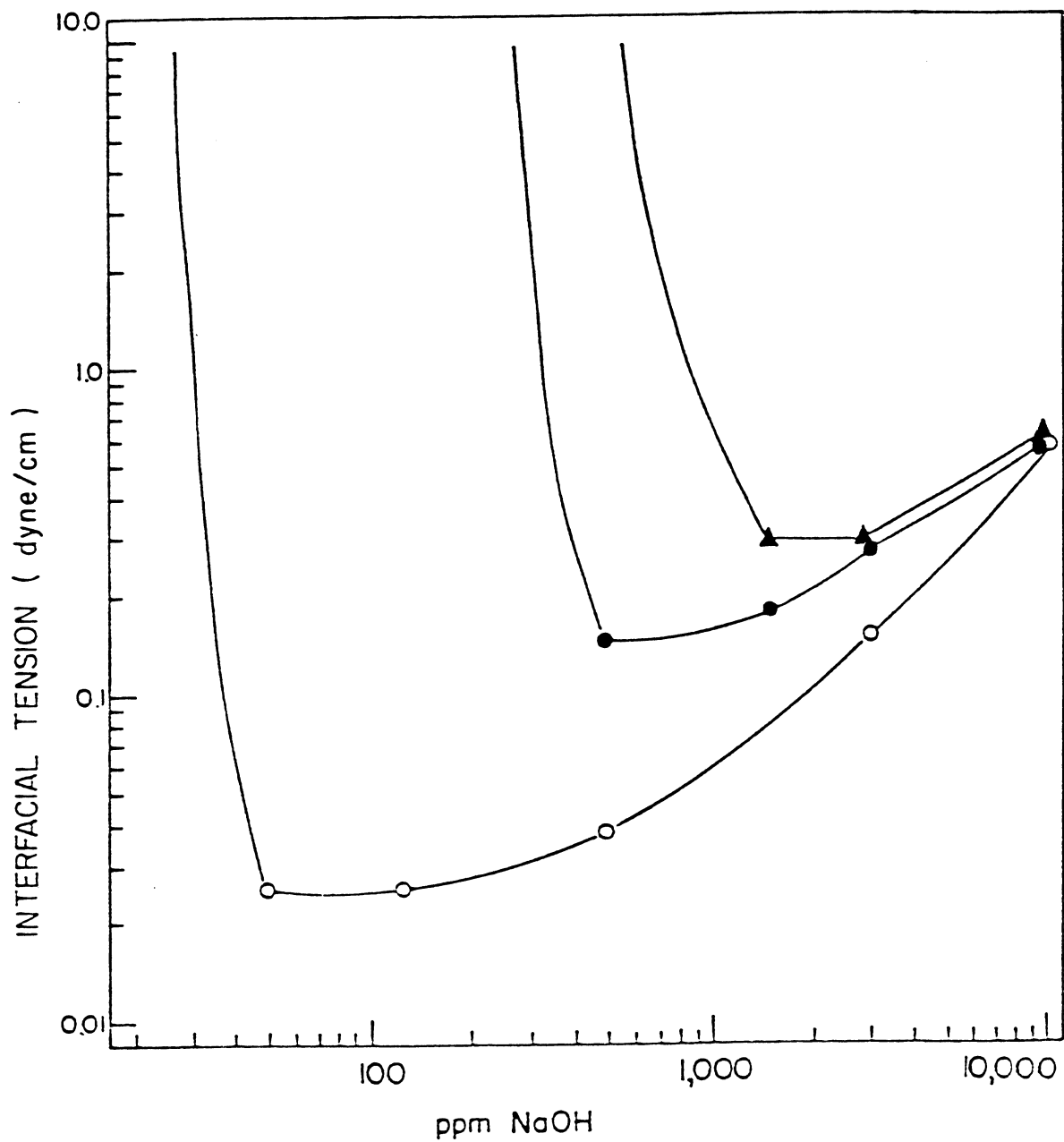


Figure 33. Depletion of Activity by Incremental Alkali Treatment. Original Crude (○) Treated with 125 ppm Alkali (●) followed by 500 ppm Alkali (▲). Further Treatment with 3,000 ppm Alkali Deactivated the Crude completely.

Table 12. Oil Recovery from a Sand-Packed Core by Alkali Flood

<u>ppm Alkali in solution</u>	<u>Recovery %<sup>*</sup> (multiple runs)</u>
500	31, 32
10,000	14
250 - 500 - 3,000	31, 36

\* Based on residual oil after secondary water flooding.

Table 13. Amount of Acid Extracted Out by Alkali from Crude Oil after each Acid Reactivation

<u>Extraction Scheme<sup>*</sup></u>	<u>Amount of Acid Extracted (Wt. %)<sup>**</sup></u>
Alkali	0.06
(Alkali - Acid) - Alkali	0.03
(Acid) - Alkali	0.10

\* 10,000 ppm NaOH solution is the alkali used; 0.2N HCl solution is the acid used.

\*\* These figures are based on materials extracted by the last round of alkali. Materials extracted by previous extractions, i.e., those within the brackets, are not included.

gave the same recovery as 250 followed by 500 ppm. This could be explained by the fact that consumption of alkali by the sand matrix at the beginning would give the local pH a value lower than that of the feed solution. Therefore flooding with 500 ppm would cause the core to spend much of the pH buildup time (about three pore volumes) in the 200 ppm's region, which is equivalent to flooding for a couple of pore volume with a 250 ppm alkali solution. Flooding with a very high 10,000 ppm solution, however, would cause the core to spend very little time in the low alkali concentration region which has been shown to give low IFT. As a result, low recovery was observed.

#### Generation of Additional Soap-Forming Acids From Crude Oil

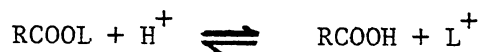
The stripping of extractable materials from the crude by the alkali extraction procedure described previously was found to coincide with the disappearance of interfacial activity from the crude sample. These acids extracted are believed to be a mixture of free acids in the crude and acids which were liberated by alkali-catalyzed hydrolysis of compounds such as certain amides in the crude. Since there are many other acid derivatives which are known not to hydrolyze significantly at alkaline pH, an acid-catalyzed hydrolysis reaction is proposed previously to liberate some of these remaining bound-acids so that they would contribute new or additional activity to the crude.

Figure 34 shows that a crude which had been deactivated completely by alkali, i.e., one which showed no activity in alkali concentration of up to 10,000 ppm, became active again after an acid treatment with a HCl solution (described previously). This implied that the oil in a reservoir which has been exhausted by alkaline floods may be activated again by an acid flood. At 25° C, the temperature at

which the experiments were conducted, the effective HCl concentration for the crudes studied could be as low as 0.05N. The figure also shows that 1N HCl has the same effectiveness as 0.2N HCl. Sulfuric acid solutions at the same concentration were found to show the same effects as hydrochloric acid.

A slightly different experiment of similarly treating a crude sample which has never been exposed to alkali, i.e., one of which activity is intact, was found to give the crude improved IFT response. The result is shown in Figure 35.

Also the deactivation by alkali and activation by acid can be repeated over and over again for a few times on the same crude sample, indicating that not all the acids are liberated and removed by one such acid-alkali cycle. An equilibrium is believed to exist between the free acid (RCOOH) and the bound complex (RCOOL):



where L is the ligand part that is bound to the acid in the complex. From the above expression it is not surprising to see that removal of free acids in the system would help shift the equilibrium toward breaking more complex molecules. That could explain why no matter how complete each acid treatment was, after the following round of alkali deactivation, one could always generate more acids, i.e., the crude was reactivated again. Of course with each cycle less and less of these complexes will be left, and that is why later activated crudes were found to have less and less interfacial activity (see Figure 36). The weight of acid extracted by each round of alkali is shown in Table 13. This implies that activating an oil reservoir more than

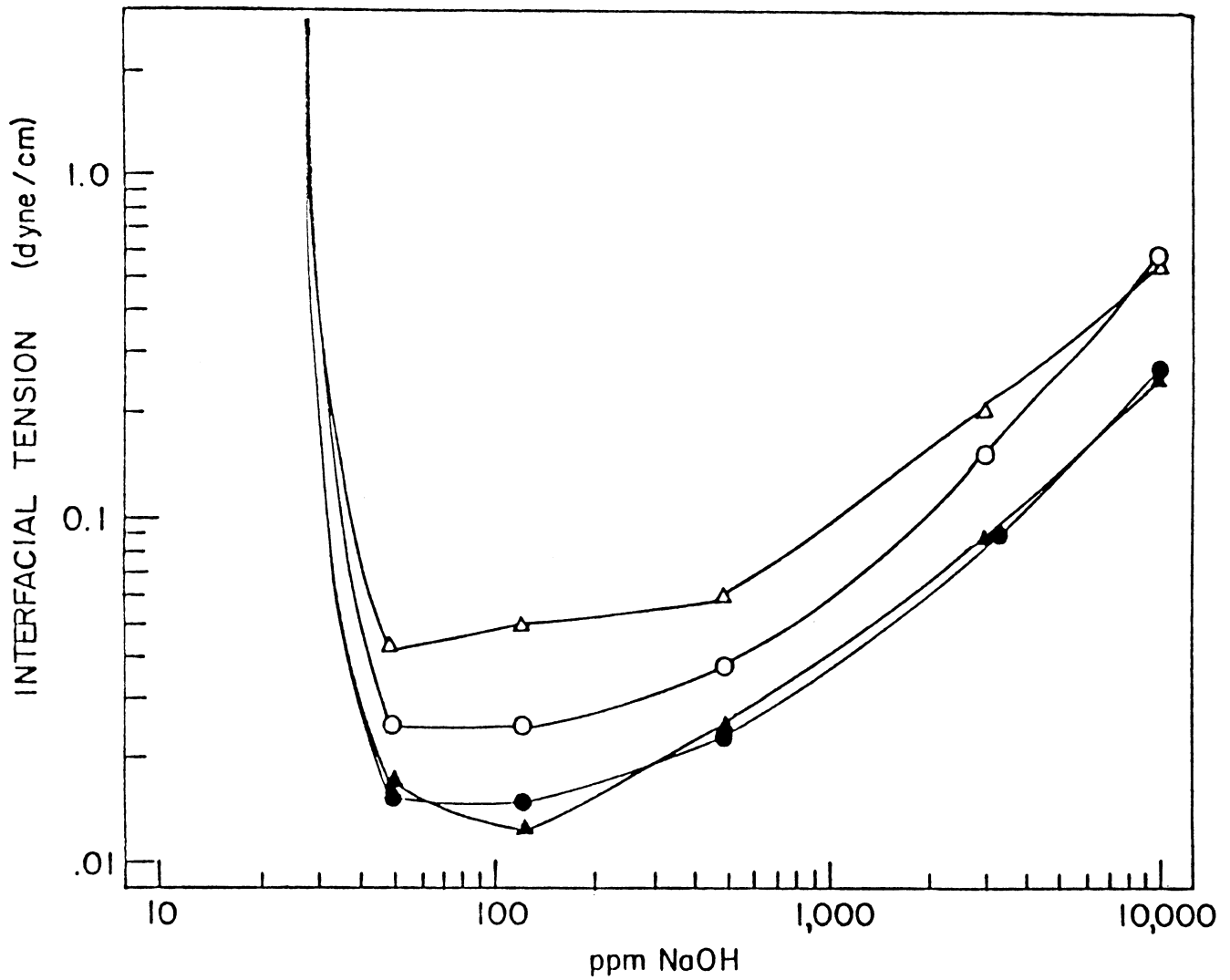


Figure 34 Reactivation of Alkali Exhausted Crude Oil by Acid Treatment. Original Crude (○) Deactivated by a 1 % Alkali solution is Reactivated by 0.05N HCl (△), 0.2N HCl (▲) or 1.0N HCl (●) respectively.

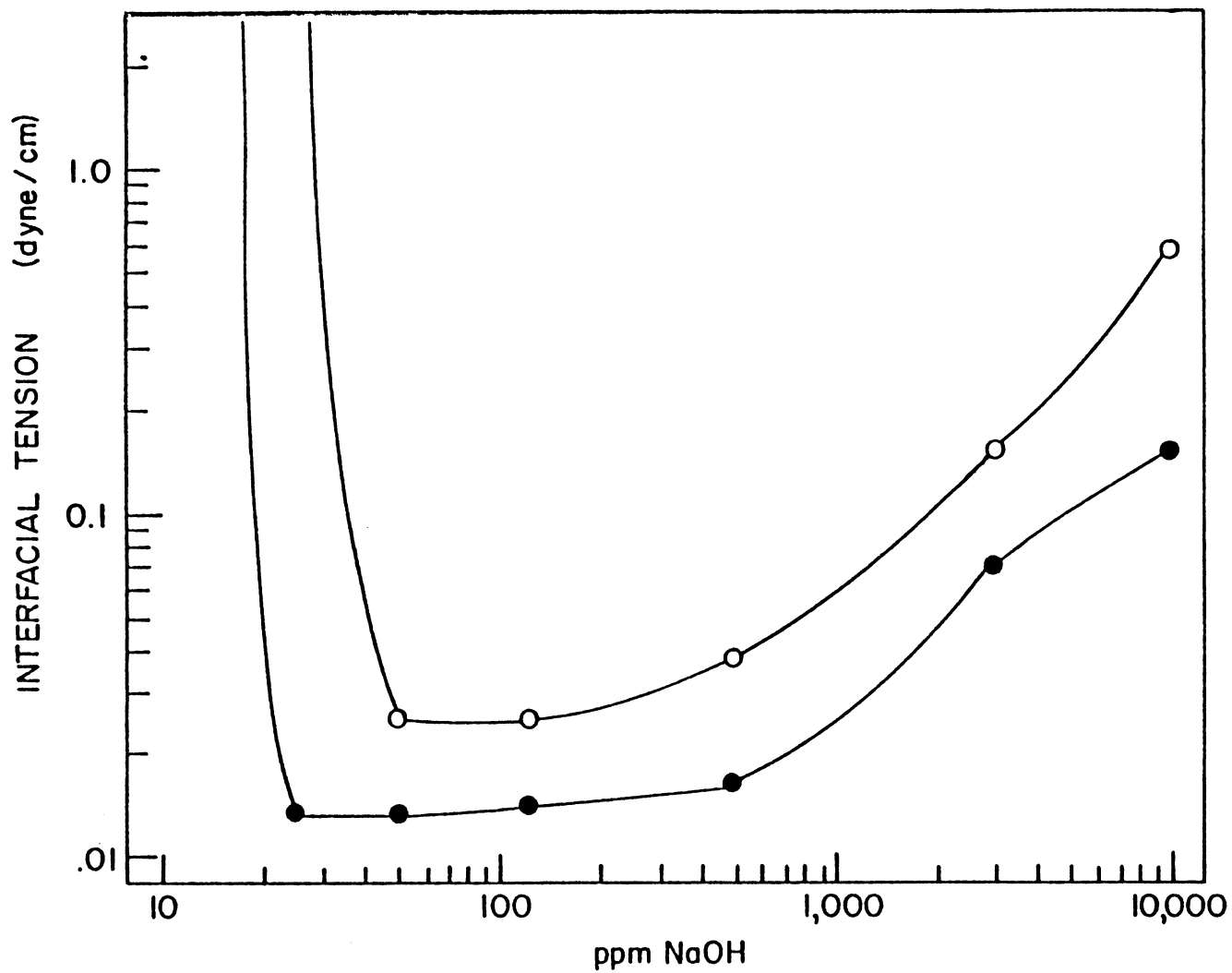


Figure 35. Increased Activity of Crude Oil by Acid Treatment.  
 Original Crude (O) Treated with 0.2N HCl Solution (●).

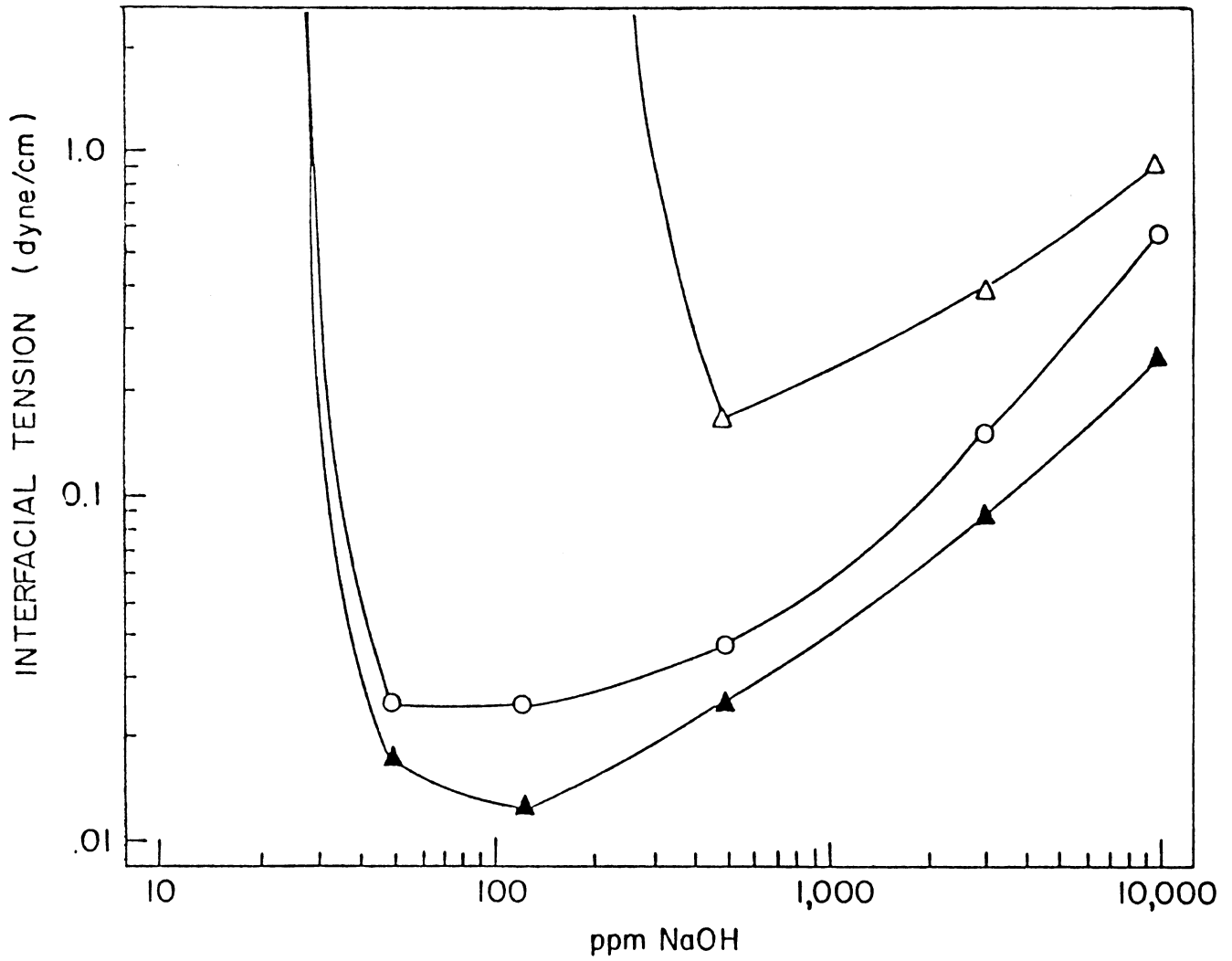


Figure 36. Repeated Reactivation of Crude Oil by Acid Treatment. Original Crude (●) Deactivated by a 1 % Alkali solution is Reactivated by a 0.2N HCl solution (▲). It is then Deactivated and Activated similarly for the Second Time (Δ).

one time may not give quite the same activity as before. This is especially true with recovery efficiency as less and less oil is now left in the reservoir after the previous alkaline floods.

With the stepwise depletion of these active elements, however, the crude has gained another potentially desirable property--the formation of a water-in-oil emulsion. This formation of water-in-oil emulsion occurs when the oil is treated with acid for the second or third round (after a previous acid-alkali round). It comes at a later, usually the fourth, round if the aqueous solution contains no NaCl. It is believed that the depletion of highly polar components such as organic acids and bases through the extraction by alkali and acid, respectively, has significantly changed the property of the crude to a point where the formation of water-in-oil emulsion is preferred over the normal oil-in-water emulsion on shaking. This may be a desirable property according to Cooke et al.<sup>22</sup> who believed that viscous (about 6,000 c.p. versus 460 c.p. of the original crude) water-in-oil emulsion droplets tend to block flow and induce a high pressure gradient which, in turn, overcomes the capillary forces of the porous media.

Core flood experiment results confirmed the potential effect of the acid treatment on oil recovery by alkaline flooding. Alkali induced recovery from a core which has been exhausted by either a flooding sequence of 250, 500 and 3,000 ppm NaOH or a single effective 500 ppm NaOH flood was found to renew after the core was flooded with a 0.2N HCl solution. Also a core pretreated with the acid was found to yield better recovery on the first round alkaline flooding than one which was not so treated. These core flood results are shown in Table 14.

Table 14. Increased Alkaline Flooding Oil Recovery from a Sand-Packed Core through Acid Treatment.

<u>Flooding Scheme</u> *	<u>Recovery (Wt. %)</u> **
(1) Alkali	31
then Acid - Alkali	26
(2) Acid - Alkali	48
then Acid - Alkali	5

\* Alkali = flooding with 250, followed by 500 and 3,000 ppm NaOH ; Acid = 0.2N HCl solution.

\*\* Based on residual oil after secondary water flooding.

As might be expected, Fraction 3, which was found to contain all the free acids in the crude, showed results similar to those of the crude when subjected to the deactivation-activation cycle. This means that Fraction 3 also contains the acid-bearing species.

Fraction 2, which showed no activity, was found to inherit some activity after an acid treatment, although the gained activity was nowhere near as strong as that of Fraction 3 (see Figure 37). This means that Fraction 2, although containing no free acids, does have a small amount of these acid-bearing species. This is supported by results of elemental analysis which showed that Fraction 2, like Fraction 3, contains a significant amount of nitrogen (see Table 8). Therefore amine-acid type of complex may constitute part of these acid-bearing species mentioned here. Nonactive Fraction 1, however, is not affected by acid treatment. This is consistent with the understanding that the fraction contains few heteroatoms such as the oxygen or carboxylic acid.

#### Evidence for the Mechanism of the Generation of Additional Activity by Acid Treatment

The presence of acid-hydrolysable species such as amides, esters and fats (tri and diesters) and base-acid associates in crude oil has been mentioned previously. Our experiment showed that pure toluene solutions of oleic acid-methyl ester, oleic monoethanolamide and L- $\alpha$ -phosphatidylcholine (lecithin), all independently showed activity generation by acid treatment similar to that observed with the crude. The results are shown in Figures 38, 39, and 40, respectively. In Figure 41 and Figure 42, the close similarity between the acid-generated activity and the activity of pure free oleic acid (included in the figures for comparison) provided further evidence

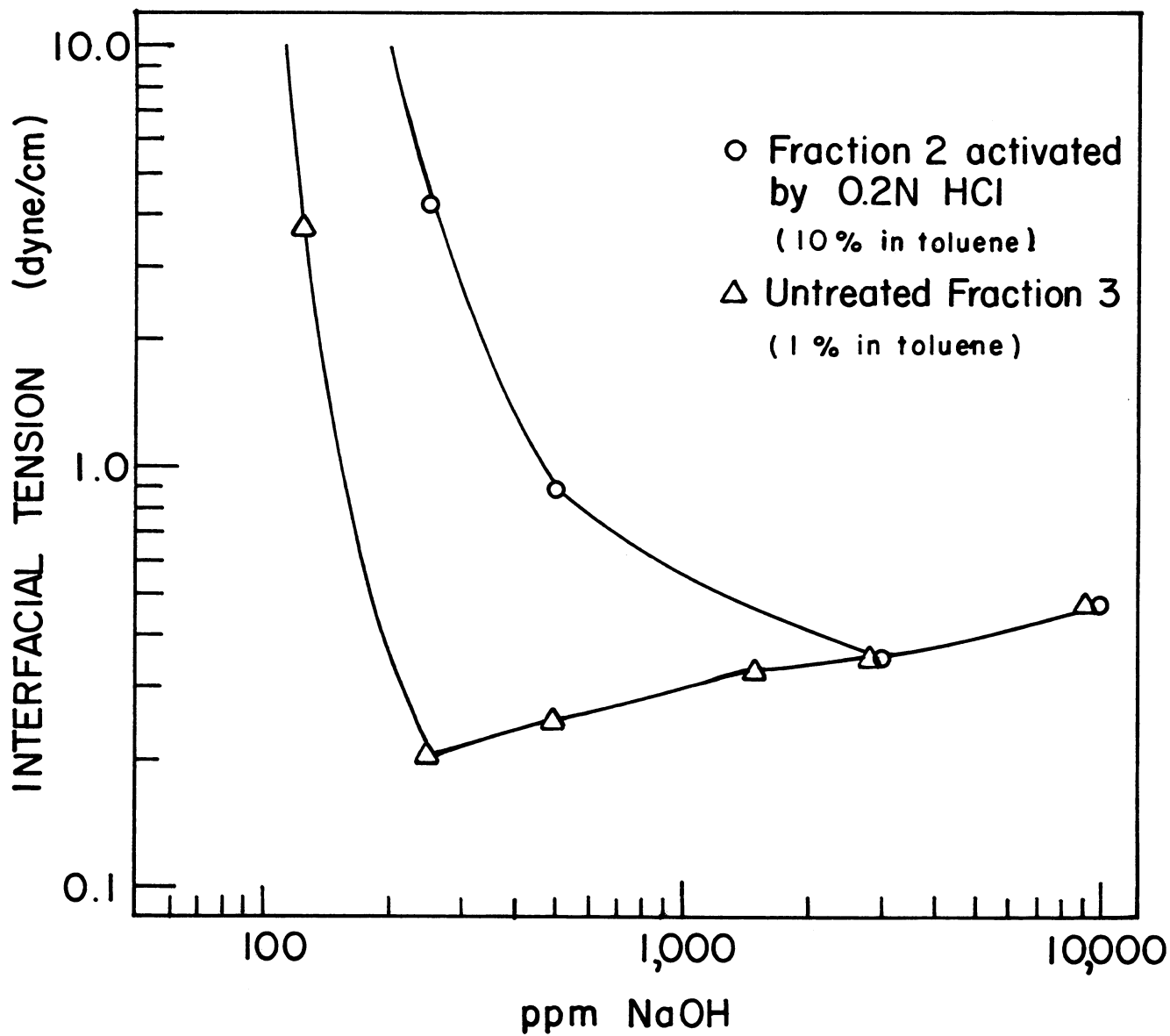


Figure 37. Acid-Induced Interfacial Activity of Fraction 2 (10 % Sample). A 1 % Fraction 3 Sample is Included for Comparison.

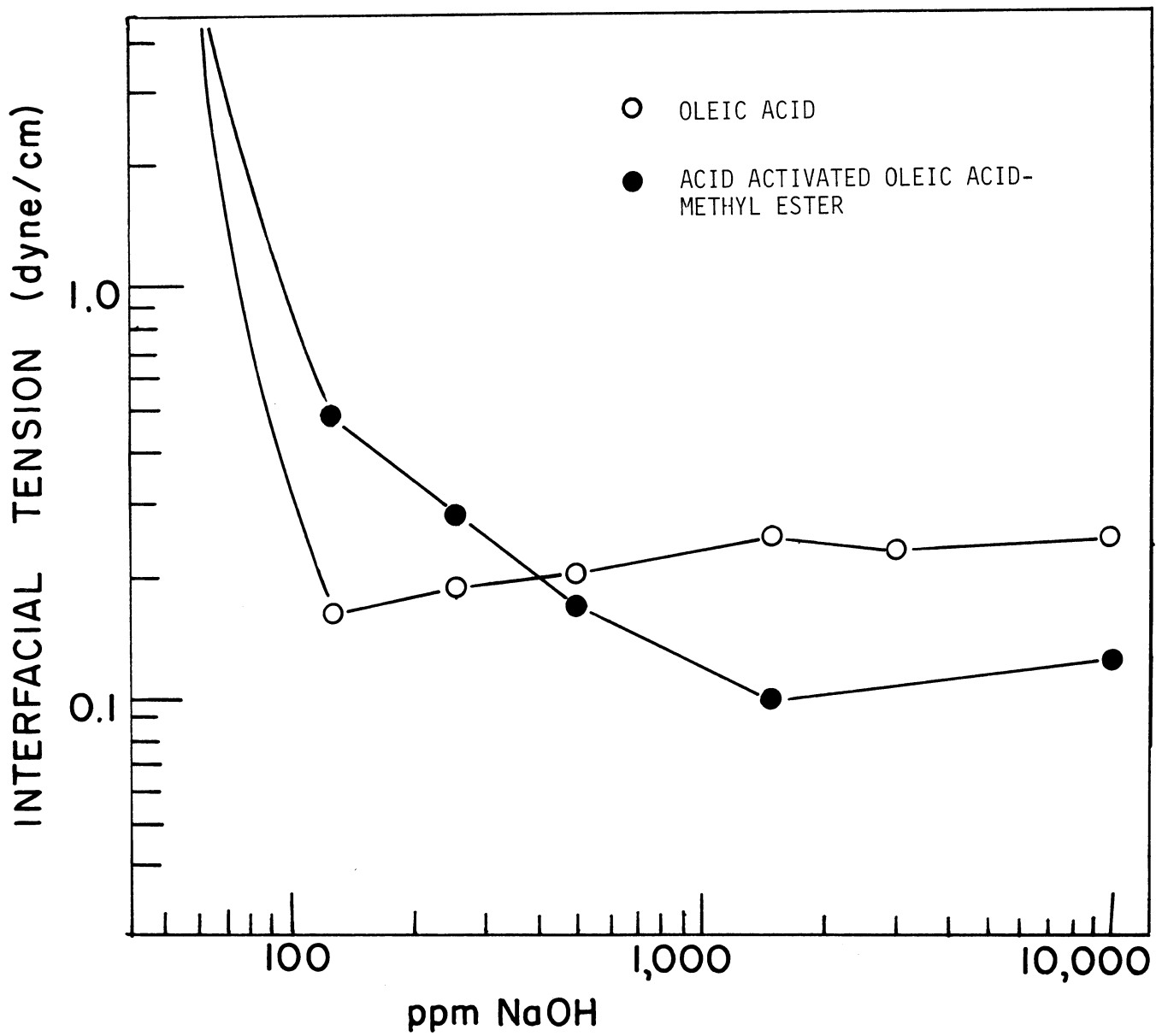


Figure 38. Acid-Induced Interfacial Activity of Oleic Acid-Methyl Ester: a 1 % Sample Pre-exhausted with Alkali.

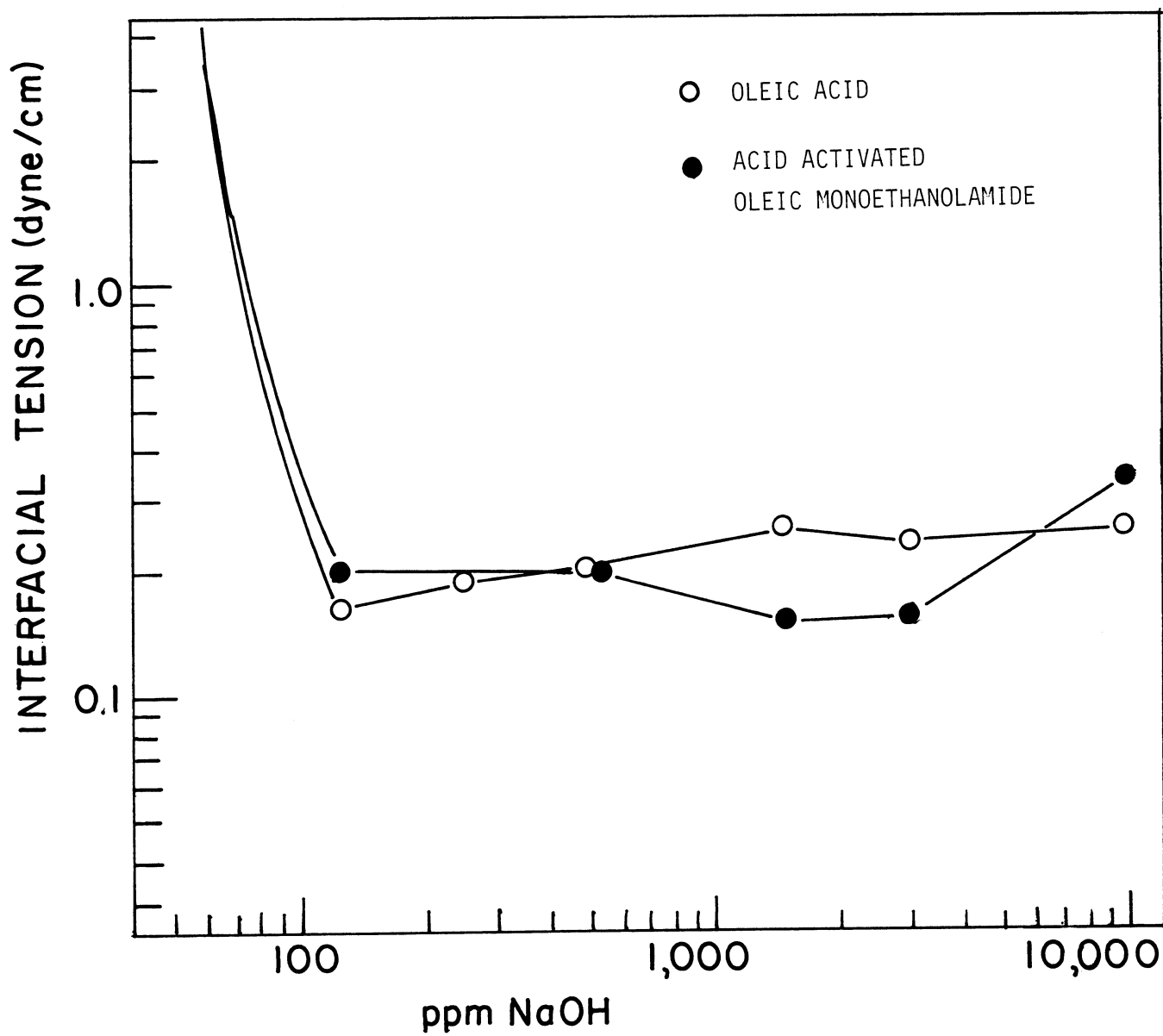


Figure 39. Acid-Induced Interfacial Activity of Oleic Monoethanolamide: a 1 % Sample Pre-exhausted with Alkali.

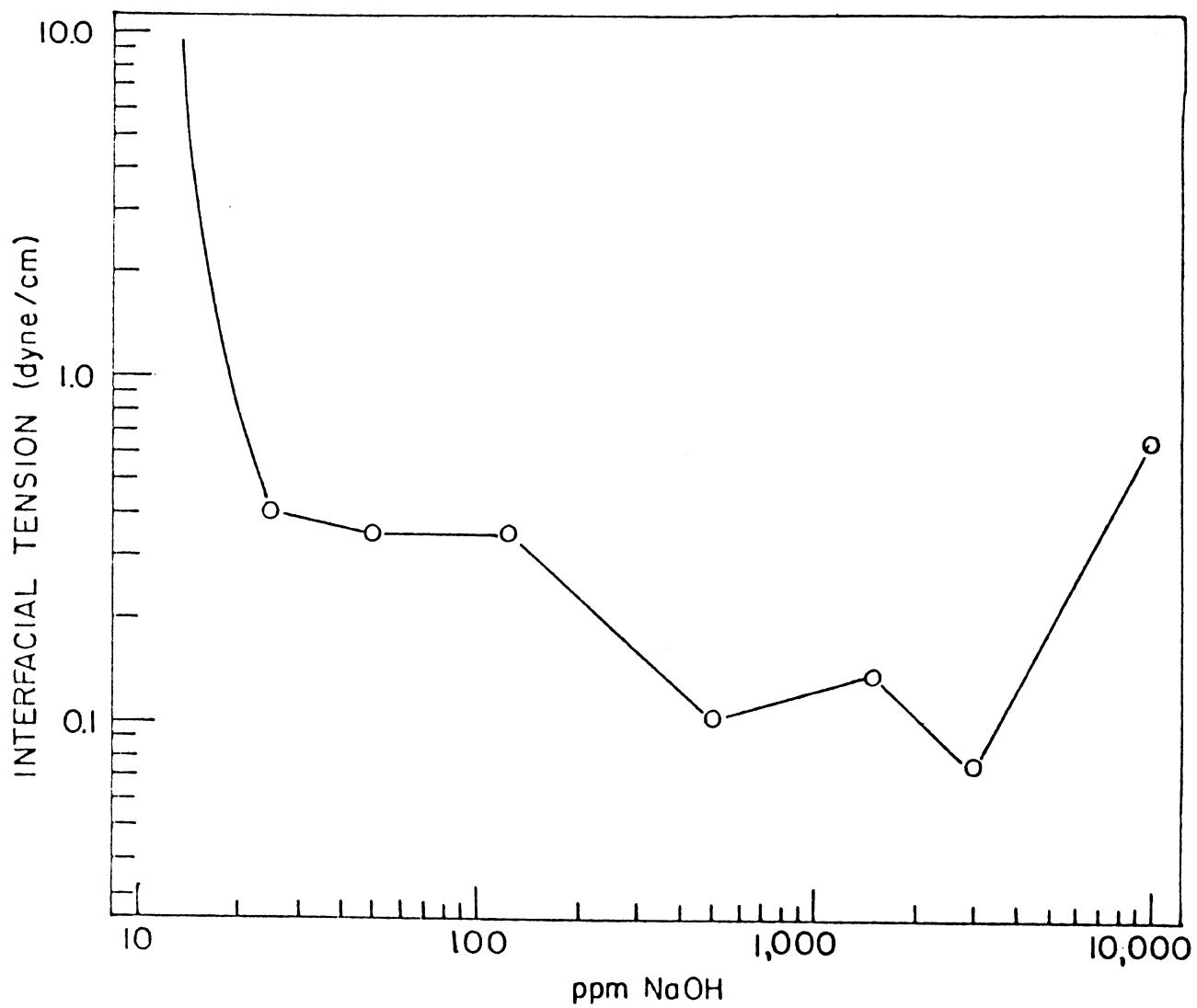
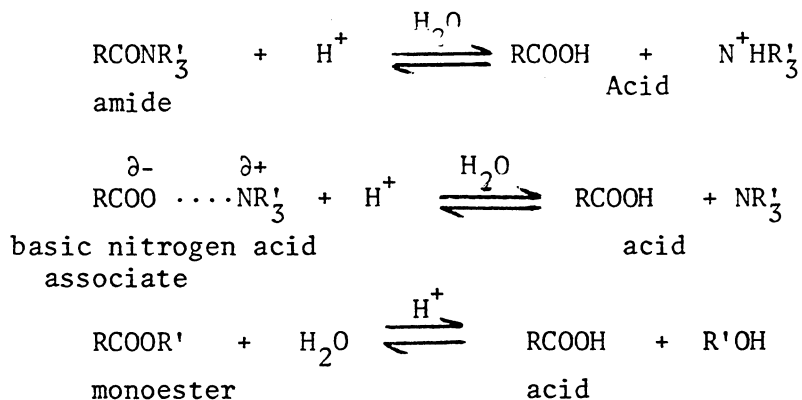


Figure 40. Acid-Induced Interfacial Activity of L- $\alpha$ -Phosphatidylcholine (Lecithin): a 1 % Sample Pre-exhausted with Alkali.

for the hydrolysis of these oleic acid-bearing species yielding free oleic acid molecules which are then responsible for the observed activity in alkali.

Another piece of evidence for the breaking up of some type of base (aliphatic amines or pyridine type basic nitrogen)-acid complexes, which include amides, was the observation that amine type of nitrogen molecules were extracted out into the aqueous phase during the acid treatment. This was identified by IR absorption spectrum which showed strong N-H absorptions at both 3,500 and 2,800  $\text{cm}^{-1}$  (Figure 41). Surprisingly, these extracted bases exhibit interfacial activity at alkaline pH (see Figure 42), although at about half the strength of the active acid extracted previously. This observation, together with the IR carbonyl absorption at 1,700  $\text{cm}^{-1}$  in Figure 41, strongly suggested that some of these bases are some kind of amino acids because pure acid could not have been extracted out by acid solution. Elemental analysis of these bases confirmed the high content of oxygen in addition to the nitrogen abundance (see Table 11).

The hydrolysis reactions of the above mentioned compounds which yield free organic acids are given below:



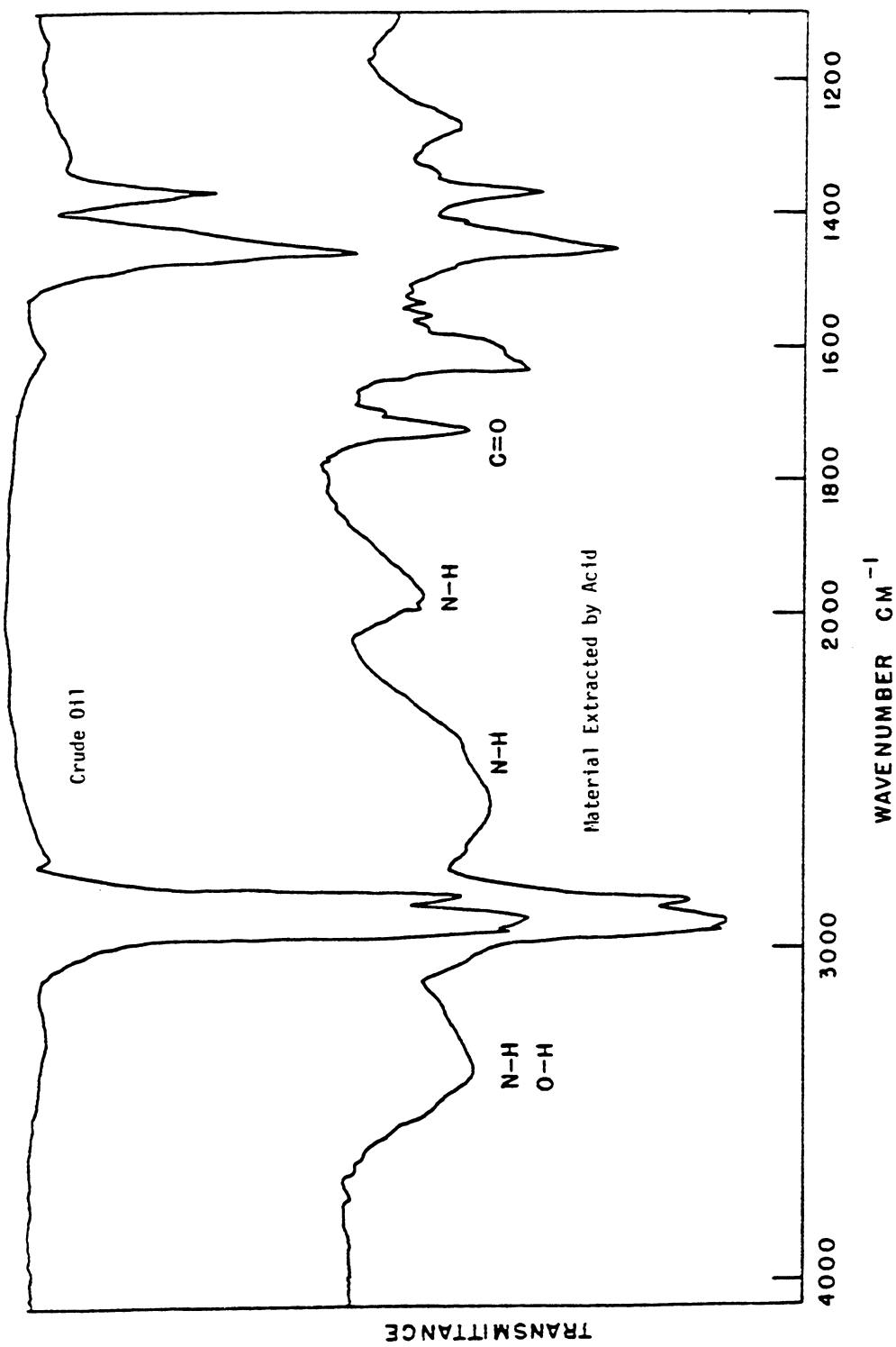


Figure 41. Infrared Spectrum of Material Extracted from Crude Oil with 0.2N HCl Solution.

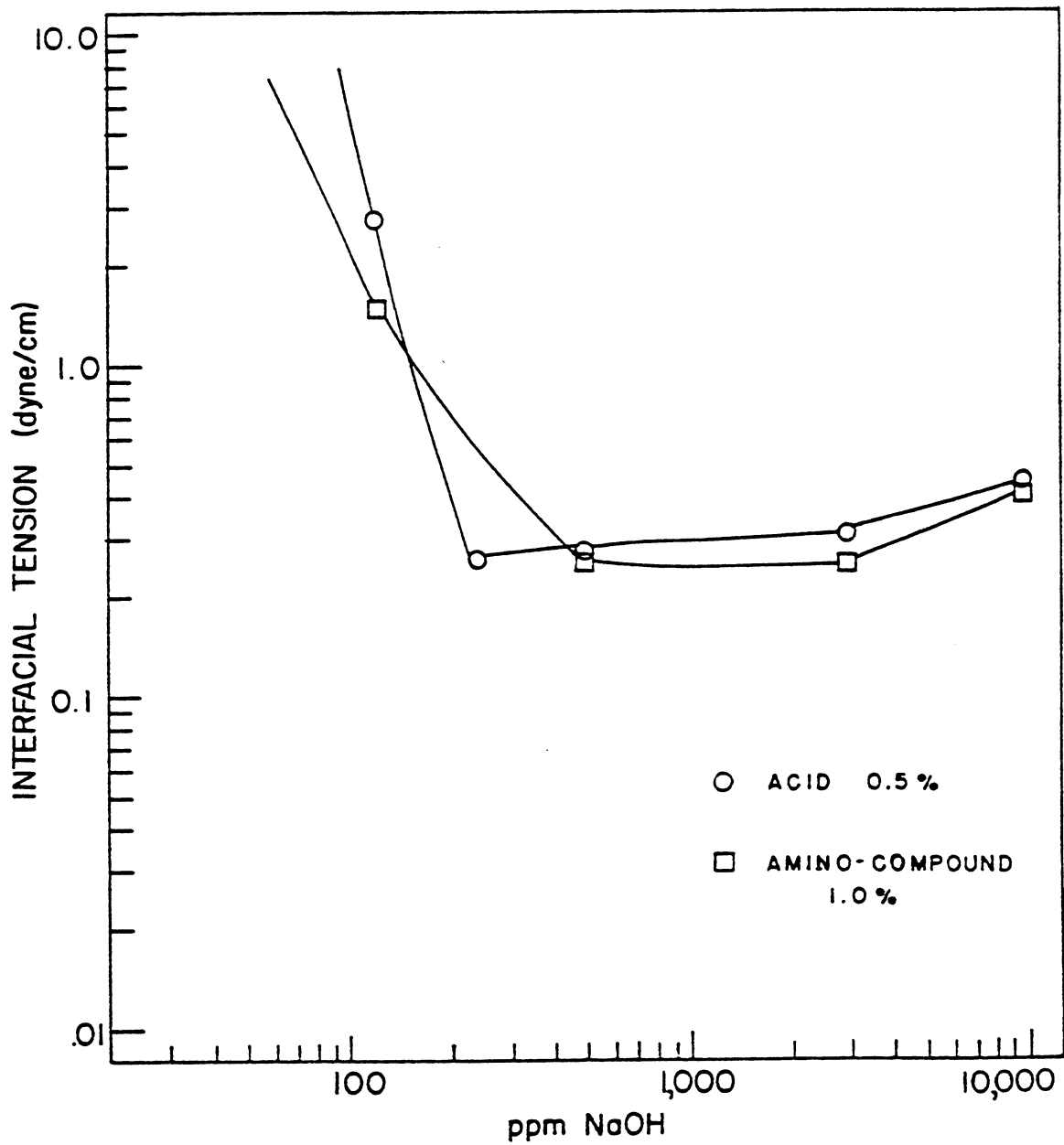
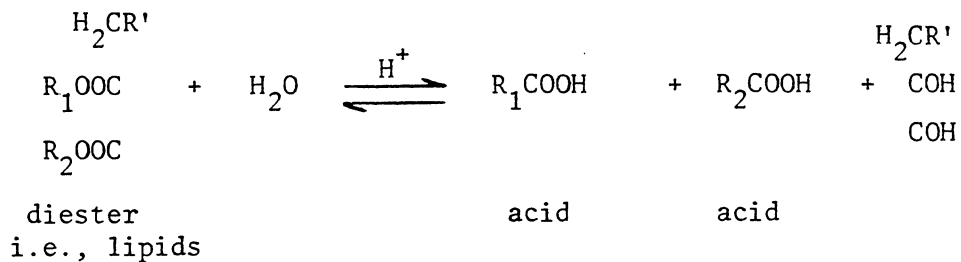


Figure 42 Interfacial Activity of Amino Material Extracted from Crude Oil with 0.2N HCl Solution: a 1 % Sample. A 0.5 % Sample of Active Acid Extracted by Alkali is Included for Comparison.



The above observations strongly suggested that the organic acid-bearing species in the crude in this case include amides and other amine-acid type associates, as well as esters (mono, di and tri-esters); and their acid-catalyzed hydrolysis reactions could be exploited to yield free organic acids capable of generating interfacial activity by soap formation at alkaline pH. The possibility that these acids were generated through oxidation can be excluded due to dilute concentration of acid used.

## CONCLUSIONS

The objective of this work was to understand the mechanisms involved in lowering the interfacial tension of acid-containing hydrocarbons in water by alkali agents. In order to do this the composition and chemical properties of three crude oils were studied. The alkali sensitive Interfacially active fractions of these crude oils were characterized and an equilibrium chemical model for the observed interfacial phenomena was developed.

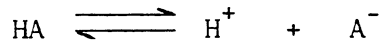
The results presented in the previous sections allow the following conclusions to be drawn:

1. The alkali sensitive surface active components of crude oil can be concentrated into a small polar fraction using silica gel column chromatography. These active components are primarily carboxylic acids.
2. The presence of sodium chloride in the alkaline aqueous solution can lower the alkali concentration required to bring about the drop in interfacial tension between oil and water. Increased salt concentration, however, causes an overall higher interfacial tension.
3. An equilibrium chemical model was proposed expressing the interfacial concentration of

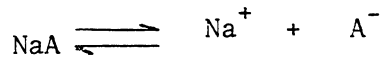
active acids as:

$$(A^-) = \frac{HA_o}{\frac{(H^+)}{K_a} + \frac{(Na^+)_{OH}}{K_s} + \frac{(Na^+)_{Cl}}{K_s} + 1}$$

where  $HA_o$  is the total concentration of active acids in the oil,  $(H^+)$  is the interfacial hydrogen ion concentration,  $(Na^+)$  is the interfacial sodium ion concentration, subscripts OH and Cl mean the sodium ions are originated from NaOH and NaCl, respectively,  $K_a$  is the ionization constant of the active acid:



and  $K_s$  is the dissociation constant of acid soap:



Interfacial tension data of the crude as well as artificial samples containing the extracted acids showed that this model gives a satisfactory description of the observed oil-alkaline solution interfacial phenomenon, including its dependence on pH ( $(H^+)$ ), alkali and salt concentrations ( $(Na^+)$ ), type of acid present ( $K_a$ ) and type of soap formed ( $K_s$ ).

4. The active acids present in the crude are shown to be a mixture of many species which ionize at different bulk solution pH. Therefore sequential flooding with solutions of different alkali concentrations is proposed to react with these different species. It is to start from the

lower end of the effective alkali concentration range because it gives lower interfacial tension. One then works one's way up to react with the remaining active species at higher alkali concentrations as long as economics allows. The theoretical alkali concentration to be used at each stage is the one that gives the interfacial tension minimum of the remaining oil. However, due to alkali consumption by reservoir rock, a slightly higher feed alkali concentration may have to be used to achieve the desired reservoir pH.

5. It is possible to generate additional soap forming acids from the crude by treating the crude with dilute solutions of mineral acids such as hydrochloric acid or sulfuric acid. This is based on the acid-catalyzed hydrolysis reaction of compounds such as esters, amides and other amine-acid associates, which yield free organic acids capable of forming soaps at alkaline pH. Similarly, acidflooding can be used to activate an oil reservoir which has been exhausted by previous alkali floods, making the reservoir sensitive to new alkali floods. It can also be used as a pretreatment prior to any first round alkali flood to enhance the interfacial activity.

#### REFERENCE

1. Silverman, S. R., in *Isotopic and cosmic chemistry: North-Holland Publishing Co.*, p. 92-102.
2. Yen, T. F., ACS Symp. Series No. 18, *Genesis and Degradation of Petroleum Hydrocarbons in Marine Environments*, 231, (1975).
3. Porfirev, V.B. and Grinberg, I.V., *Trudy L'vovsk. geol. ob-va, ser. geol. No. 1*(1948).
4. Porfirev, V.B., *Izv. AN SSSR, ser. geol.*, No. 6 (1955).
5. Brod, I.O. and Eremenko, N.A., "*Fundamentals of Petroleum and Gas Geology*", Izd. MGU (1953).
6. Cox, B. B., *Bull. Am. Ass. Pet. Geol.*, 30, No. 5 (1946).
7. Teodorovich, G.I., *Neft. Khoz.*, No. 12 (1952).
8. Brod, I.O. and Levinson, V. G., "*Origin of Petroleum and Petroleum-Gas Accumulation*", Gostoptekhizdat, (1955).
9. Andreev, P.F., Bogomolov, A.I., Dobryanski, A.F. and Kartsev, A.A., "*Transformation of Petroleum in Nature*", Pergamon Press (1968).
10. Donnon, *Zeit. Physikal. Chem.*, 31, 43 (1899).
11. Hartridge, H. and Peters, R., *Proc. Roy. Soc. (London)*, A101, 348 (1922).
12. Peters, R., *Proc. Roy. Soc. (London)*, A133, 140, (1931).
13. Danielli, R., *Proc. Roy. Soc. (London)*, B122, 155 (1937).
14. "*Bailey's Industrial Oil and Fat Products*", D. Swern, E., Vol. 1, John Wiley & Sons (1979).
15. Fryer, P.J. and Weston, F.E., "*Technical Handbook of Oils, Fats and Waxes*", Vol. I & II, Cambridge Univ. Press (1939).
16. Squires, F., U.S. Patent No. 1,238,355.
17. Atkinson, H., U.S. Patent No. 1,651,311 (Nov. 29, 1927).

18. Subkow, P., U.S. Patent No. 2,288,857 (July 7, 1942).
19. Sarem, A.M., U.S. Patent No. 3,805,893 (April 23, 1974).
20. Nutting, P.G., Oil & Gas J., 25, 32, 106 (1927).
21. Nutting, P.G., Oil & Gas J., 27, 146, 238 (1928).
22. Cooke, C.E., Jr., Williams, R.E. and Kolodzie, P.A., J. Pet. Tech., Dec., 1365 (1974).
23. Leach, R.O., Wagner, O.R., Wood, H.W. and Harpke, C.F., J. Pet. Tech., Feb., 206 (1962).
24. Ban, A., Oil & Gas J., July, 149 (1977).
25. Raimondi, P., Gallagher, B.J., Bennett, G.S., Ehrlich, R. and Messmer, J.H., SPE 5831, SPE Symp. on Improved Oil Recovery, Tulsa, OK (March 22-24, 1976).
26. Emery, L.W., Mungan, N. and Nicholson, R.W., J. Pet. Tech., Dec., 1569 (1970).
27. Grave, D.J. and Johnson, C.E., Jr., J. Pet. Tech., Dec., 1353 (1974).
28. McAuley, R.G., paper presented at the 28th Ann. Tech. Meeting of Pet. Soc. of CIM, Edmonton, Alberta (May 30-June 3, 1977).
29. Wotring, D.H., SPE Improved Oil Recovery Field Reports, June, 113 (1975).
30. Weinbrandt, R.M., Paper C-4, 5th Ann. DOE Symp., Tulsa, OK, (Aug. 23-24, 1979).
31. Phillips Petroleum, Oil & Gas J., April, 92 (1979).
32. Campbell, T.C., paper presented at the 50th Ann. Calif. Region Meeting (April 9-11, 1980).
33. Campbell, T.C., paper presented at the 50th Ann. Calif. Region Meeting (April 9-11, 1980).
34. Chang, H.L., Canadian Patent No. 1037863 (filed Feb. 24, 1976).
35. Jennings, H.Y., Jr., SPE J., June, 197 (1975).
36. Johnson, C.E., J. Pet. Tech., 28, 85 (1976).
37. Reisberg, J. and Doscher, T.M., Prod. Monthly, Nov., 43-50 (1956).
38. Jennings, H.Y., Jr., Johnson, C.E., Jr. and McAuliffe, C.D., J. Pet., Tech., Dec., 1344 (1974).

39. Wagner, O.R. and Leach, R.O., Trans., AIME 216, 65 (1959).
40. Mungan, N., J. Pet. Tech., Feb., 247 (1966).
41. Ehrlich, R.R., Hasiba, H.H. and Raimondi, P., J. Pet. Tech., Dec., 1335 (1974).
42. Seifert, W.K. and Howells, W.G., Anal. Chem., 41, 786 (1969).
43. Seifert, W.K. and Teeter, R.M., Anal. Chem., 41, 554 (1969).
44. Seifert, W.K., Prog. Chem. Nat. Prod., Springer-Verlag, 1-49 (1975).
45. Dunning, H.N., Moore, J.W. and Denekas, M.O., Ind. Eng. Chem., 45, 1759 (1953).
46. City of Long Beach and Thums Long Beach Co., First & Second Ann. Reports, DOE SAN/1396 (Oct., 1976 - May, 1978).
47. Bansal, V.K., Chan, K.S., McCallough, R. and Shah, D.O., J. Canad. Pet. Tech., 17, 1 (1978).
48. Dezabala, E.F., Vislocky, J.M., Rubin, E. and Radke, C.J., SPE 8997, SPE 5th Int. Symp. on Oilfield and Geothermal Chem., Stanford, CA (May 28-30, 1980).
49. Snyder, L.R., Anal. Chem., 41, 314 (1969).
50. Snyder, L.R., Anal. Chem., 41, 1083 (1969).
51. Latham, D.R., Preprints, Div. Pet. Chem., ACS, 19, 25 (1974).
52. Cayias, J.L., Schechter, R.S. and Wade, W.H., ACS Symp. Series No. 8, Absorption at Interfaces, 234 (1975).
53. Erdman, J.G., U.S. Patent No. 190,829 (June 22, 1965).
54. "Carotenoids", Otto Isler, Ed., Halsted Press, N.Y., p. 785 (1971).
55. "Carotenoids", Otto Isler, Ed., Halsted Press, N.Y., p. 36 (1971).
56. Pasquarelli, C.H. and Wasan, D.T., paper presented at Third Int. Conf. on Surface & Colloid Science, Surface Phenomenon In Enhanced Oil Recovery Sect., Stockholm, Sweden (Aug. 20-25, 1979).
57. Farmanian, P.A., et al., Symp. on Chem. of Oil Rec. Div. Pet. Chem., ACS, Anaheim, Ca., (March 12-17, 1978).
58. Baker, E.W., et al., JACS, 3631 (1967).

59. Gouy, G., J. Phys., 9, 457 (1910).
60. Chapman, D.L., Phil. Mag., 25, 475 (1913).
61. Stern, O., Z. Electrochem., 30, 508 (1924).
62. Davies, J.T. and Rideal, E.K., Proc. Roy. Soc. (London), A193, 417 (1948).
63. Payens, Th. A. J., Phillips Research Reports, 10, 425 (1955).











